

⁰ Shear Failure of Reinforced
Concrete beams under uniformly
distributed loading.

James J. Idathara

A thesis submitted in fulfilment
for the Degree of Master of Science
(Engineering) in the University of Nairobi

1973

DECLARATIONS

This thesis is my original work and has not been presented for a degree in any other University.

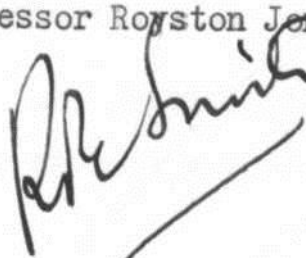
A handwritten signature in black ink that reads "Gathara". The signature is written in a cursive style with a large, stylized initial "G".

James J.
Gathara.

This thesis has been submitted for examination with our approval as University supervisors.

A handwritten signature in black ink that reads "Royston Jones". The signature is written in a cursive style with a large, stylized initial "R".

Professor Royston Jones.

A handwritten signature in black ink that reads "R. B. L. Smith". The signature is written in a cursive style with a large, stylized initial "R".

Professor R. B. L. Smith

CONTENTS

Acknowledgements		i
List of Tables		ii
List of Ei Tires		iv
List of Plates		viii
Notations		ix
Summary_ c^> \		1
Chapter 1 •	Introduction	6
Chapter 2 •	Literature review	11
Chapter 3 •	General behaviour of reinforced %	19
-	concrete beams	
Chapter 4 •-	Experimental work	38
Chapter 5	Analysis of test results	73
Chapter 6	Conclusions and discussion	112
Chapter 7	Recommendations for future work	116
Bibiliography		120
Appendi 2es		125

ACKNOWLEDGEMENTS

The author is indebted to Professor R.B.L. Smith, University of Nairobi, under whose guidance this research project was carried out. His valuable advice and helpful suggestions are recorded with thanks.

The author also wishes to thank Professor R. Jones,

University of Nairobi, for his constant encouragement at all stages of this research.

%

The University of Nairobi concrete laboratory staff were of great help during the experimental stage of this research. Their co-operation is very much appreciated.

Thanks are due to the Ministry of Works, Materials Branch, for the assistance rendered in the testing of steel reinforcing bars.

The author is very grateful to UNESCO mission for providing funds to conduct a great part of this research.

LIST OF TABLES

Table	Title	Page
4.1	Test results	47
4.2	Test results	48
4.3	Maximum concrete strains	49
5.1	Summary of graphical solutions for $T(=C)$ and k	95
5.2	Test and calculated values of x^{\wedge}	96
5.3	Actual and theoretical web reinforcement	97
5.4	Comparison of modes of failure, actual and predicted web reinforcement	98
5.5	Predicted values of web reinforcement, r, f by equation 5.22 for different values of t	99
5.6	Values of web reinforcement predicted by equation 5.24	100
Appendix C		
C1	Strain values for beam G1/1	140
C2	" 01/2	143
C3	"• 01/3	146
C4	»' 01/4	149
Table	Title	Page
C5	Strain values for beam 02/1	152
C6	02/2	153
155	G2/3	
C		
7		

C8	Strainvalues for beam G-2/4		
09	tf	03/1	156
			158
CIO	ft	03/2	159
Oil	III	03/3	158
012	H*	03/4	161
Appendix D			
D1	Details of beams and test of results Smith		162
Appendix F			
F1	Rotations for beam	01/1	174
F2	« ft	G1/2	175
?3	It	01/3	176
F4	111	01/4	177
F5	II'	02/1	178
F6	If	02/2	178
F7	It	02/3	179
F8	II	02/4	179
F9	f1	03/1	174
F10	It	03/2	180
F11	f1	03/3	181
F12	It	03/4	181

LIST OF FIGURES

<u>Figure</u>	<u>Title</u>	<u>Page</u>
1.1	Shear force and Bending moment diagrams for simply supported beam under two concentrated loads.	9
1.2	Shear force and Bending moment diagrams for simply supported beam under uniformly distributed loading.	10
3.1	Development of a flexural crack to a diagonal tension crack formation	33
3.2	of web shear cracks Stresses	33
3.3	acting on a finite element Free-body diagrams without web reinforcement	33
3.4	(a) Before redistribution (b) After redistribution Free-body diagrams with web reinforcement	34
3.5	(a) Before redistribution (b) After redistribution Deformation conditions according to Regan	35
3.6	Deformation conditions according to Walther Moment-rotation relationship	36
3.7		36
3.8		37

Figure	Title	Page
4.1	Stress-strain characteristics for the 14.70 mm square high tensile twisted bars used for the main reinforcement	50
4.2	Stress-strain characteristics for the 5.64 mm diameter mild steel rods used for the stirrups	51
4.3	Comparison of test and calculated modulus of rupture	52
4.4	Location of mid points <of gauge lengths for strain measurement	53
4.5	Loading arrangement for group G1 beams	54
4.6	Loading arrangement for group G2 beams	55
4.7	Loading arrangement for group G3 beams	56
4.8	Crack patterns of group G-1 beams	57
4.9	Crack patterns of group G2 beams	58
4.10	Crack patterns of group G3 beams	59
4.11	Direct and shear stress distributions	60
4.12	Variation of concrete strain with load-beam G1/1	61
4.13	It G1/2	62
4.14	ft 01/3	63
4.15	ft G1/4	64
4.16	It G2/1	65
4.17	It G2/2	66
4.18	tft 02/3	67

4.19	Width of concrete strain with		6
			8
4.20	ft	G3/1	6
4.21	It	G3/2	7
			0
			7
4.22	If	G3/4	1
4.23	It	G3/4	7
			2
5.1	Critical section		101
5.6			
5.2	Relationship between	and L/d	102
5.3	Relationship between	ratio of actual	104
	web reinforcement to the calculated		
	quantity and ratio of ultimate moment to		
	flexural capacity		103
	Concrete and steel strain variation		
5.4			101
5.5	Graphical solution of	equations	
		5.12 (b)	
	and 5.17 for $T C = C$	and k	101
	Development of regression equation for		
	predicting web reinforcement considering shear		
	stresses		
5.7	Development of regression		
	equation for predicting web reinforcement		
	considering bending moments		10
			5
5.8	Deflection profile of a beam before		10
	failure		6
5.9	Influence of web reinforcement on mid		
	span rotations		
A	(a) for $l/d = 6$		10
	(b) for $L/d = 8$		7
			10
			8
	(c) for $L/d = 10$		10
			8

<u>Figure</u>	<u>Title</u>	<u>Page</u>
5.10	Influence of web reinforcement on ratio of ultimate moment for beams with web reinforcement to ultimate moment for beams without web reinforcement	109
5.11	Influence of ratio of effective length to effective depth on ratio of ultimate moment for beams with web reinforcement to ultimate moment for beams without web reinforcement	110
5.12	Comparison of test and calculated ratios of ultimate moment for beams with web reinforcement to ultimate moment for beams without web reinforcement	111
Appendix A		
A1	Physical properties of group G-1beams	126
A2	Physical properties of group G-2beams	127
A3	Physical properties of group G3 beams	128

LIST OF PLATES

Plate	Title	Pag
Appendix B		
B1	Beam G1/3 at failure load	12
		9
		12
B2	Beam 01/3 showing concrete spalling	9
		13
B3	Beam G1/4 at failure load	0
		13
B4	Beam 01/4 showing concrete spalling	0
		13
B5	Diagonal tension failure of beam 02/1	1
B6	Close-up of the failure diagonal crack of beam G2/1	13
		1
		13
B7	Beam 02/2 before load application	2
		13
B8	Shear-compression failure of beam 02/2	2
B9	Close-up of failure section of beam 02/2	133
B10	Beam 02/3 before load application	13
		2
B11	Diagonal cracking of beam G2/3 during loading	13
		4
B12	Combined shear and flexure failure of beam 02/3	13
		4
B13	Diagonal cracking of beam G2/4 during loading	13
		5
B14	Close-up of diagonal cracks of beam 02/4 during loading	13
		5
B15	Flexural failure of beam 02/4	13
		6
B16	Diagonal tension failure of beam 03/1	13
		6
B17	Close-up of failure diagonal crack of beam 03/1	13
		7
B18	Beam 03/2 before load application	13
		7
B19	Shear-compression failure of beam 03/2	13
		8
B20	Shear-compression failure of beam 03/3	13
		8
		13
B21	Beam 03/4 before load application	9
B22	Combined shear and flexure failure of beam 03/4	

Figure

Title

139
Page

x -

NOTATIONS

Areas:

A_g^{\wedge} = cross-sectional area of steel dm tension
 A_{yy} = cross-sectional arera of one stirrup
(two rods)

Bending Moments:

M = bending moment

$M_{\frac{sg}{s}}$ = ultimate shear-compression moment

M_o = shear-compression moment without web

reinforcement

M_{sw} = moment of resistance in shear compression at
critical section for shear compression
failure

M_p = bending moment at flexural cap acity

M_p' = bending moment at flexural capacity
at critical section for diagonal
cracking

M_n = bending moment at ultimate load at
critical section for diagonal cracking

M_{v1} = bending moment corresponding to

diagonal cracking load.

= ultimate bending moment M_{u_w} =

ultimate bending moment with web
reinforcement

$M_{u'}$ = ultimate bending moment without web
reinforcement

M_{xT} = bending moment at x^{\wedge} from support

Distances:

a = shear span

b = breadth of rectangular beam

d = overall depth of rectangular beam d_1 =
effective depth of rectangular beam

L = x_i
 l_a = effective span of beam
 s = lever arm
 x_1 = horizontal spacing of stirrups distance along axis of beam from support value of x at
 x_2 = critical section for shear compression value of x at critical section for diagonal cracking

Forces:

Q = total shear force
 Q_{cr} = shear cracking force
 Q_w = shear force carried by one stirrup (two rods)
 $\%$
 $<^*u$ = ultimate shear force
 T = tensile force resisted by main steel
 0 = compressive force resisted by compression zone
 w = uniformly distributed load per unit length of span total load on beam
 W = total diagonal cracking load on beam total ultimate load on beam
 $w =$
 $"cr$
 $w =$
 $'■a$

150 x 300 mm cylinder strength of concrete

Stresses:

σ_c = modulus of rupture of concrete
 V = allowable tensile stress in stirrups
 $V -$ yield stress of web reinforcement
 $f_w - f$ = stress in main steel corresponding to
 $y_w =$ ultimate concrete strain
 τ = shear stress at flexural capacity
 τ_{st} = shear stress at initial shear cracking load
 σ_F
 σ_{cr}

τ_x = ultimate shear stress

U = 150 nun cube strength of concrete.

Othersr

r = ratio Of main steel = $A^/bd^$

r_w = ratio of web reinforcement = $A^/bs$

e_u =ultimate concrete strain

A =deflections

m, n', t, V, cp) T^ocand (5 are
R, 9, defined
inthe text.

+

SUMMARY

The main object of this investigation was to establish an expression to predict the quantity of web reinforcement that would be required to prevent shear failure in rectangular reinforced concrete beams under uniformly distributed loading and enable attainment of flexural capacity. The general behaviour and strength of such beams were also studied.

Twelve beams were tested, and the variables considered in this study were:-

- (1) the span, hence effective length/effective depth ratio
- (2) the amount of web reinforcement.

All the beams, 230 mm deep by 127 mm wide reinforced by three 14.70 mm square cold twisted bars as main steel with effective depth of 200 mm, were tested on simple spans of 1.2, 1.6 and 2.0 m. Three beams, one of each span, were without web reinforcement. The remainder were provided with 5.61 mm diameter, mild steel stirrups with a yield stress of 320 N/mm². For all the beams with stirrups, the ratio, of web reinforcement was varied from 0.137 to 0.783# such that some beams were intentionally under-reinforced for shear so as to study clearly the function of the web reinforcement in resisting the shearing forces and its actual contribution to the strength of the beams.

The beams were tested at ages between 46 and 50 days and the mean concrete cube strength was 45.8 N/mm².

All the beams were tested under a system of eight point loads applied through steel rollers and plates to simulate uniform loading. For the three spans considered, the steel plates were the same such that in the shortest span the plates were separated by 50 mm; in the other spans the distances were 100 and 150 mm respectively. . The load was applied by %
20 kN increments. After each increment the deflections at mid span and quarter points were determined, the concrete strains were measured on one face of the beam with a demountable demec gauge and the crack patterns were studied. The diagonal cracking load was recorded as the load at which the major diagonal crack crossed the neutral axis.
Finally the ultimate loads and the modes of failure were recorded. Some beams were found to fail in shear, others in flexure and the remainder in combined shear and flexure.

The beams with the shortest span and with web reinforcement exceeded the flexural capacity by up to 34%. This was attributed to the closeness of the steel plates placed on the top surface of the beam on which the point loads were applied.

When the plates were very close as in this case they had the effect of increasing the lever arm and therefore the ultimate moment.

After the analysis of the deflection readings at mid span and quarter points the rotation capacity with relation to web reinforcement and effective length/ effective depth ratio was studied.

The concrete strain distribution indicated that after the formation of the diagonal crack, the upper portion of the beam near the supports became subject to eccentric loading which resulted in a reversal of the nature of the strains. In the two longer spans, the beams with most web reinforcement had tensile strains towards the failure load.

In the attempt to establish an expression for predicting the quantity of web reinforcement necessary for flexural capacity, the test results of the author were analysed together with the test data collected by Smith in 1970. Smith tested eleven beams all of 230 mm deep by 150 mm wide reinforced by three 16 mm diameter rods as main steel with effective depth of 200 mm. The beams were tested on simple spans of 2.44, 3.04 and 3.60 m under a distributed system of eight point loads. Three beams, one of each span, were without web reinforcement and the remainder had 3.2 mm diameter mild steel stirrups with a yield stress of 265N/mm² .

The ratio of web reinforcement varied from 0.068 to 0.41075. The mean concrete strength was 34.4N/mm².

The expression tentatively suggested by Smith for beams of short spans such as those tested by the author predicted very high estimates of web reinforcement that would have been desired for flexural capacity. Consequently it was attempted to establish a general empirical expression applicable for all cases of effective length/effective depth ratio based on the consideration of shear stresses and bending moments. Several empirical equations were derived using v regression models. Out of these, one equation expressing the quantity of web reinforcement in terms of shear stresses corresponding to flexural capacity and diagonal cracking load, was selected for predicting the quantity of web reinforcement required for beams subjected to uniformly distributed loading to attain flexural capacity.

Since it is not possible to establish the influence of all the variables that affect the shear strength of reinforced concrete beams rationally an attempt was made to express the total contribution of web reinforcement empirically-. An equation was established expressing the ratio of the ultimate moment for beams with web reinforcement to the ultimate moment for beams without web reinforcement in terms of web reinforcement and effective length/effective depth ratio.

To extend the scope of the subject, it is suggested that future research would be desirable with the aim of establishing a general expression either empirically or rationally. Recommendations have been made with regard to theoretical approach, test programme ., loading arrangement, crack observation and study of T-beams.

CHAPTER 1

INTRODUCTION

1.1 GENERAL REMARKS

Shear failure in a complex problem. The study of the behaviour and ultimate strength of reinforced concrete rectangular beams failing in shear due to concentrated loading has received very wide attention. Under such loading, the shear span, a , is subjected to a constant shear force and a linearly varying bending moment (figure 1.1). It has been possible, therefore, to establish expressions for the prediction of diagonal cracking load, ultimate shear compression moment and the critical section. A survey of literature reveals that very little work has been done on T-beams regarding shear failure and the development of any expressions has not been possible.

However, when beams carry uniform loading distributed over the entire span, the shear span is subjected to a linearly varying shear force and a parabolically varying bending moment as shown in figure 1.2. In addition, the compressive zone in the entire length of the beam comes under the action of vertical stresses due to the loading; these stresses increase the strength of the compressive zone because when they act in conjunction with the normal bending stresses, they create a biaxial state of compressive **stress under which concrete is known to exhibit higher strengths (14) 1**

In uniform loading the critical section is not as

1 Numbers in parentheses indicate references in the bibliography•

apparent as in the case of concentrated loading and the analysis is more', difficult. Recent research has, however, resulted in the development of expressions for ultimate shear strength, critical section for diagonal cracking load and the quantity of web reinforcement required for attainment of flexural capacity. Unfortunately some expressions are of limited validity due to lack of sufficient test data to extend the scope of the evidence.

1.2 OBJECTIVES AND SCOPE

This report is concerned with the study of reinforced concrete rectangular beams under uniformly distributed loading. The general objective of this study was to investigate the behaviour of beams under uniform loading and the transition between shear and flexural failures. The main considerations were:

- (1) Observation of the development of cracks.

The propagation of the flexural cracks into diagonal cracks and the formation of any web-shear cracks were studied. Particular attention was given to the major diagonal crack especially its intersection point with the extreme tensile concrete fibre.

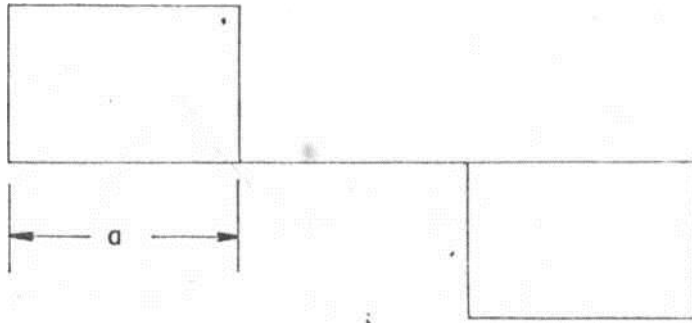
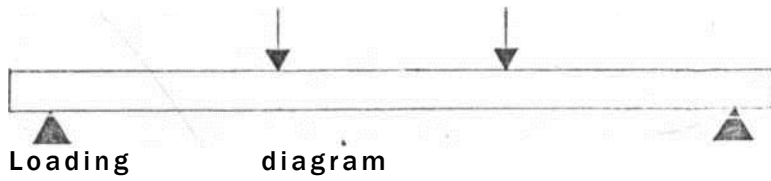
The distances from the support to the intersection point were determined and related to I/d_i ratios.

- (2) Determination of concrete strains during progressive load application. The concrete strain distribution with relation to the applied load was investigated.
- (3) Determination of the diagonal cracking and the ultimate loads.
- (it-) Investigation of the amount of web reinforcement required for

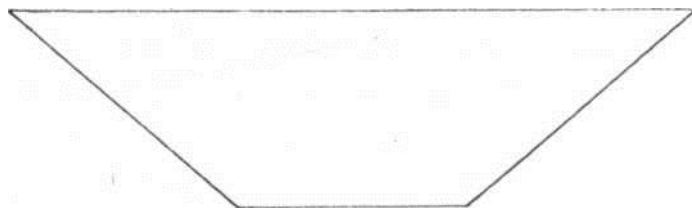
the achievement of flexural capacity. This formed the main part of the study and empirical equations were established.

- (5) Investigation of the influence of the web reinforcement on rotation capacity.
- (6) Contribution of web reinforcement.

For this study twelve beams were tested. All were of similar cross-section and were divided into three groups of L/d ratios 6, 8 and 10. The amount of web reinforcement varied so that some beams failed in shear and the others in flexure.

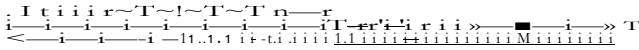


Shear force diagram



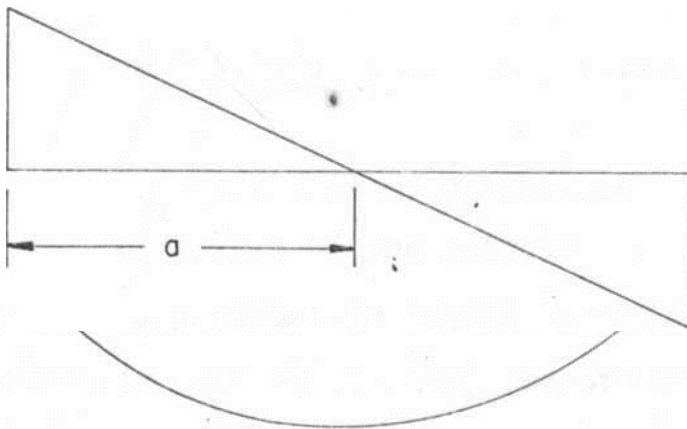
Bending moment diagram

FIGURE I . I : Shear force and bending moment diagrams for simply supported beam under two concentrated loads.



A : ----- I

Loading diagram



Shear force diagram

Bending moment diagram

FIGURE 1.2; Shear force and bending moment diagrams for simply supported beam under uniformly distributed loading.

CHAPTER 2

LITERATURE REVIEW

The first published theory regarding web reinforcement was due to Ritter (1) who suggested in 1899 that vertical stirrups, which are stressed in tension, may be designed by means of equation 2.1

$$Q = A_w f_w l_a \dots\dots\dots (2.1)$$

S

where Q = total shear resistance
 A_w = area of one stirrup f_w = allowable tensile
 stress in stirrups l_a = lever arm
 S « horizontal spacing of stirrups.

This was the concept of "truss analogy" which forms the basis of present day recommendations of design codes (3). According to this analogy, the concrete is assumed to act as diagonal members resisting compression only while the shear reinforcement acts as tension members. Since the dowel action of the longitudinal reinforcement and the compression zone of concrete do resist shear, the codes' stipulation that the whole shear force must be resisted by shear reinforcement only is conservative. As a result of the experimental and theoretical investigations that have been carried out for many years, many empirical expressions have been developed, but none of them is of general application.

The work of Watstein and Mathey (8) refuted the validity of the usual assumptions that longitudinal reinforcement does not transfer vertical shear across a diagonal tension crack and that the maximum compressive strain within the shear span is developed at the extreme fibre. After carrying out extensive strain measurements in steel and concrete, they concluded that after the development of a diagonal crack, sections which were initially plane did not remain plane and the maximum compressive strains in the concrete occurred some distance below the

i

extreme fibre. The longitudinal reinforcement was found to carry considerable vertical shear across a crack, but this force decreased rapidly as the load approached maximum. The contribution of the longitudinal reinforcement in resisting vertical shear is in agreement with the information reported by Hognestand (1) who referred to some 170 documents published between 1897 and 1951.

In order to find an equation for the shear cracking load and the ultimate shear-compression moment, Smith (9) analysed results of 250 tests of simple beams under concentrated loading performed by previous research workers; the range of shear span/ effective depth ratio was from 1.52 to 1.5. As a result of the analysis, he modified Laupa's equation

(2.2) and presented it in the form of equations 2.3 and **2,k**

$$V M,^2 \quad (2.3)$$

$$(\sqrt{p - 0.17p}) d | a$$

$$f_t^{\text{SC}} \sqrt{bd}^2 \quad (>nr - 0.17p) \quad \dots (2.4)$$

where $p = 100r$

Smith reported that the function $(\sqrt{p - 0.17p})$ had a satisfactory correlation with Laupa's equation.

Concerning the regions already cracked in flexure, Smith (9) discussed the implications of Paduart's work and concluded that the transition point from diagonal tension to shear-compression failures at $a/d, j = 2.4$ actually refers to an initiation of diagonal cracking at a section where $M/Qd = 1.2$.

Ramakrishnan (11) tested 110 beams designed to fail in shear subjected to one or two point loads. After analysis of the results, it was concluded that a fully mathematical and rational solution was not possible in the case of beams subjected to combined bending and shear unless a number of assumptions, which may not be strictly true, were made.

As a result of his more recent work on shear Regan (12) reported that shear cracks can be of two types

- (a) the more common cracks forming in regions already cracked in flexure (flexural-shear cracks) and

- (b) the cracks forming in previously uncracked regions (web-shear cracks).

Regarding web-shear cracks, Regan did not give any test evidence to support his suggestion; nevertheless the concept is similar to "shear-proper", a term used by Laupa (t-) to denote the mode of failure of beams whose shear/moment ratio was too large for the criterion of shear-compression to be valid. Regan presented an equation for the total shearing resistance of the form

where V_u = ultimate shear force

$$V_u = 0.30 \frac{100 A_{st}}{bd_1} u \}^{0.4} bd_1 \gamma^{bc} \dots (2.5)$$

G = projected length of a shear crack in the direction of the span.

Regan reported that numerous tests had shown that the lengths of cracks critical for shearing can be taken as

$$c = 1.5d$$

where d' is the depth to centre of lowest longitudinal bars when stirrups are used; that is if the main bars are at one level, $d' = d - j$. Equation 2.5 is subjected to special detailing qualifications whereby shear reinforcement crossing a shear crack can be assumed to yield prior to failure at that crack. Under such detailing qualifications, the shear forces carried by vertical stirrups can be calculated by the term r^{bc} of equation 2.5.

While the problem of shear failure regarding beams subjected to concentrated loading has received much attention, investigations of shear failure of beams subjected to uniform loading seems to have been neglected. Consequently there is little published literature and test evidence in this field.

Whitney (13) analysed the test results reported by Morrow and Viest and found that the shear strength is not a simple function of concrete strength, but depends largely on the amount of flexural reinforcement and its efficiency. Assuming a uniform ultimate moment, M_u , from end to end of the beam, Whitney proposed the following equation for the ultimate shear strength

$$V_u = \left(50 + 0.26 \frac{M_u}{l} \right) b d \quad (2.6)$$

where

$a = k l$

= shear span expressed as a variable

with l equal to half the span of the beam and k varying with the beam span.

Whitney showed analytically that the critical section for uniformly loaded beams without web reinforcement was between six-and seven-tenths of the distance from the centre to support.

This showed good agreement with the results of tests of a further 18 uniformly loaded beams without shear reinforcement reported by Bemaert and Siess. In addition the value of shear at first diagonal tension cracking showed good agreement with the following

$$q_{cr} = 70 + 0.54 \frac{M_u}{d^2} \sqrt{\frac{d}{l}}$$

equation derived
from the test
results of the 18

beams

(2.7).

Another theory was proposed by Ojha (14) when he reported an iterative method of calculating the failure load of uniformly loaded reinforced concrete rectangular beams without shear reinforcement. The development of the equations for uniformly loaded beams was based under one or two point loads. Using "distortion energy" principle, Ojha was able to predict mathematically the section of failure. The critical section was found to lie at a distance equal to from 1.45 to 2.25 times the effective depth of the beam measured from the support. The theoretical approach was tried out with test results of 27 beams, but it did not show good agreement for beams with high l/d ratios.

In 1970 Smith (10) discussed Som's equation for diagonal cracking load for beams under point loads without web reinforcement with $a/d = 2.4$ and concluded that the equation may be used for any system of loading if applied at sections for which $M/Qd = 1.2$. Smith further established equations for the critical section for shear-compression moment and the quantity of web reinforcement required to prevent the beam to fail below flexural capacity and to sustain sufficient rotation.

The predictions of diagonal cracking load and the estimation of the quantity of web reinforcement were supported by test evidence of eleven beams with varying spans and the amount of web reinforcement and under simulated uniform loading. Furthermore there was a close agreement between the requirements of AGI Building Code and the optimum ratios of web reinforcement deduced from the tests for the achievement of full flexural capacity. Nevertheless the evidence was based upon few tests results with L/d varying between 12 and 18 and Smith recommended

I

*

that further tests are required to extend the scope of evidence, particularly with regard to the effects of low L/d ratios.

The author's investigation, therefore, is in line with Smith's recommendation and a full critical derivation of his method of analysis is given in the analysis chapter of this report.

CHAPTER 3

GENERAL BEHAVIOUR OF REINFORCED

CONCRETE BEAMS

In order to understand the mechanism of shear failure and the factors that influence it, it is necessary to investigate the behaviour of reinforced concrete beams in both elastic and plastic stages. It is only with the knowledge of shear failure mechanism that methods to design beams to resist shear and attain their flexural capacity can be developed. '

3.1 FLEXURAL CRACKS

In the initial stages of loading a beam, and before any cracks appear, the beam shows an elastic behaviour and the load-deflection relationship is linear. When the load is increased, flexural cracks begin to form at the tensile face of the beam and then extend upwards some going above the tensile steel level. Some of the cracks are very small indeed and can be clearly seen only with a magnifying lens. Further increase of load results in additional flexural cracks and increase in width and vertical extension of the already formed cracks.

At low loads when the beam is uncracked or cracked in flexure only, the action of the web reinforcement does not come into play and therefore, in effect, beams with and without web reinforcement

resist shearing force in a similar manner; the total shearing force is resisted by the compression zone of the concrete, the dowel action of the longitudinal reinforcement and the force due to aggregate interlock along the cracks (12).

3.2 DIAGONAL (SHEAR) CRACKS

Diagonal tension cracks or shear cracks can be divided into two types according to the origin of their formation.

3.2.1 Flexure-Shear Cracks. These cracks develop in regions of high shear within the shear span. As the load is increased, some of the already formed flexural cracks bend away from the support to become diagonal tension cracks. With further load increase, the shear cracks extend diagonally upwards and downwards and flatten as they approach the top surface of the beam and at the level of the

longitudinal tensile reinforcement. The development of a flexural crack to a diagonal tension crack is illustrated in figure 3.1.

3.2.2 Web-Shear Cracks. The web-shear cracks are rare. They occur in regions of high shear and relatively low bending stress as for example in the webs of I-sections near a single support. In rectangular sections they occur very near the support within the shear span as shown in figure 3.2.

Web-shear cracks do not occur if there are flexural cracks available to be converted into diagonal cracks.

Even though shearing stress τ in figure 3.3 is often regarded as the primary cause of shear failure, a beam cannot be subjected to pure shear without bending moment. A direct bending stress σ is always present so that its combination with the shearing stress produce diagonal tensile stress which frequently causes the initial shear cracking

(13,16). This principal stress therefore is the

cause of shear cracks and ultimately shear failure. The diagonal crack that makes the beam collapse is termed the major or critical diagonal crack. It is usually the longest and widest crack. Recent research has led to the development of expressions for locating the starting point of diagonal crack, the failure section and the inclination of the critical diagonal crack (10, 11.).

3.3 BEHAVIOUR AFTER SHEAR CRACKING-

The diagonal tension cracks extend upwards and thereby reduce the depth of the compression zone.

The diagonally cracked concrete cannot resist any of the transverse shear force and, therefore, if the beam is able to sustain further increases in load, a redistribution of the internal stresses takes place. It is only after the formation of the diagonal crack that web reinforcement carry load; consequently after

this stage, beams with and without stirrups behave differently,

5.3.1 Behaviour of Beams Without Stirrups. A free-body diagram of the cracked section of a beam without web reinforcement before and after redistribution of the internal forces is shown in figures 3.4(a) and 3.4(b) respectively.

The diagonal cracked concrete does not resist any of the shearing force Q . Considering figure 3.4(a), for vertical equilibrium,

$$Q + T_2 \sin \alpha = C_1 \cos \alpha \quad (3.2a)$$

for horizontal equilibrium,

$$T_2 \cos \alpha = C_1 \sin \alpha \quad (3.2a)$$

and taking moments

about 0,

$$Qx_1 = T_2 l_a + d_2 (x_1 - x_2) \quad (3.3a)$$

where

d_2 = shear transferred by dowel

action at section 2 T_2 = main steel

tension at section 2

At section 1 the resultant forces balance external bending moment, thus

$$M = H^a \quad (3.4)$$

The values of x_1 and x_2 can be obtained from a plot of the crack pattern and C_1 is assumed to act at the middle of the compression zone. T_1 and T_2 are determined from strain measurements.

Upto the formation of the diagonal crack, T_2 has been found to be small compared to $T^{(8)}$. When the load is increased the value of T increases rapidly to a value close to V . By equations 3.3(a) and 3.1, when T_2 approaches the dowel force D_2 approaches zero. When D_2 equals zero, the breakdown or redistribution of forces is said to have taken place and the total shear is carried by the concrete compression zone. This situation is shown in figure 3.4(b) where by statics

$$Q - S_{12} \dots \dots \dots (3.1b)$$

$$T_1 = C_{12} \dots \dots \dots (3.2b)$$

$$S_n \sim V_a \dots \dots \dots$$

In beams without stirrups T_2 is likely to increase with excessive extension of the steel. If this happens, the diagonal tension crack penetrates high into the compression zone and finally shears through the rest of the beam depth. This causes true diagonal tension failure which is a common feature of tests of beams without web reinforcement.

3.3.2 Behaviour of Beams With Stirrups. Figures 3.5(a) and 3.5(h) illustrate the free-body diagrams of the cracked section of a beam with web reinforcement before and after the redistribution of forces respectively. After the formation of the shear crack and before the redistribution of the internal forces, the total shearing force is resisted by the dowel action of the main steel, the compression zone of concrete and the stirrups crossed by the crack, considering figure 3.5(a), for vertical equilibrium,

$$Q - S_{12} + \sum_{i=1}^n D_2 \dots \dots \dots (3.5a)$$

for horizontal equilibrium,

$$T_2 = C_{12} \dots \dots \dots (3.6a)$$

and taking moments about 0,

$$Q_{xi} = \frac{Q_w a^2}{x_1^2} + \sum_{i=1}^n \frac{Q_{wi} a_i^2}{x_2^2} \quad (3.7a)$$

As in the case of beams without stirrups, at section 1 the resultant forces balance the external bending moment thus

$$Q_w a^2 = \sum_{i=1}^n Q_{wi} a_i^2 \dots\dots\dots$$

where n is the number of stirrups crossed by the diagonal crack. The values of x-j, x2 and a^ can be obtained from a plot of the crack pattern. ^ and

Qw are determined from strain measurements.

As the load is increased, the same sequence of transfer of forces takes place as in beams without web reinforcement except that after the breakdown of the dowel force, the total shear force is resisted by the compression zone of concrete together with the stirrups crossed by the shear crack as shown in figure 3.5*Ob).

By statics,

(3.5b)

$$\langle 3 = \sum_{i=1}^n 2^5 x_i Q_i \rangle$$

(3.6b)

$$Q_i = T_i l_a + \sum_{i=1}^n Q_{wi} a_i$$

(3.7b)

In addition to carrying a part of the shear force, the web reinforcement increases the ability of the concrete compression zone and the longitudinal reinforcement to resist shear by limiting the growth of the diagonal cracks and checking their penetration into the compression zone, and by preventing the dowel force from splitting the concrete along the longitudinal steel level. Thus in effect, shear reinforcement prevents sudden failure so that collapse occurs only after substantial deflection (6).

In the absence of shear reinforcement, the diagonal tension cracks result in a separation of the 'blocks' on both sides of each crack. When shear reinforcement is provided, connection of the 'blocks' will resist the dislocation tendency of the member. It is this dislocation concept that Ojha (li.) in 1967 referred to as shear rotation in his consideration of the shear strength of rectangular reinforced concrete beams using 'distortion energy' principle.

The conclusion arrived at by Watstein and Mathey (8) that maximum compressive strains occur some distance below the extreme fibre can be explained by figures 3.4'0>) and 3.5(b).

After the breakdown of the dowel force the compressive thrust becomes more inclined to section 1 and acts as an eccentric force on the concrete above the diagonal crack. This produces a reversal of strain and, in general, the strains at the extreme fibre of the compressive zone decrease rapidly and in some cases tensile strains may occur at this surface.

3 ~~X~~ COMPATIBILITY CONDITIONS

After the formation of shear cracks, sections which had previously been plane no longer remain plane.

%

Consequently the normal flexural elastic neutral axis depth is invalid for sections crossed by shear cracks and must be replaced by one in terms of integrated deformations. The neutral axis depth used by many previous investigators is not generally equal to the ultimate flexural neutral axis depth because in most shear failures the main steel does not yield at failure. The compatibility condition can be expressed in two forms.

3.U.1 Regan's Approach (17).

If section 1-1 in figure 3.6 undergoes negligible or no deformation during loading and section 2-2 is a plane section that remains plane during loading, the neutral axis depth at section 2-2 is given by the equation

$$\frac{\epsilon_c}{3T} = \frac{\epsilon_s}{\lambda} \quad (3.9)$$

where A_{cc} = total shortening of the extreme compressed fibre
between sections 1-1 and 2-2.

Δs_t = corresponding lengthening of the main steel
between section 1-1 and
2-2.

n = neutral axis depth factor.

~~3.2~~ Walther's Approach (17). in this approach the total deformation in the region of a shear crack is considered to consist of a rotation about the head of the shear crack and a deformation of the web. this deformation increases the width of the shear crack in the middle of the web relative to its width at the level of the steel (figure 3.7). Combining the two types of deformation, the neutral axis depth factor

is expressed by equation 3.10.

where

$$\frac{A_{cc} \Delta s_t}{A_{st}} = k_q \frac{n}{1-n} \sin \theta \quad (3.10)$$

Δs_t = deformation of main steel

k_q = width of shear crack at steel level. θ =

angle between the shear crack and

the direction of the member k_q = coefficient

greater than or equal to unity

= Δs_t " Δs_{cr}

r

3.5 MODES OF FAILURE

There are normally three recognised types of failure of reinforcement concrete beams namely:-

- (a) Bond and anchorage failure
- (b) Flexural failure
- (c) Shear failure.

It is necessary to be able to differentiate between the above different types in order to know which type of failure a beam undergoes.

3.5.1 Bond and Anchorage Failures. In reinforced

concrete, bond and anchorage failure is due to poor bond characteristics of steel and concrete. This type of failure is prevented by providing an extra length of the main reinforcement such that the average bond stress does not exceed the permissible bond stress stipulated in the modern codes of practice. A.C.I - A.S.C.E. Committee 326(17) recommends that the main steel should be extended beyond its permissible cut-off point according to flexural theory by a distance equal to the effective depth. The equivalent additional length may also be provided by means of hooks or other types of anchorages.

1.5.2 Flexural Failures. When a concrete beam is over-reinforced and is adequately reinforced against

shear, it fails by the crushing of concrete or splitting of the concrete over the vertical cracks caused by bending stress in the compression zone. However, if the beam is under-reinforced, and cannot fail in shear, it fails by the yielding, or very rarely, breaking of the longitudinal reinforcement caused by tensile bending stress.

3.3.3 Shear Failures. Shear failures are preceded and caused by the

diagonal tension cracks which may start as flexural cracks or as pure web-shear cracks. The criterion of shear failure has been the cause of a controversial issue among investigators over the years -whether it occurs at some limiting value of shear force or bending moment. It has now been established that for any given combination of moment and shear, there will be a mode of failure which is critical. Whereas beams with a high $M/Qd-j$ ratio fail in flexure, beams with low $M/Qd-j$ ratio fail in shear. In between it is a combination of flexure failure and shear failure which divides into two types-shear-compression failure and diagonal tension failure.

Shear-compression failure. As the load is

increased the diagonal tension crack penetrates the compression zone of concrete. After the breakdown of the dowel force, the neutral axis rises and the external load is supported by an inclined, arch-like, thrust that gives great intensity of compression above the diagonal tension crack. The horizontal component of the thrust at the support is resisted

by the tension steel acting as a tie as shown in figures 3A(b) and 3.3(b). If the geometry of the crack and the loading configuration are such that stability of the arch action is achieved, collapse of the beam is caused by failure of concrete at the crown of the arch (section 1-1). This is the type of failure which led earlier investigators such as Zwoyer and Siess (3), Moody and Viest (6) and Jones

(7) to develop a new analysis of shear failure known as shear-compression theory. Shear-compression failure is more common to beams with short shear spans and the collapse load is often several times the initial diagonal cracking load. The ultimate load for

shear-compression failure is given by the

equation

$$C^a = k_1 k_3 f_c' b k d_1 (d_i - k_2 k d_1) \dots (3.11)$$

where

M_{sc} Shear compression moment ultimate shear force

$\frac{Q_u}{a}$ = shear span

= average longitudinal compressive stress

in the compressive zone at failure

$k d_j$

= depth of compressive zone at failure

$k_2 k d_1$

= depth to centre of compressive zone at failure.

= breadth of section.

The coefficients k^a and k_2 are Hognestad's (2) stress

block factors

$$k-jk.^{\wedge} = 26.9 + 0.35f_c'$$

$$22.1 + f_c'$$

$$k_2 - 0.5 - f_c'$$

55?

Coefficient f_c is neutral axis depth/effective depth ratio, indicating position of neutral axis at failure.

(b) Diagonal tension failure. The critical diagonal tension crack extends rapidly beyond the neutral axis and backwards by a tearing action at the main steel

%

level. When the crack extends through the compressive zone the load carrying capacity is reduced. After the breakdown of the dowel force, the beam becomes unstable and almost with no further load increase it splits into two and collapses immediately, i.e. the collapse load is close to the initial shear cracking load. Diagonal tension failure is common to beams without web reinforcement.

3.6 LOAD - DEFLECTION RELATIONSHIP

If the load-deflection relationship is known, it is possible to study the behaviour of the beam at working loads and to estimate the limit of safe working loads. Since the deflection is different for bending and for shear failures, the load-deflection relationship would give a guide in distinguishing between flexural and shear failures.

Whereas in flexural failure the deflection is solely due to bending, in shear failure the total deflection is the sum of the deflection due to bending and the deflection contributed by the opening up of the diagonal tension cracks. This is evidenced by taking deflection readings on the top and bottom surfaces of the beam. In some instances, the bottom surface deflections are found to be twice the top surface deflections.

A study of the moment-rotation relationship indicates that reinforced concrete is truly plastic in the steel-yield bending failure for low percentages of main steel. However, whereas shear-compression failure reduces the ductility of reinforced concrete, diagonal tension failure may prevent it altogether (figure 3.8).

At low moments beams with and without web reinforcement behave in the same manner and therefore the slopes of curves in figure 3.8 for the different modes of failure remain the same until diagonal cracking when stirrups become effective.

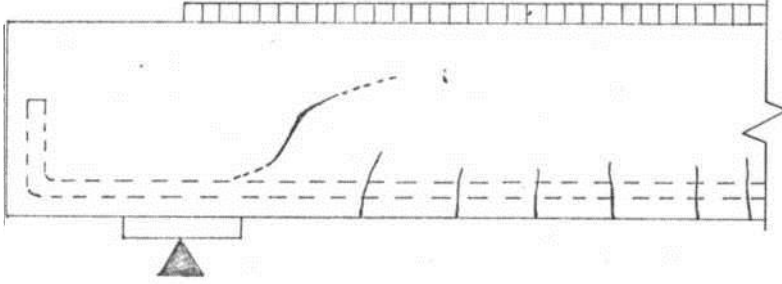


FIGURE 3.2: Formation of web-shear cracks. to a diagonal tension crack.

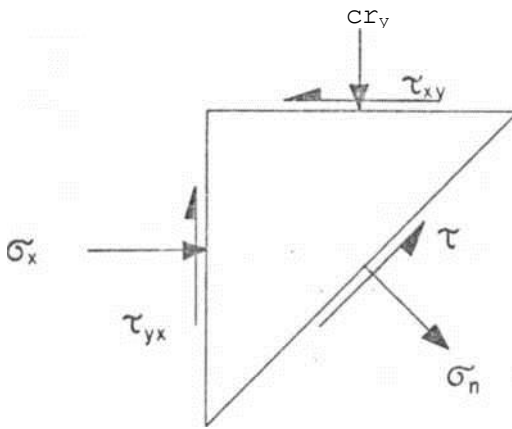
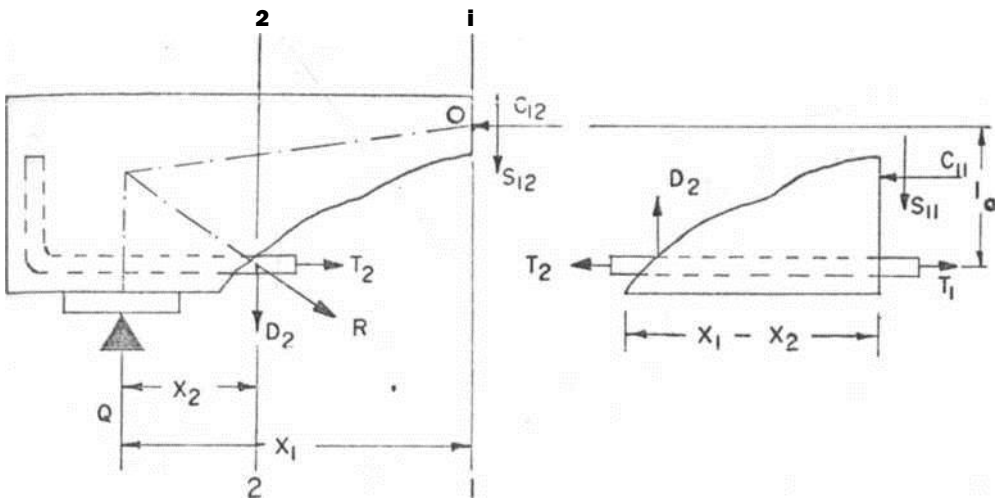
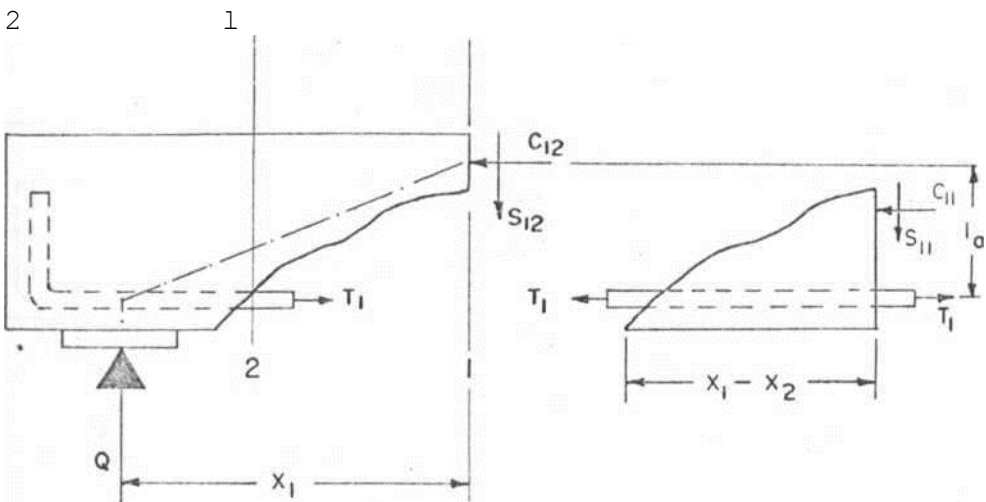


FIGURE 3.3! Stresses acting pn a
finite element.



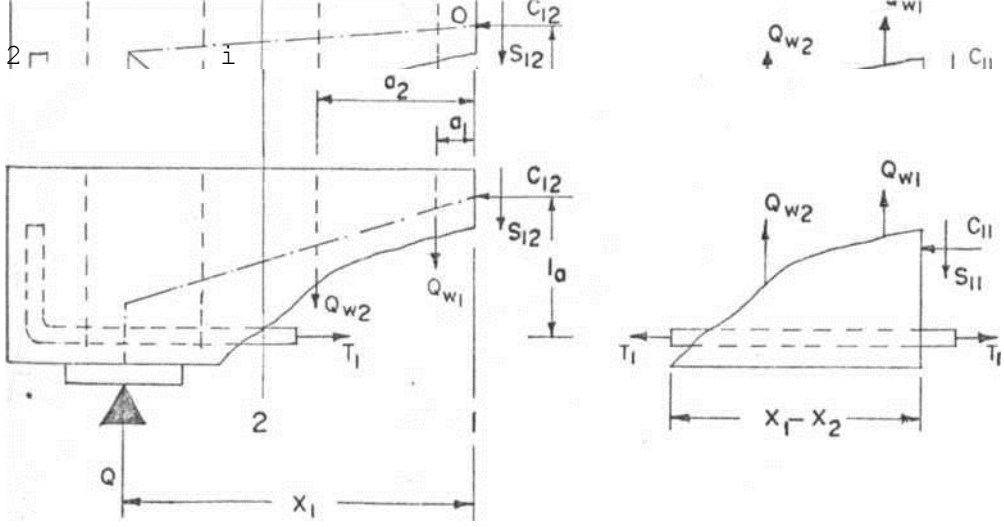
(a) Before redistribution



(b) After redistribution

FIGURE 3.41 Free-body diagram without

web reinforcement.



7

(a) Before redistribution

(b) After redistribution

FIGURE 3.5! Free-body diagram with

web reinforcement.

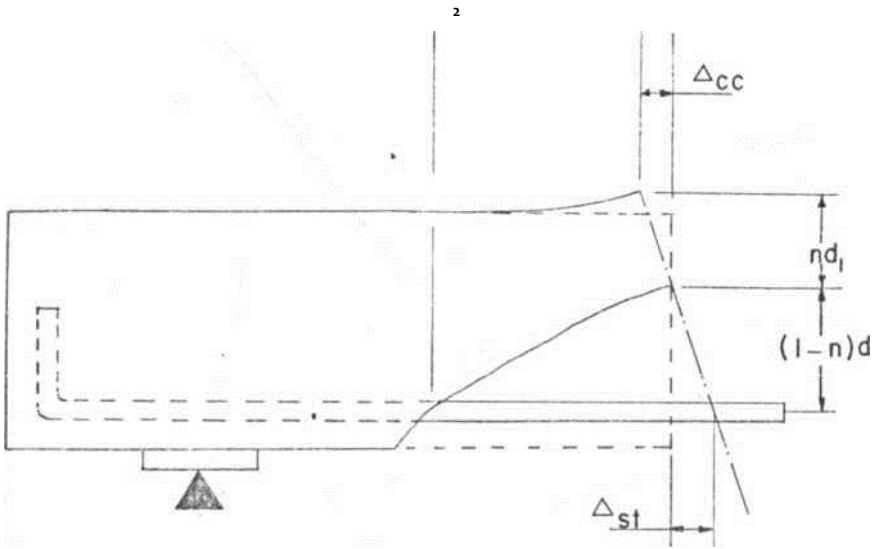
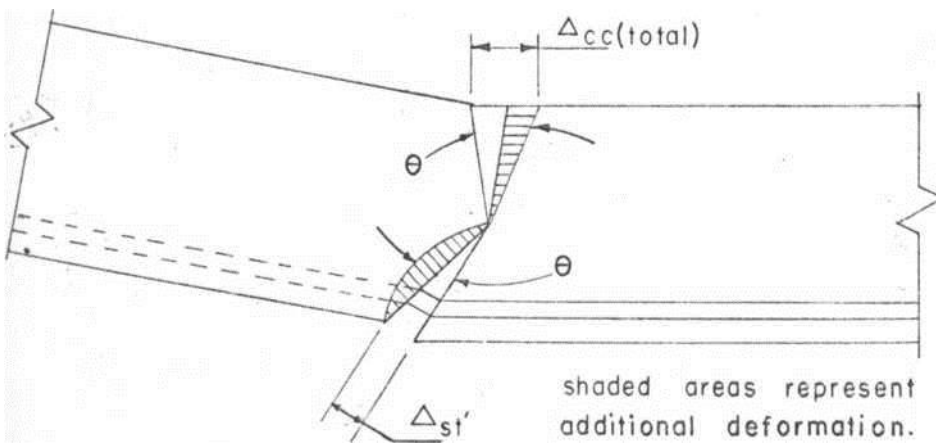


FIGURE 3.6*. Deformation conditions according to Regan.



.. FIGURE 3.71 Deformation conditions

according to Walther.

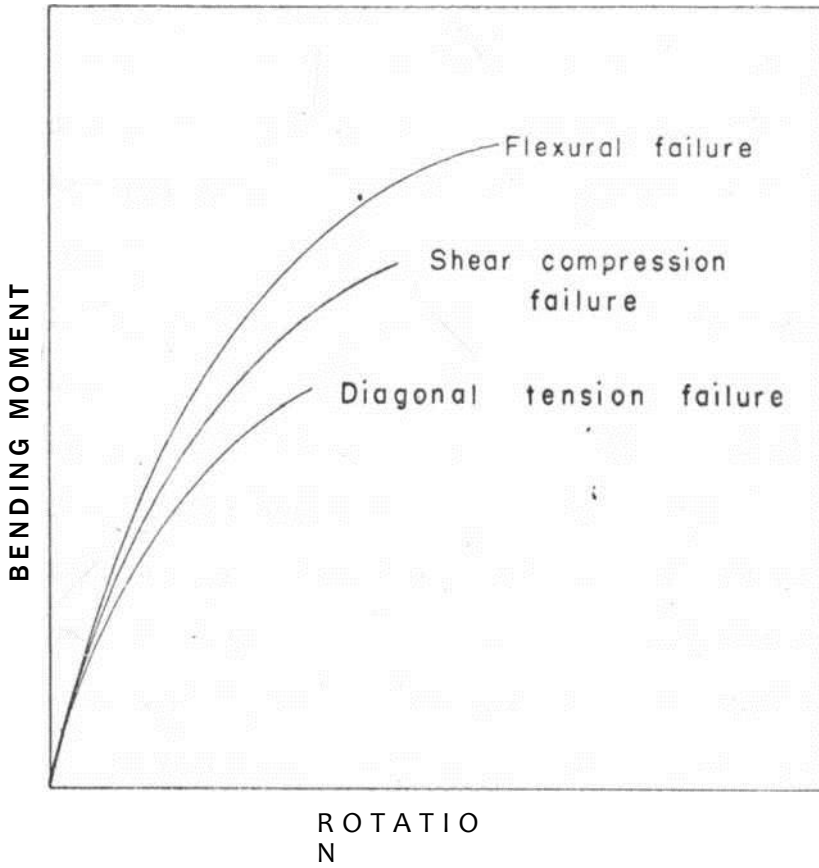


FIGURE 3.8'. Bending moment-rotation relationship.

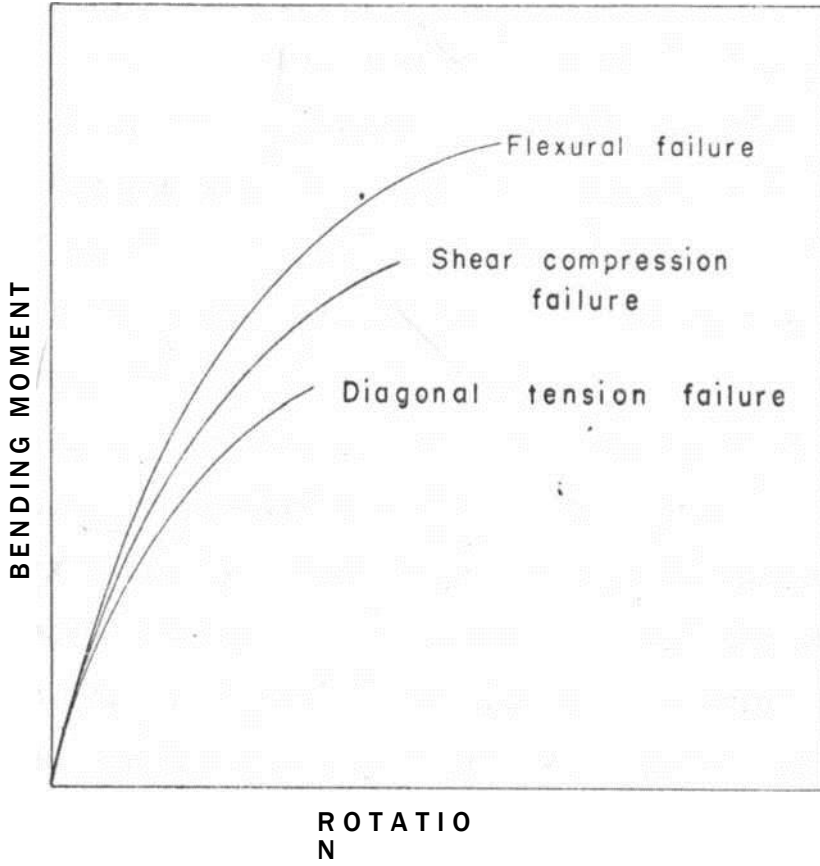


FIGURE 3.8'. Bending moment-rotation relationship.



CHAPTER *U*

EXPERIMENTAL WORK

1.1 TEST SPECIMENTS

Twelve beams, divided into three groups G1, G2 and G3, were designed to provide information on the shear resistance of web reinforcement, distribution of strain in concrete and the formation of cracks.

All the beams, 230 mm deep and 127 mm wide, were reinforced by three U-.70 mm square high yield cold twisted bars with effective depth d_e of 200 mm. The three groups had overall lengths of 1.7,

2.1 and 2.5m

respectively. Figures A1, A2 and A3 in appendix A show, the physical properties of all the beams. Three beams, one of each span, had no web reinforcement.

The remainder had vertical stirrups of 5.6 mm diameter mild steel rods the spacings of which were varied so that the amount of web reinforcement varied from

0.157% to 0.785%. The stress-strain characteristics for the main steel and for the stirrups are given in figures 4.1 and 4.2. respectively.

The concrete mix 1:X.5 ordinary Portland cement to Athi River Sand and two sizes of aggregate, 9.X and 18.8 mm, water/cement ratio 0.5 was designed to have a 150 mm cube strength, f_{cu} of $X0N/mm^2$ at 28 days. All the beams were cast in a wooden mould. Together with each beam three cubes, three cylinders and three modulus of rupture specimens were made for control purposes.

The compaction was done with an internal vibrator.

The test beam and the control specimens were cured in a curing room until a day before testing.

L.2 TESTING

L.2.1 CONTROL SPECIMENS. The cubes and the modulus of rupture specimens were tested in accordance with B.S.1881:1970(18) to obtain the cube strength u and the modulus of rupture f_t' . The cylinders were not provided with a capping during testing as required by the B.S. specifications and consequently the test values of the cylinder strength f_c' which were all less than $0.75 u$ were disregarded. The average values of u and f_t' for all the beams are given in Table L.1. For calculations, $f_c^* = 0.8u$ and $f_t^* = 0.79 \sqrt{f_c^*}$ were used. The test and calculated values of f_t^* are compared in figure L.3.

L.2.2. LOCATION OF DEMEC DISCS. For the purposes of determining the strain distribution in concrete demec discs were fixed on one face of each beam, symmetrically about the centre line, with "durofix" and allowed to set overnight. All the discs were fixed at a gauge length of 200 mm. By assuming the behaviour at the mid point of the gauge length, was representative of the behaviour of the entire gauge length, figure L.4 shows such positions as the points of strain measurement for half the span.

L.2.3 LOADING ARRANGEMENT. The beams were tested on simple spans of 1.2, 1.6 and 2.0 m under a distributed system of eight point loads applied through steel rollers and contact plates. Such a loading system, which is a good approximation to continuous distributed loading, does not result in non-uniform loading and horizontal shear restraint (10). The beams rested on one steel plate on one side while the other side rested on two steel plates separated by a thinner plate and two layers of grease so that horizontal movement was possible during

load application. Figures 4.5, 4.6 and 4.7 show the loading arrangements for the three groups of beams tested.

4.2.4. DEFLECTION GAUGES. Deflection gauges calibrated in 0.01 mm were fixed on the lower testing machine platten with magnetic stands at mid span and quarter points. Near the failure loads the limits of the smaller gauges at quarter points were exceeded and thereafter only the mid span deflections were taken.

4.2.5 LOAD INCREMENTS. Before loading, the initial strain and deflection readings were noted. The load was then applied in 20 kN increments. After each increment the strain and deflection readings were recorded and the crack formation observed.

4.3. TEST RESULTS

4.3.1 Concrete strengths. The ages of the test

specimens varied from 46 to 50 days. The actual concrete cube strength, u varied from 42.2 to

49.5 N/mm² with an average of 45.8 and a standard

deviation of 2.65 N/mm² for all the beams. The modulus of rupture varied from 4.51 to 5.44 with a

mean of 4.90 N/mm².

4.5.2 Diagonal cracking and ultimate loads. The

diagonal cracking loads obtained from the tests are given in Table 4.1. These are the loads at which the diagonal cracks crossed the neutral axis. This

observation was performed visually and since the head of the diagonal crack was always very small and sometimes invisible to the naked eye, the accurate value of the diagonal cracking load could not be determined. Hence the reported values are only approximate. It is clear from the results in Table 4.1 that the diagonal cracking load is influenced by web reinforcement. For the second and third beams in each group the ratio $W_{cr}(\text{test})/W_{cr}(\text{calc.})$ was higher than for the first beams which had no web reinforcement. In groups G-2 and G-5 the last beams, which had most web reinforcement, the ratio was lower than for the beams without stirrups. These test results further show that the ratio decreased with the increase in span.

4.5.5 Cracks and modes of failure. The crack patterns of all the beams are illustrated in figures 4.8, 4.9 and 4.10. The initial flexural cracks appeared in the regions of high bending moment around the beam mid span.

The load at which the flexural cracks first appeared varied depending

upon the span of the beam.

This load was from 120kN for beams of group G1 to 80kN for beams group G3. With increase in loading the already formed flexural cracks widened and extended upwards. In addition new cracks formed between the existing ones and in uncracked regions. The presence of web reinforcement did not affect widening, extension or the formation of the flexural cracks. Generally no flexural crack was observed to form within a distance equal to the beam depth from the support. This is a characteristic behaviour reported by previous investigators (9). When the applied load was equal to the diagonal cracking value, the flexural cracks in regions of high shear, i.e. nearest the supports, developed into diagonal cracks in some beams. In other beams like G1/2 (right side), G2/2(right side), G2A (left side) and G3A (left side) diagonal cracks originated as web-shear cracks. These cracks first appeared at about the neutral axis level in regions very close to the supports where no flexural cracks had formed. The occurrence of web shear cracks was not acknowledged by many previous investigators and the first mention was perhaps by Laupa A) when he suggested "shear-proper" type of failure.

It is incorrect to assume that all diagonal cracks always begin as flexural cracks.

The origin of diagonal cracks depends upon the relationship of "bending moment and shear. When a section is uncracked in flexure, i.e. a section very near the support, it would be reasonable to neglect the effect of steel altogether. Then the direct stress σ_x and shear stress τ_{xy} distribution are of the form shown in figure 4.11. At such a section the shear to

moment ratio is high and diagonal cracks would commence as web shear cracks in the region of the neutral axis where the shear stress is high. The web shear crack would then propagate both ways with increase in loading. However, if shear to moment ratio is not high flexural cracks may first develop and some of them propagate to diagonal cracks.

The most distinct formation of web shear crack was exhibited by beam G 2/4 (left side). The crack marked 'X' first appeared at about mid depth of the beam at 160KN. With increase in loading, it propagated diagonally both upwards and downwards. The downward propagation was directly towards the support and not the edge of the reaction plate. This is further evidence that web shear cracks occur since at the support there is no bending moment and therefore no flexural cracks. Another unique aspect of G2/4 was the formation ..of the crack marked *Y' at the top surface. This crack appeared at a load of 200 KN and at a load of 220 kN it had extended vertically downwards below the neutral axis.

After the formation of the diagonal cracks, the propagation of the flexural cracks was either terminated in the region of the neutral axis or was very gradual. With further increase in loading the diagonal cracks extended upwards and also downwards in the case of web shear cracks. This extension was accompanied by increase in width. Further development of the cracks depended upon the span and amount of web reinforcement.

All the beams without web reinforcement failed in shear. Beam G3/1 failed in shear-compression after the diagonal crack had extended to the extreme fibre of the compression block. The two major diagonal cracks had also split back at the main steel level as seen in figure 4.10(a). Beams G1/1 and G2/1 failed in diagonal tension. After its formation, the diagonal crack extended gradually until at loads approaching the failure value, the propagation to the top fibre and the accompanying widening were very rapid producing an unstable state that caused sudden collapse. In G1/1 the major diagonal crack formed at 240kN but failure did not occur until the load was 300kN. The collapse moment was lower than the calculated flexural capacity ($M_u/M_f = 0.913$). In beam G2/1 the major diagonal crack appeared at 120kN and collapse occurred at 148kN. As in beam G1/1, the failure moment for G2/1 was lower than the calculated flexural capacity ($M_u/M_f = 0.620$).

In beams G2/2, G3/2 and G3/3, the flexural

cracking was more pronounced than in the beams without web reinforcement and the major diagonal crack was accompanied by many minor shear cracks.

These beams failed by shear-compression.

In beams G1/2, G2/3 and QJ/A, after the major diagonal cracks had penetrated far into the compression zone, the flexural cracks around the mid span extended rapidly upwards and caused the beams to fail by combined bending and

shear with concrete spalling at the top(figures 4.8(b), 4.9(c) and 4.10(d)).

%

Although the remaining beams cracked extensively in shear, the development of the flexural cracks around the mid span did not terminate as in the other beams falling in shear, and ultimately the beams failed in flexure 4.8(c & d) and 4.9(d)).

Some photographs taken during the experimental stage are presented in plates B1-B23 in appendix B.

4.3.4 STRAINS. Extensive concrete strain measurements were made with a demountable mechanical strain gauge

with a calibration factor of 1 division = 0.882×10

-5

All the strain measurements are given in Tables C1 to C12 in appendix C. For handy reference

the maximum compressive and tensile strains recorded are presented in Table 4.3.

The variations of concrete strains with the applied load are illustrated in figures 4.12 to 4.23.

It was not possible to fix demec discs at the extreme fibres due to unevenness of the edges and therefore the furthest strains were measured at 10mm from the top and bottom surfaces. From the strain distributions it can be deduced that

(a) With regard to span, the trend was that as the span increased corresponding strains decreased.

(b) In all the beams tested, at the sections nearest to the supports the compressive strains first increased with increasing

%

load and then decreased still with increasing load. In most cases these strains changed to tensile after the formation

of the diagonal crack.

- (c) Considering web reinforcement, the concrete strains had no direct relationship and no deduction could be made.

TABLE 4.1 - TEST RESULTS

BEAM No.	CONC ^{ET} gT ^{ENGTH}				DIAGONAL LOAD (kN)	CRACKING	$\lambda_{cr}(\text{test})$
	u	$f_c' = 0.8u$	$f_t' = 0.79HV$	$f_t(\text{test})$			
G1/1	48*0	58.4	4.90	4.62	104.5	160	1.55
G1/2	47.5	58.0	4.86	5.15	104.0	170	1.63
G1/3	48.0	58.4	4.90	4.48	105.0	180	1.71
G1/4	44.0	55.2	4.70	4.51	100.0	170	1.70
G2/1	45.8	55.0	4.67	4.90	90.2	150	1.66
G2/2	49.5	59.5	4.96	5.40	96.5	180	1.87
G2/3	42.2	55.8	4.59	4.57	96.6	180	1.87
G2/4	45.4	34.6	4.65	4.76	90.4	120	1.55
G3/1	45.5	54.5	4.65	5.02	86.0	115	1.54
G3/2	42.4	55.8	4.59	5.44	84.6	120	1.42
G3/3	49.2	59.5	4.96	5.17	92.0	150	1.42
G3/4	48.0	58.4	4.90	4.98	90.5	120	1.55

TABLE. 4.2 - TEST RESULTS

BEAM Ho.	ULTIMATE LOAD (KN)	ULTIMATE MOMENT (kNm)	FLEXURAL CAPACITY (KNm)	to	MODE OF * FAILURE	LEVER ARM
	Wu	Mu	Mr			mm
G1/1	300	43.0	19.2	0.915	DT	115
G1/2	425	63.7	49.0	1.30	SC-F	206
G1/3	UO	66*0	19.2	1.34	F	213
OlA	396	59.5	17.8	1.24	F	191
G2/1	118	29.6	17.7	0.620	DT	97
G2/2	218	19.6	19.8	0.995	SC	139
G2/3	257	31.4	47.2	1.090	SC-F	169
G2A	238	17.7	17.6	1.00	F	157
G3/1	128	32.0	17.1	0.672	SC	103
G3/2	180	15.0	47.2	0.951	SC	118
G3/3	183	15.8	19.8	0.920	SC	117
G3A	207	51.8	49.2	1.030	SC-F	167

*

W - Diagonal tension failure SC - Shear-compression failure ^ * Flexural failure

SC-F-Combined shear-compression and flexural failure*

TABLE if>3: MAXIMUM CONCRETE STRAINS

BEAM No.	CONCRETE STRAINS × 10 ⁻⁵					
	SECTION A		SECTION B		SECTION C	
G1/1	* -202	*** +165	- 31	+302,	- 18	+ 197
61/2	-U7	+82,6	- U8	+375	- 8	+ 12,1
61/5	-L00	+880	-158	+396	- 30	+ 187
G1A	-37A .	+860	- 70	+330	- 10	+ 128
G2/1	-103	+163	- 70	+ 93	- 15	+ 13
G2/2	-106	+L17	-260	+555	- 10	+ 187
G2/3	-306	+292	-22,0	+232	- 25	+ 2,1
G2A	-UQ6	+U2	-279	+380	- 12	+ 111
G3/1	- 91	+138	- 11	+ 23		
G3/2	-220	+126	- 16	+123		
G3/3	-112	+210	- 4	+ 39		
G3A	-193	+350	- 12	+12,0		

* - ve - Compressive ** * ve - tensile

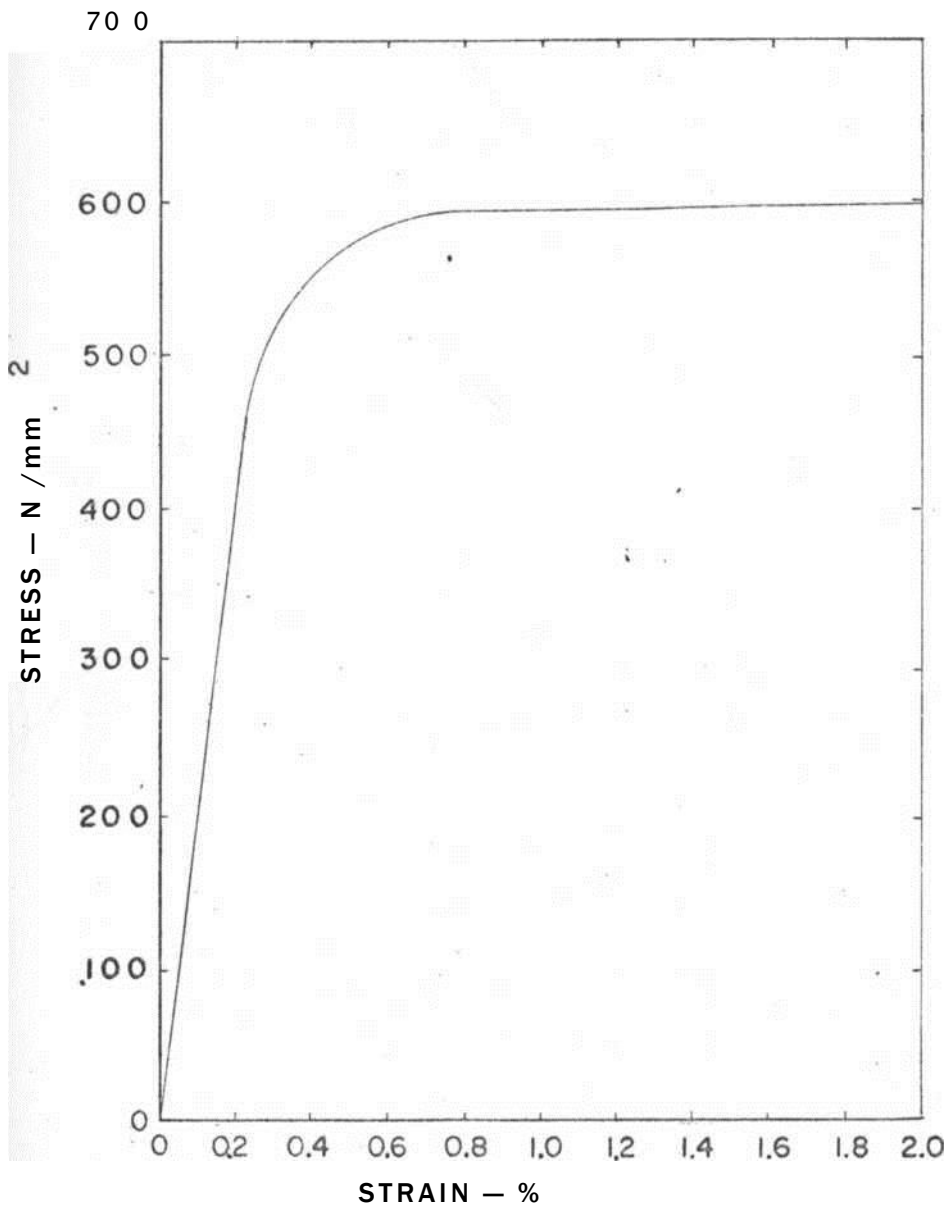


FIGURE 4-1 . * Stress-strain characteristics for the 14-70 mm square high tensile twisted bars used for the main reinforcement.

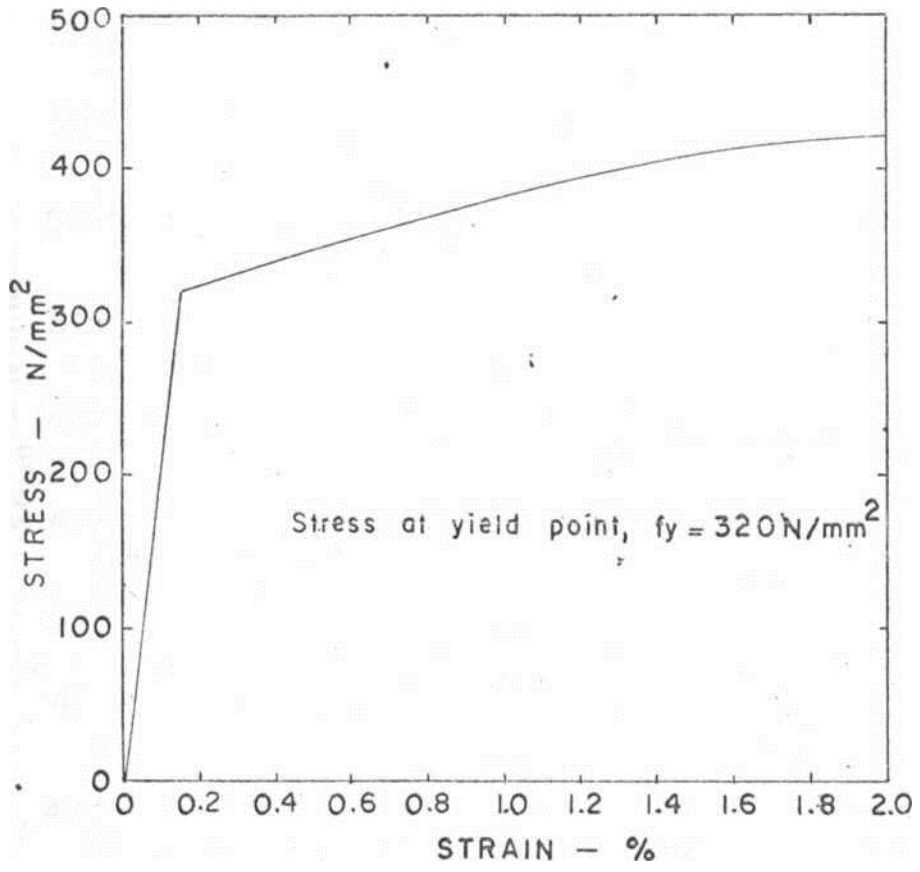


FIGURE 4-2'. Stress strain characteristics for the 5-64mm diameter mild steel rods used for the stirrups.

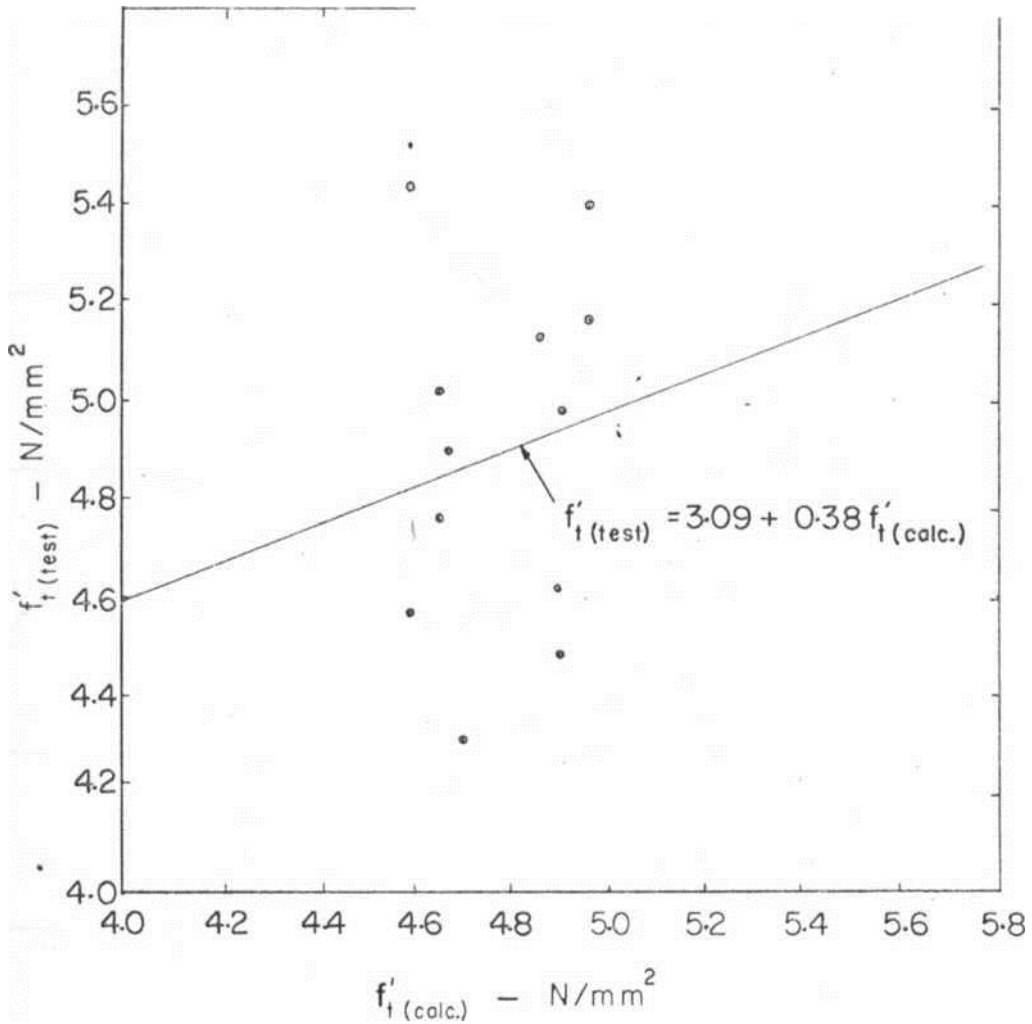
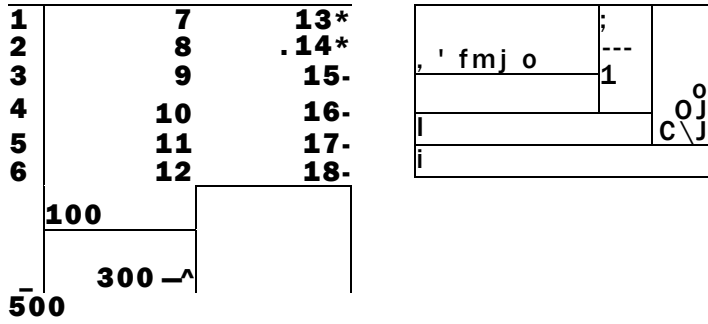
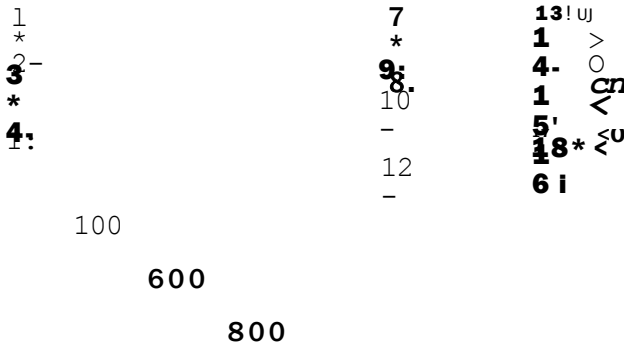


FIGURE 4-3! Comparison of test and calculated values of modulus of rupture.

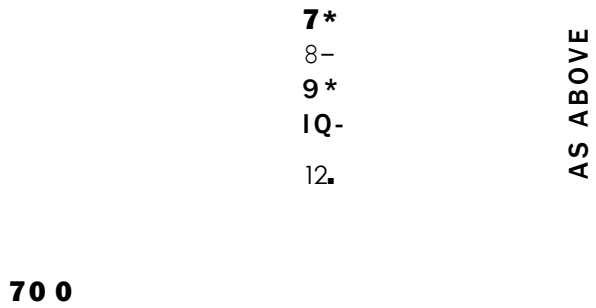
GROUP G1



GROUP G2



GROUP G 3



ALL DIMENSIONS IN mm.

FIGURE 4.4! Location of mid points of gauge lengths for strain measurement.

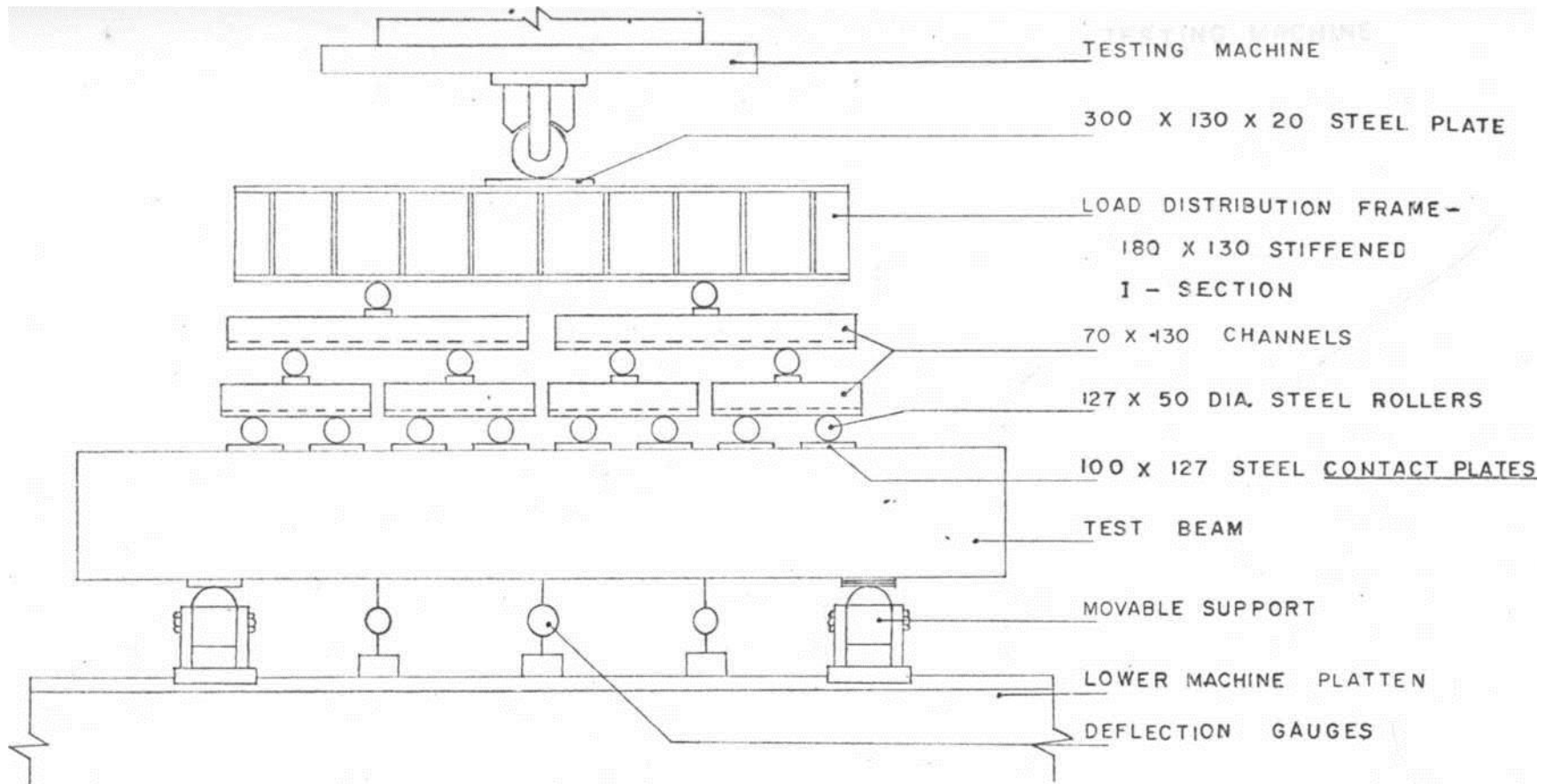


FIGURE 4.5: Loading arrangement for group G1 beams.

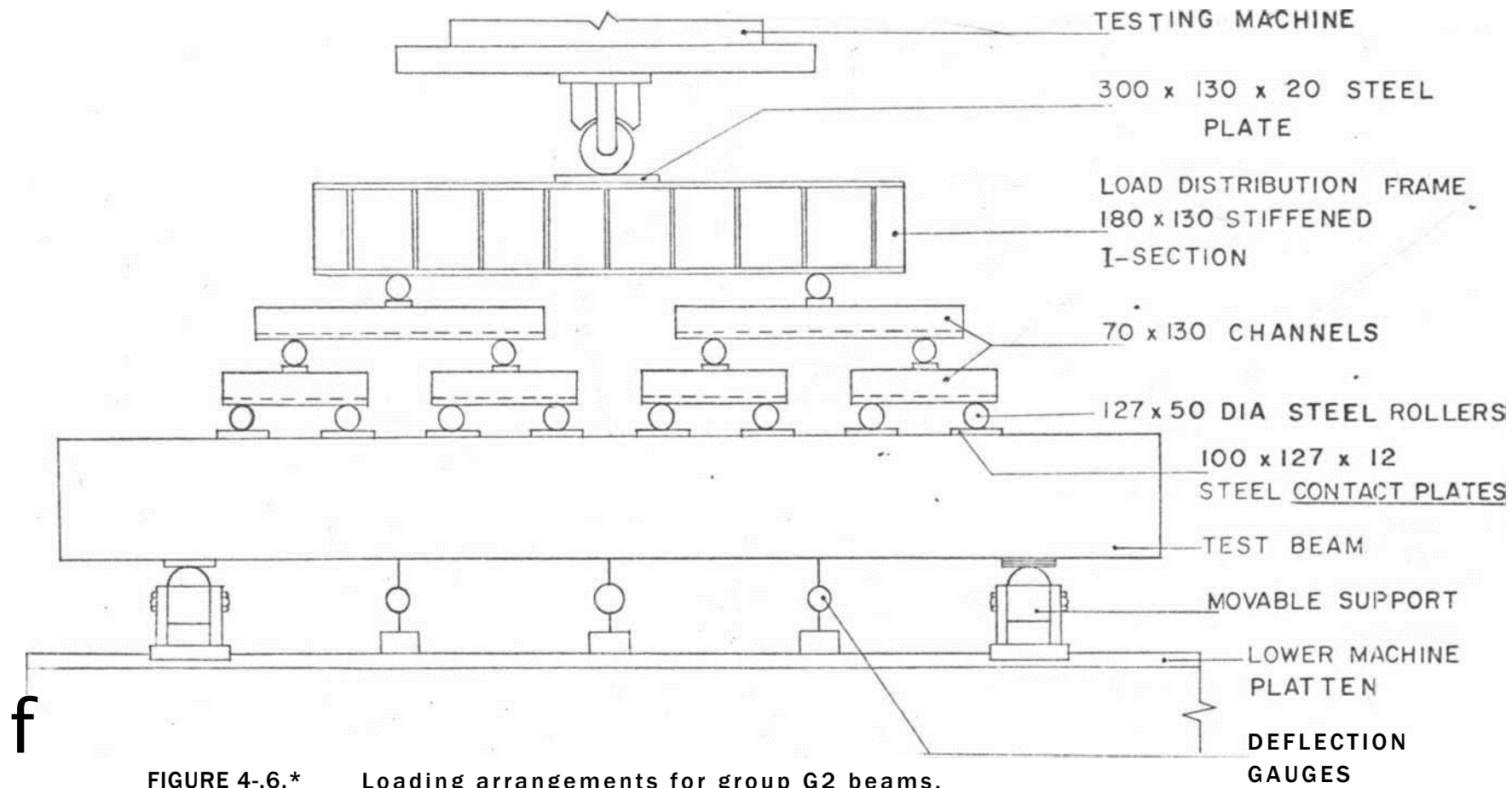


FIGURE 4-6.* Loading arrangements for group G2 beams.

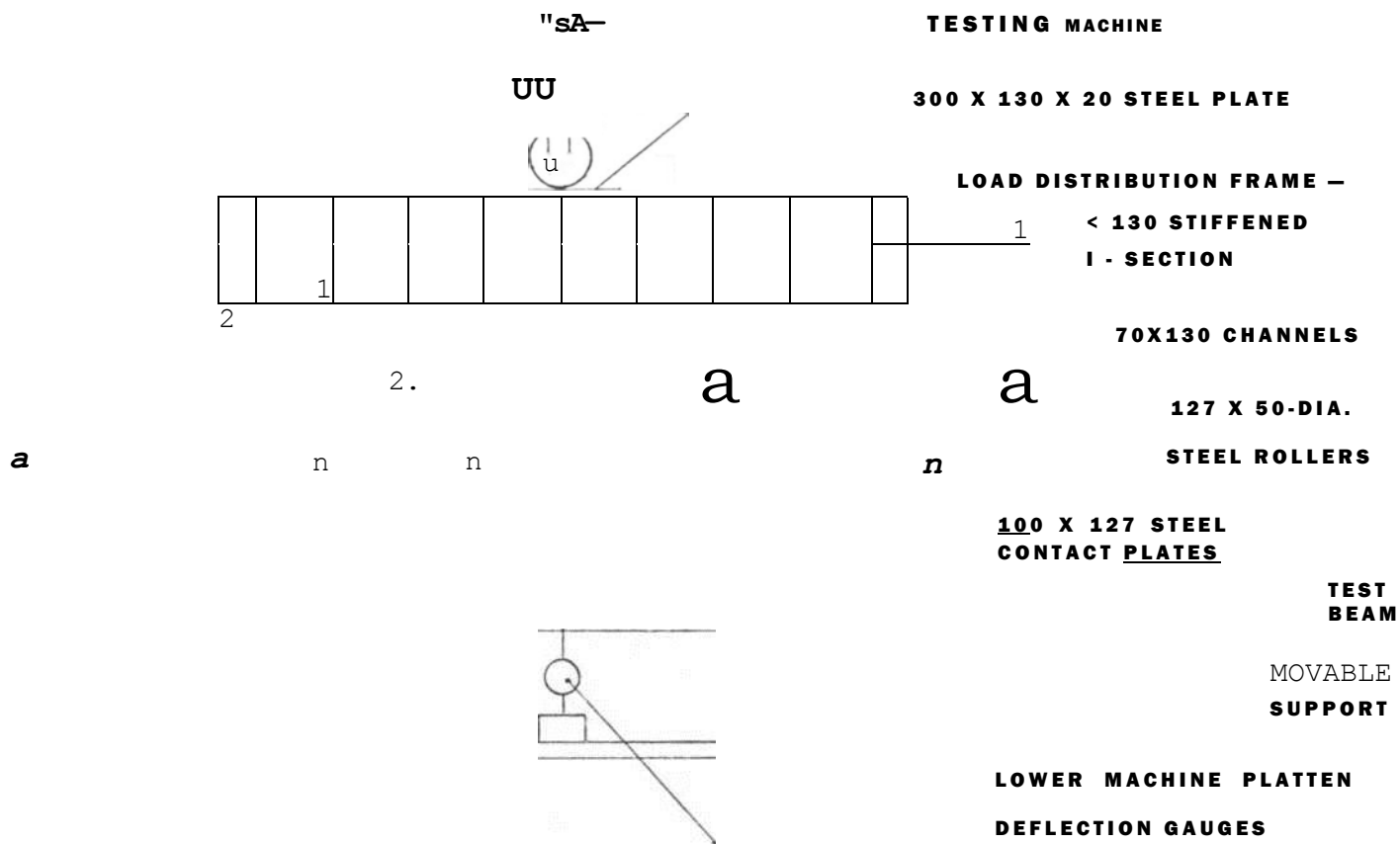
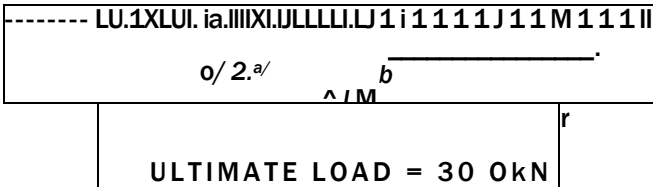
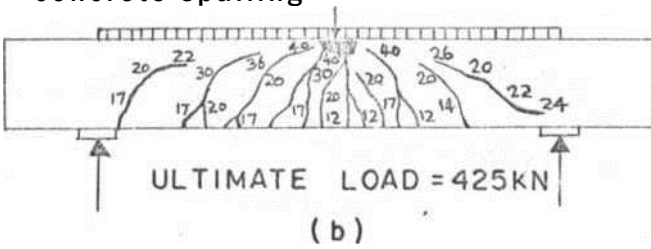


FIGURE 4.7; Loading arrangements for group G3 beams.

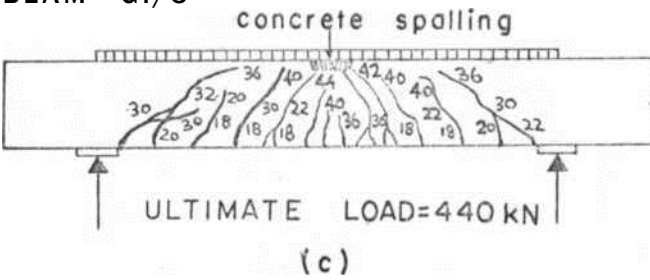
BEAM GI/1



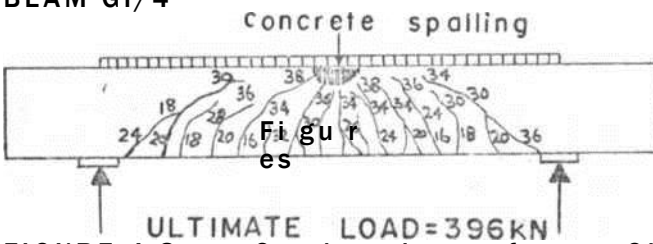
BEAM GI/2
* concrete spalling



BEAM GI/3



BEAM GI/4

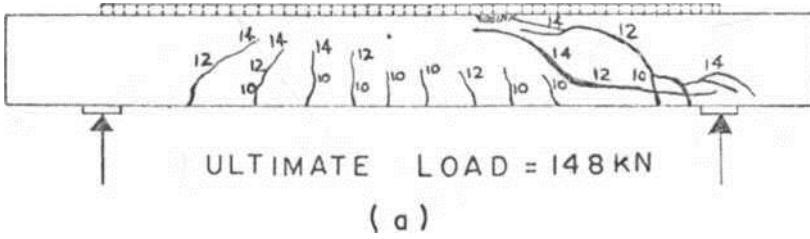


(d)

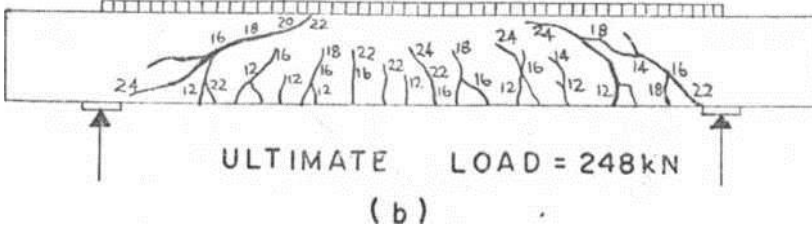
FIGURE 4.8: Crack patterns of group GI beams.

along cracks indicate loads in KN x 10.

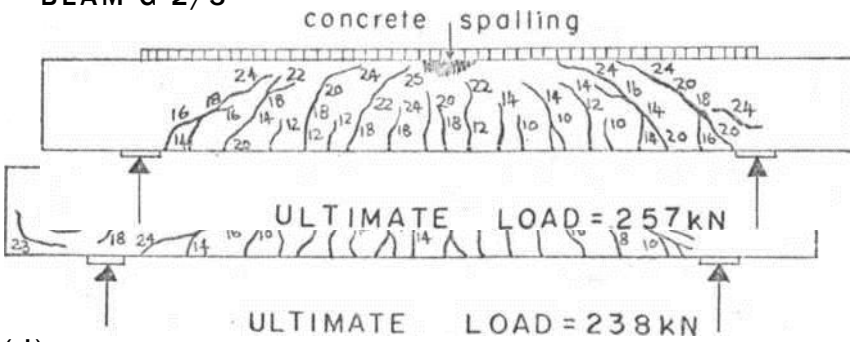
BEAM G 2/ 1



BEAM G 2/2



BEAM G 2/3



(d)

FIGURE 4.9: Crack patterns of group G2 beams

BEAM G 2/4
concrete spalling

Figures along cracks indicate loads
in kN x 10.

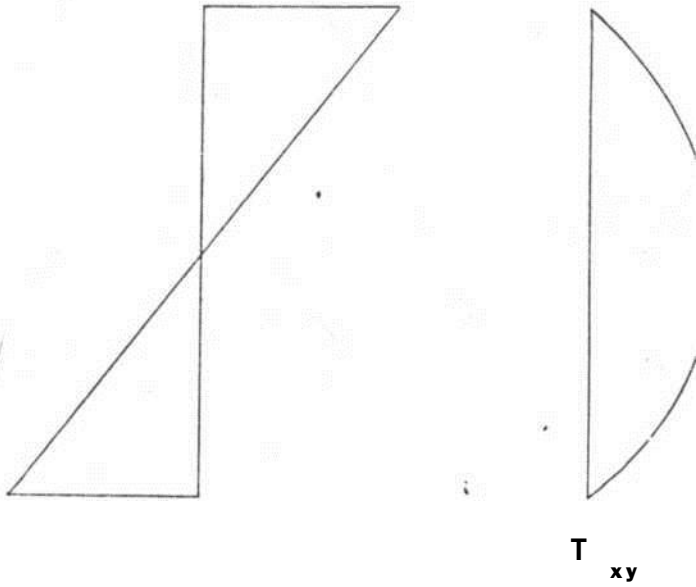


FIGURE 4.11; Direct and shear stress distributions.

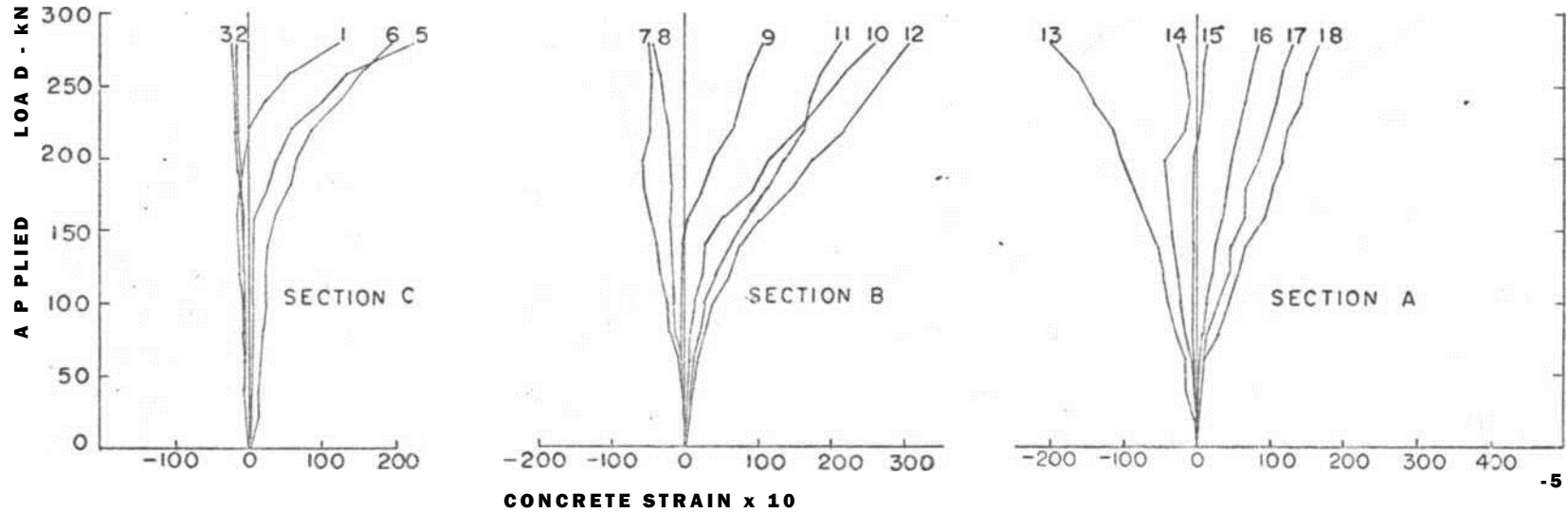
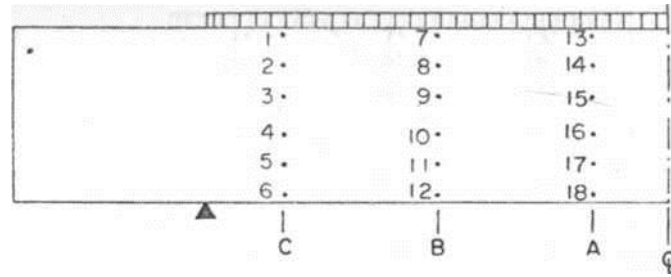


FIGURE 4.12: Variation of concrete strains with applied load — beam GI/1.

2*	7'	13*
3*	9*	15*
4 •	10-	16»
5-	1 1*	17-
6-	12-	18:
c	B	A <k

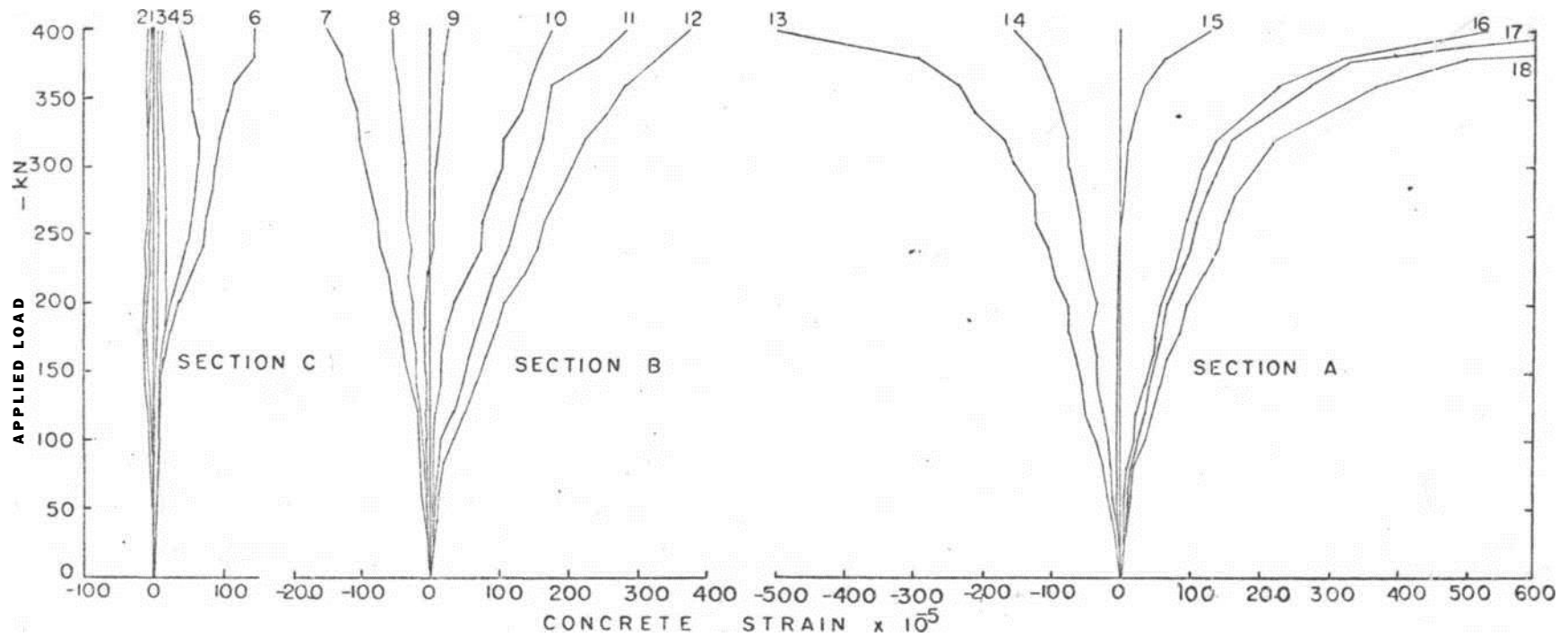


FIGURE. 4.13:

Variation of concrete strains with applied load — beam GI/2.

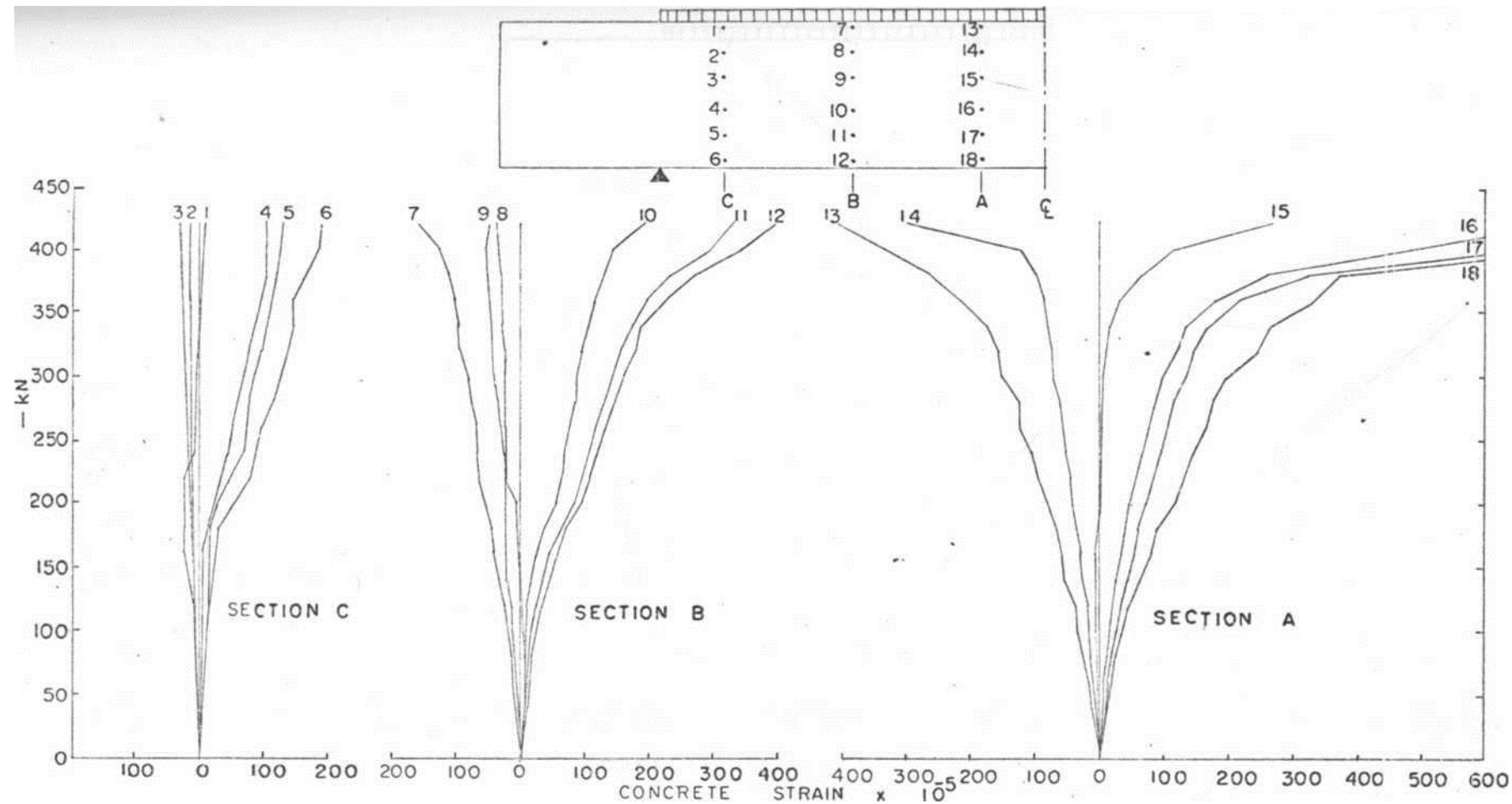


FIGURE 4.14:

Variation of concrete strains with applied load — beam G1/3.

FIGURE 4.15*. Variation of concrete strain with applied load

G1/4.

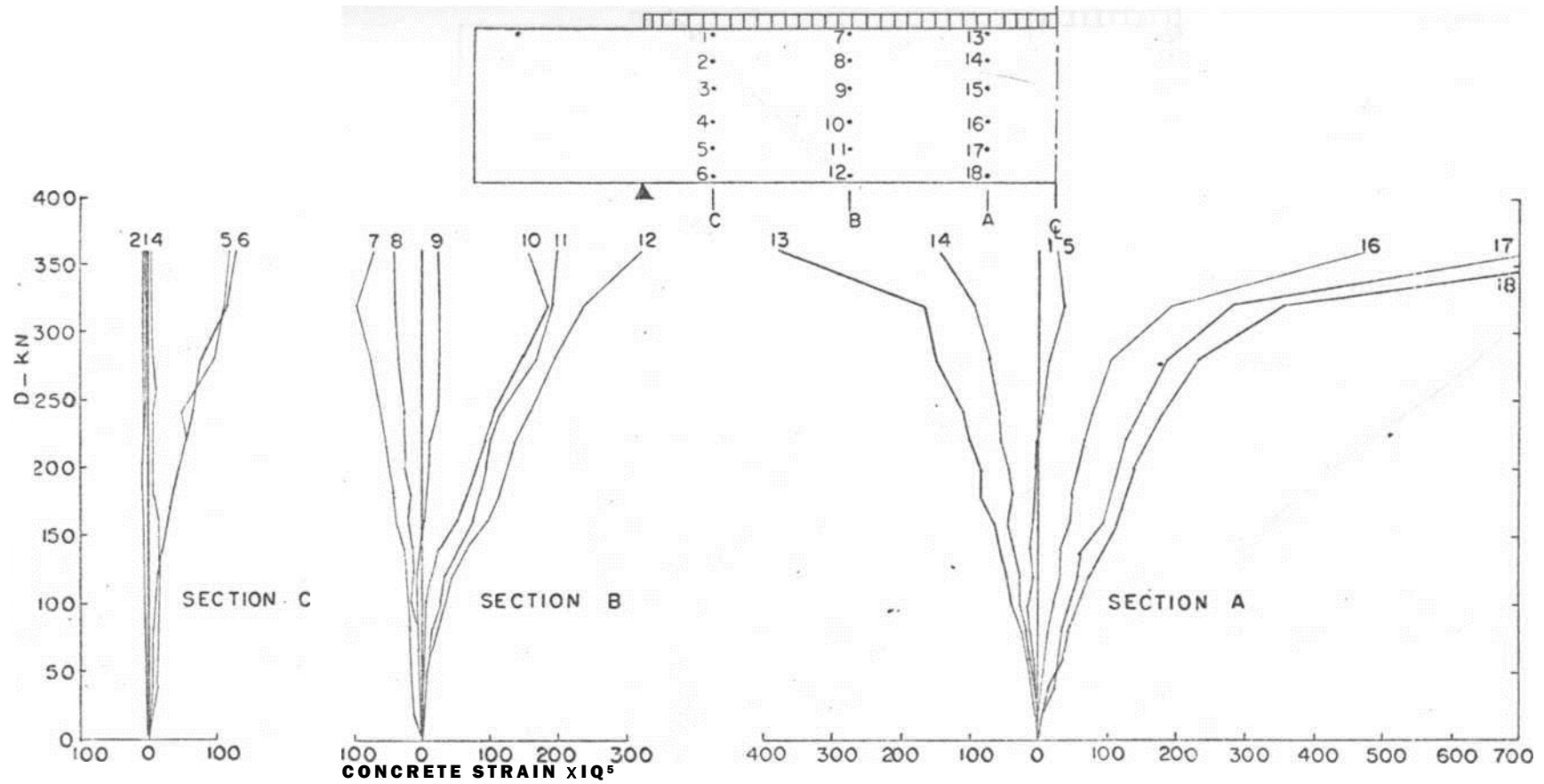


FIGURE 4.14:

Variation of concrete strains with applied load — beam G1/3.

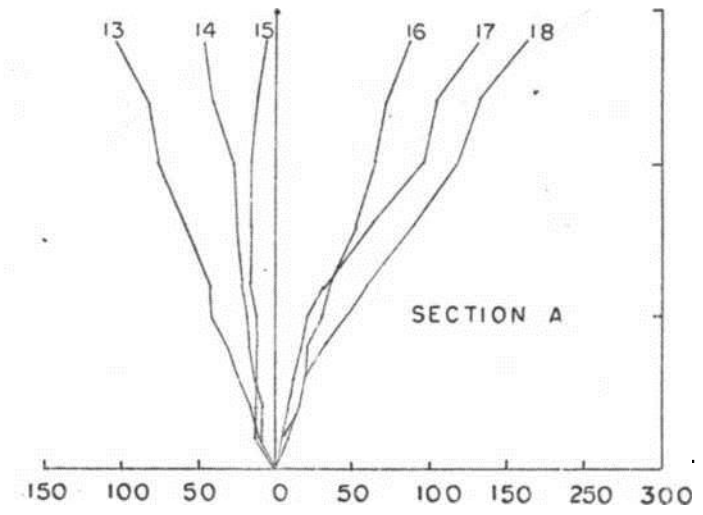
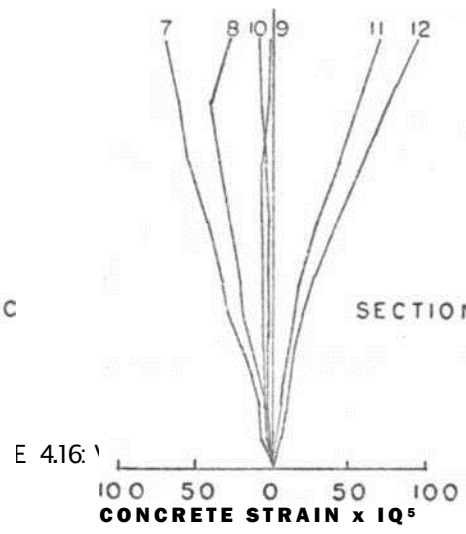
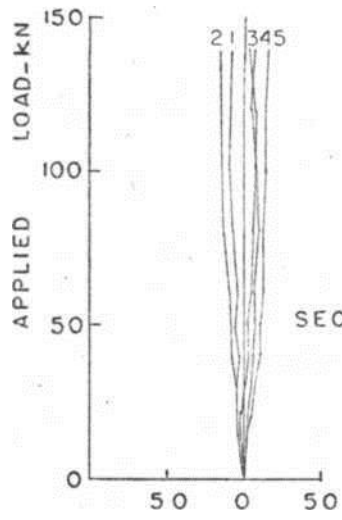
FIGURE 4.15*. Variation of concrete strain with applied load

G1/4.

umriri 1.1111111111111111 n 111 m i j

1*	7*	13*
2'	8*	14^
3*	9-	isl
4.	10*	.6f
5-	11-	•7f
6.	12-	19*

Δ I | I
 C | B | A
l n i a l
 I •
 7*
 mi



E 4.16 \

FIGURE 4.17: Variation of concrete strains with applied load — beam G2/2.

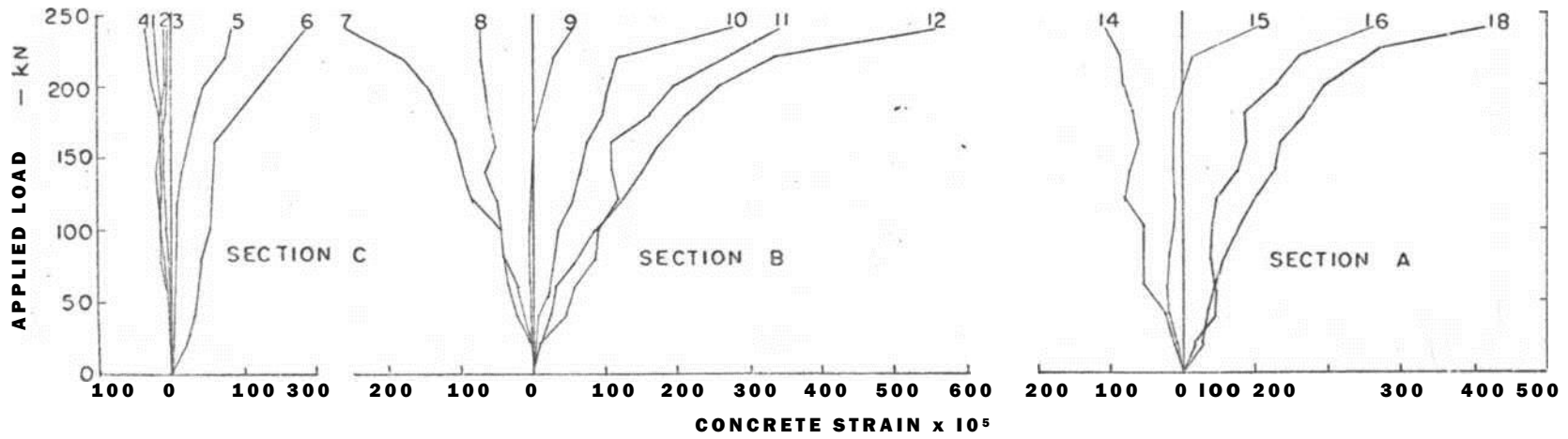
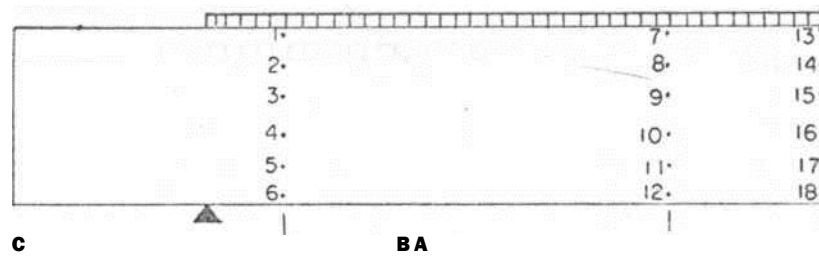


FIGURE 4.18; Variation of concrete strains with applied load—beam G2/3,"

rmxi.j'i i.n 11111 r.ixirrrrTT m^iaxiTT

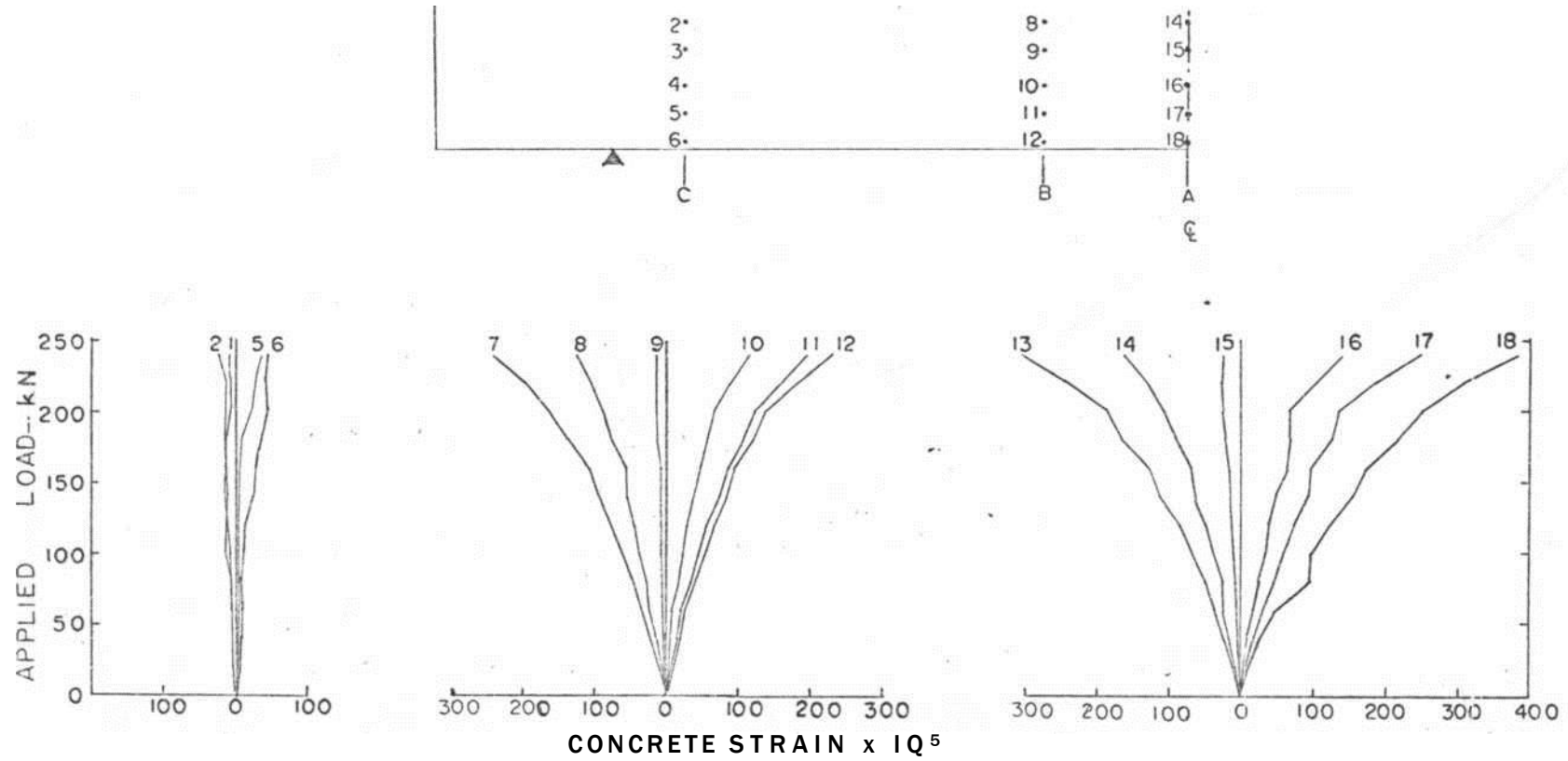


FIGURE 4.17: Variation of concrete strains with applied load — beam G2/2.

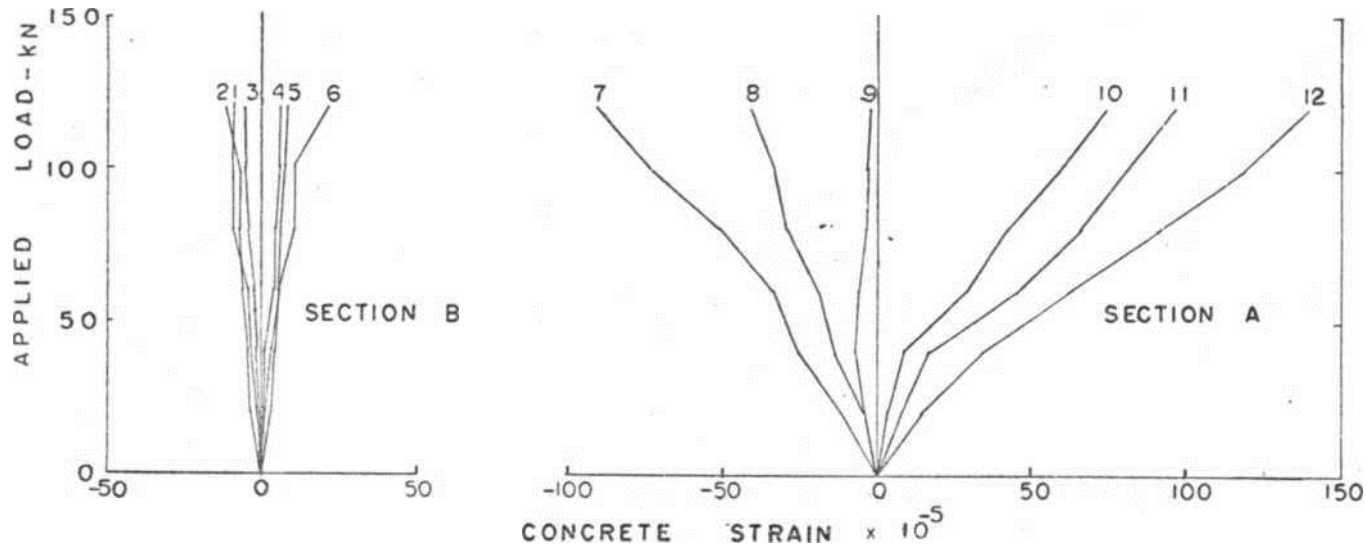
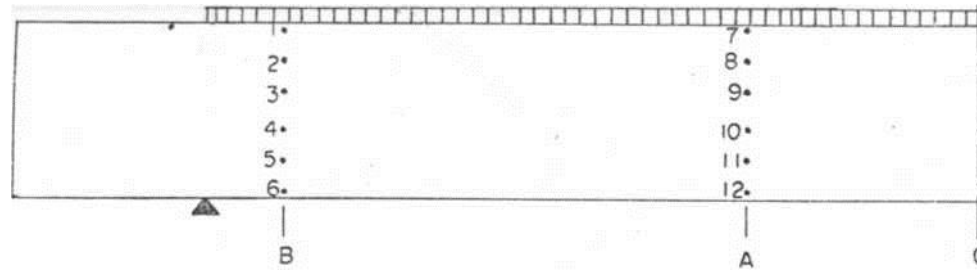


FIGURE 4.21! Variation of concrete strains with applied load—beam G3/2

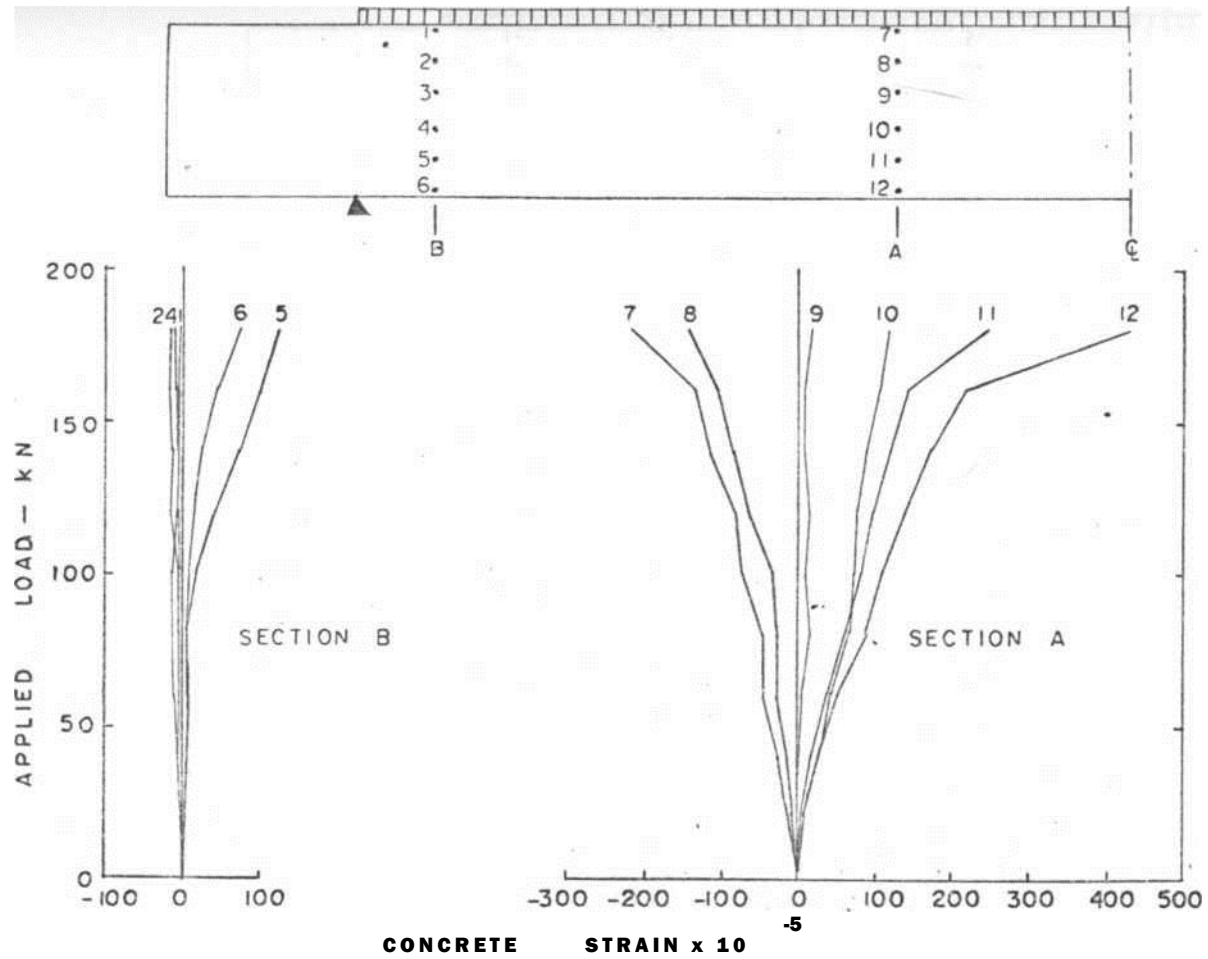


FIGURE 4-20:

Variation of concrete strains with applied load—beam G3/I.

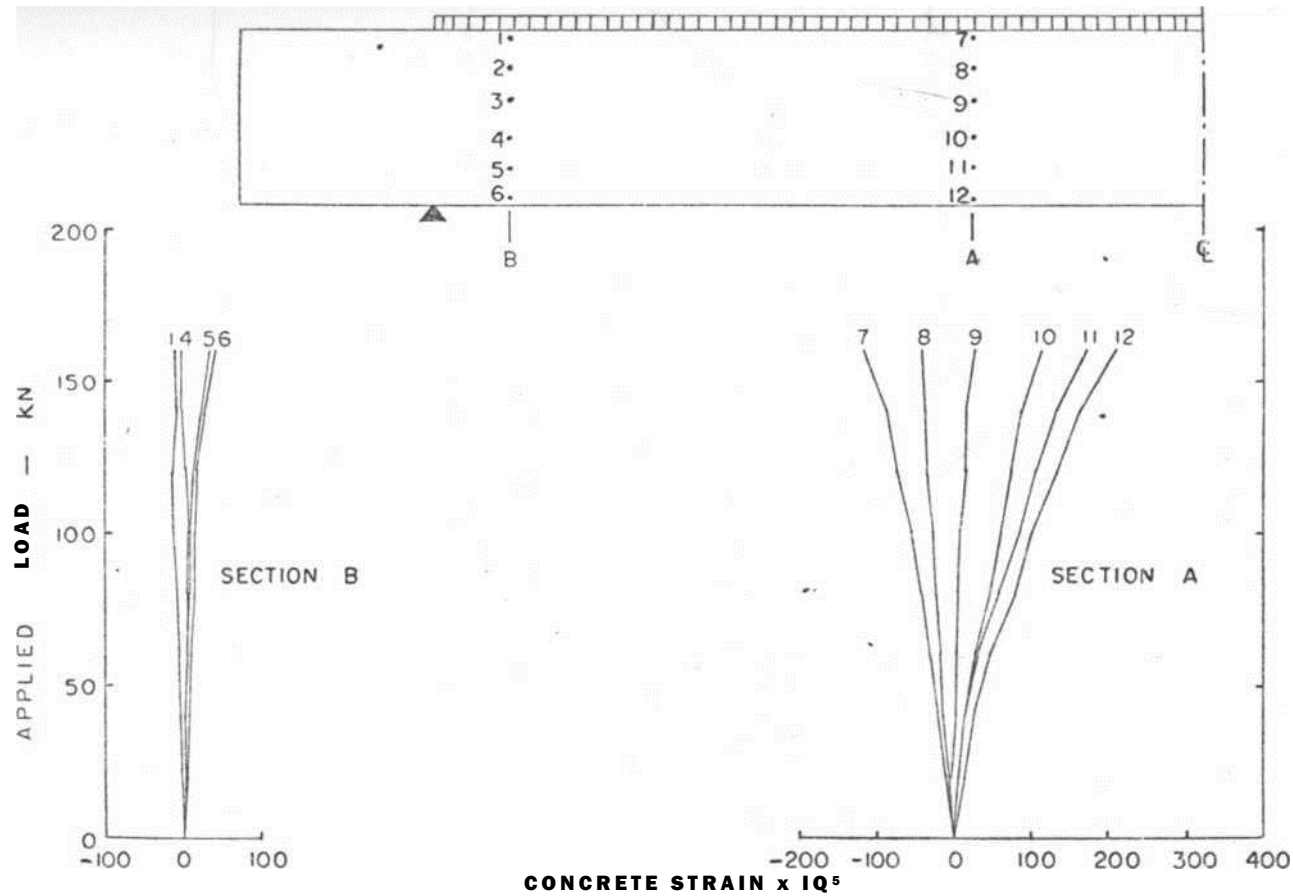


FIGURE 4.22'. Variation of concrete strains with applied load—beam G3/3.

CHAPTER 5

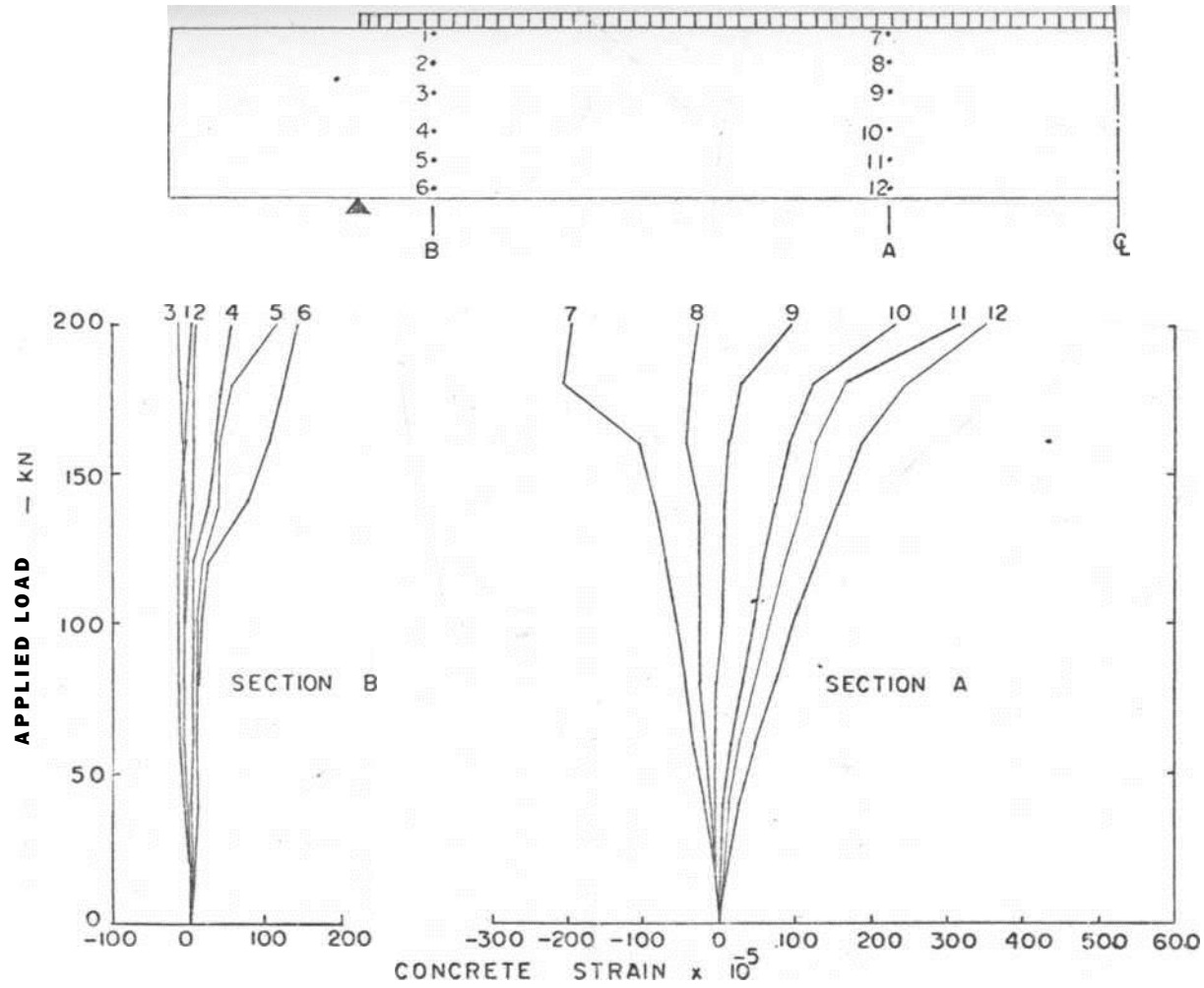


FIGURE 4.231 Variation of concrete strain with applied load—beam G3/4.

ANALYSIS OF TEST RESULTS5.1 SMITH'S APPROACH (10)

Smith applied the existing knowledge of shear failures under isolated point loads and presented a method of predicting the diagonal cracking load and the section of diagonal crack initiation. The critical section for shear-compression moment and the quantity of web reinforcement required for the attainment of flexural capacity were also investigated.

5.1*1 Determination of the Diagonal Cracking load.

The estimation of the diagonal cracking load is a prerequisite to the design of web reinforcement. Unfortunately there has not been a generally accepted definition of the diagonal cracking load. Krefeld and Thurston had suggested that the diagonal cracking load might be associated with a rapid propagation of a diagonal crack accompanied by a sudden increase of deflection and the first signs of horizontal splitting along the main tension reinforcement. Smith argued that since the phenomena considered by Krefeld and Thurston do not always coincide, the definition is not entirely satisfactory. An alternative definition was adopted - the load at which a diagonal crack crosses the neutral axis. As mentioned earlier in this report, unless an accurate method of observing crack propagation is employed, it is difficult to determine with precision the load at which a diagonal crack crosses the neutral axis.

Smith studied the results of the work of Paduart and Walther and deduced that the critical section corresponding to $a/d-j = .2 A$ was given by

$$\frac{M}{Qd_i} = 1.2 \dots\dots\dots (5.1)$$

but since for uniformly distributed loading at any section

$$-L = x_2 \frac{(L-x_2)}{2(I/2-x_2) d_i} \dots\dots\dots (5.2)$$

where x_2 is the distance between the section and the nearest support, the critical section for initiation of diagonal tension cracking is given by the quadratic equation

$$x_2^2 - x_2(L + 2.4d_i) + 1.2 Ld_i = 0 \dots\dots\dots (5.3)$$

obtained by substituting for M/Qd_i in equation 5.1 from equation 5.2.

It was further found that the critical section was given by equation 5.1 for the value of the shear cracking load obtained by the following equation which was developed by Som with $a/d-j = 2A$.

$$Q_{cr} = (jD-13 + 0.022i.(3 - a/d.,)^2] R ft'bd-, \dots$$

where $R = (1 + 70r)$ for $r \leq 0.0125$

$$= 1.57(1 + U-r) \text{ for } r > 0.0125 \text{ } r =$$

$$A_{st}/bd-j$$

The factor $(3 - a/d-j)$ is taken as zero if $a/d \leq 3$.

It was concluded that the diagonal cracking load as predicted by equation 5.4- with $a/d^{\wedge} = 2.K$ may be used for any system of loading if applied to sections for which $VQd^{\wedge} = 1.2$.

5.1.2 Determination of Critical section for shear-Compression and web reinforcement requirement.

• **b** ,

In this investigation it was assumed that a diagonal crack initiated at the section at which $M/Qd^{\wedge} = 1.2$, at a distance \wedge from the support. Its

horizontal projection $c = X_1 - X_2$ as shown in figure 5.1. At a distance x_1 from the support, for uniformly distributed loading .

$$= \frac{1}{2} (L - x_1) \dots \dots \dots (5.5).$$

The moment of resistance in shear-compression at this section including the effect of web reinforcement is given by

$$M_{sw} = M_s + \frac{snV_y w}{b} (x_1 - x_2)^2 \dots \dots \dots (5.6).$$

where M_s = shear-compression moment without

web reinforcement and is constant between the support and the critical section for initiation of diagonal cracking.

$f'w$ = ratio of web reinforcement

T = efficiency factor which was to be investigated (= 1.0 if all web reinforcement traversing the diagonal crack attains yield stress **f_{yw}**).

The critical value of c is given by the condition for the minimum value of $(M_{sw} - M_{x1})$ i.e.

$$\frac{d(M_{sw} - M_{x1})}{dx_1} = r_w f_y b (x - j - x_2) - w(L - 2x - j) \dots \quad (5.7)$$

The moment of resistance was equated to the bending moment at the critical section and substituted for $r_w f_y b$ from equation 5.7.

$$M_{sw} - M_{x1} = w(L - 2x - j) \left(\frac{L^2}{2} - Lx - x^2 \right)$$

The critical section for shear-compression failure is therefore given by

$$x_1 = \frac{Lx - x^2}{L - 2x - j} = \frac{fr - V}{1 - 2V} \frac{T}{L} \quad (5.8)$$

where $p = \frac{fr - V}{wL^2}$ and $V = \frac{V}{T}$

In beams of high $L/d - j$ ratios, the equation for the amount of web reinforcement required to prevent failure $\hat{\text{flexural capacity}}$ was derived from equation 5.7.

$$r_w f_y b = w \left(\frac{1 - 2V}{1 - 2V} \right) \dots \dots \dots (5.9)$$

In beams of small L/d - j ratios, if

$$\frac{\sim \wedge}{1-2} < 2 V$$

equation 3.8 implies $x_j < 2x_2$ for such beams it was tentatively assumed that the critical section for shear-compression is given by taking $x_j = 2x_2$. Then by equating equations 3.3 and 3.6 at a section at which $x_j = 2x_2$,

$$M_s + \frac{\phi w L^2}{4} + \frac{1}{2} \eta r_w f_{yw} b (L)^2 = M_s + \phi w x_2 (L - 2x_2) w L^2$$

Therefore, $r_w =$

$$(5.10)$$

3.1.3 SMITH'S TEST RESULTS.

The above equations for predicting the diagonal cracking load (3.4) and for estimating the quantity of web reinforcement (3.9) were supported by the test evidence of eleven simply supported beams under a distributed system of eight point loads. All the beams, 230 mm deep by 130 mm wide, reinforced with three 16mm diameter bars were tested on spans of 2.44, 3.04 and 3.60 m; the L/d-ratios were 12, 13 and 18 respectively. Except one beam of each span, the remainder had varying amounts of web reinforcement of a yield stress $f_{yw} = 263\text{N/mm}^2$. The mean concrete cube strength, f_c was 34.4 N/mm equivalent to 130mm cylinder strength, $f_c^* = 27.6\text{N/mm}^2$.

For the calculation of the shear-compression moment, Smith used the equation he had established earlier

$$M_s = (\rho - 0.17\rho) f_t^* b d^2 \dots\dots\dots (5.11)$$

which gave the same result as Laupa's equation

$$\rho = \frac{M_s}{f_t^* b d^2} \sim n^* \left(0.57 - \frac{A - 0.5 f_c'}{690} \right)$$

where $n^* = \text{elastic neutral axis factor} \Rightarrow \frac{r_m}{r_m + 2n - r_m}$

$$m = 5 + 69 f c'$$

Hognestad's (2) stress block factors were used to calculate the flexural capacity with $f_c' = 27.6 \text{ N/mm}^2$

$$M_F = C d_1 (1 - k k_2) \dots\dots\dots (5.12a)$$

$$G = f_c' k b d \dots\dots\dots (5.12b)$$

All the three groups of beams tested by Smith had $x_j > 2x_2$ and therefore only equation 5.9 was used for calculating the required quantity of web reinforcement defining it in terms of the efficiency factor η .

In that equation Q_p was calculated by

$$\eta = \frac{M_s}{G} \dots\dots\dots 15.15)$$

and V was obtained from the theoretical curve in figure 5.2. The details of beams and test results of

Smith's work are given in Table D1 in appendix D.

For each beam with web reinforcement, the actual web reinforcement $(r_w f_{yw})A$ was compared with the predicted quantity $T^{\wedge} r_w f_{yw}$ and the result is presented in terms of M_u/M_F in figure 5.3 together with the author's test results.

5.2 AUTHOR'S TEST RESULTS

5.2.1 Flexural Capacity. Hognestad's stress block

factors $k_1 k_3$ and k_2 were used to calculate the flexural capacity. These factors are given below for ease of reference.

$$k_1 k_3 = \frac{26.9 + 0.35 f_c'}{22.1 + f_c'} \quad (5.U)$$

$$k_2 = 0.50 - f_c' / 55 \quad (5.15)$$

The ultimate concrete strain, ϵ_u , was determined by the following equation also due to Hognestad.

$$\epsilon_u = 0.004 - f_c' / 55 \quad (5.16)$$

CTx io³

The tensile force resisted by the main steel was obtained by the equation

$$T = A_s t_{st} \dots \dots \dots (5.17)$$

A_s = total area of main steel t_{st} = stress in the main steel corresponding

to the ultimate concrete strain and the compressive

force resisted by the compression block of concrete was obtained by the equation 5.12b.

For each beam several suitable values were assigned to k to obtain various depths, d_n , of the compression block. With these values and ϵ_u from equation 5.16 the corresponding steel strain ϵ_s and hence the steel stresses were obtained from figure 5.4- and the stress-strain characteristics for the main steel in figure 4-.1 respectively

Tensile forces (equation 5.17) and the corresponding compressive forces (equation 5.12b) were plotted against the assumed values of k. The point of intersection of the graphs (figure 5.5) gave the correct values of k and T (=c) corresponding to the ultimate concrete strains. In this analysis it was assumed that

- (a) the strain diagram is linear and the steel strain is a proportion of the concrete strain at the same level, and
- (b) the longitudinal tensile stress developed in the concrete is negligible in the equilibrium equations of forces.

These assumptions had no experimental verification but they were unavoidable. Table 5.1 is a summary of the results obtained by the above procedure and were used in the calculations that follow. The flexural capacity M_p was calculated by equation 5.12a with C and k as given in table 5.1. The total load at flexural capacity, W_p , and the ultimate moment, M_u , were obtained by the well known formulae

$$WF = 8M_F A \dots\dots\dots (5.18)$$

$$M_u = W_u L / 8 \dots\dots\dots (5.19)$$

where L = effective span
 W_u = total load at failure.

5*2.2 Diagonal Cracking Load. Son's equation (5A) was used for the calculation of the diagonal cracking load. Since for the beams used in

Ms study

$$\begin{aligned}
r &= \mathbf{0.0229} \\
R &= 1.57(1 + IV \times 0.0229) \\
&= 2.07 \\
b &= 127 \text{ mm} \\
*1 &= 200 \text{ mm}
\end{aligned}$$

Som's equation reduces- to

$$\begin{aligned}
Q_{d,j} &= 7.27 \text{ ft}^3 \text{ KN when } f_t^* \text{ is in} \\
&\text{N/mm}^2 \dots\dots\dots (5.20).
\end{aligned}$$

For each beam the calculated modulus of rupture was used. Equation 5.20 gives the diagonal cracking load at the section at which $M/Q_{d-j} = 1.2$. For any other section, the diagonal cracking load, W_{cr} was obtained by the following equation derived from similar triangles of the shear force diagram

$$\begin{aligned}
\mathbf{Her} - 20^{\wedge} &\dots\dots\dots (5.21) \\
&JJ - \wedge x < 2
\end{aligned}$$

where x_2 = distance along the axis of beam from the support to the critical section for diagonal cracking.

The values of X^2 were obtained from the theoretical curve in figure 5.2. The test values of X^2 are presented in Table 5.2 and the dotted curve through the mean of X^2t/L in figure 5.2 shows a good correlation between the experimental and theoretical curves within the limits of $1/d^4$ of the beams tested.

5*2,5 Web reinforcement required for flexural capacity. In all the beams tested except

group Cr3, x_j was found to be less than $2x_2$ * For beams in group G-1, x_j/x_2 varied from 1,23 to 1.28 with a mean of 1,26; for group G2, x_j/x_2 varied from 1.55 to 1.66 with a mean of 1.60 and for group G3, the ratio varied from 2.02 to 2.13 with a mean of 2.07* Equation 5,10 was therefore applicable to beams in groups G-1 and G2 which had web reinforcement.

The quantity of web reinforcement required for group G3 beams was evaluated by both equations 5,9 and 5,10

since this group was an intermediate case by the fact that $x^$ was almost equal to $2x_2$ # Values of r^r_{wf} by both equations were nearly the same. The actual web reinforcement $(r_{;vf^v})A$ for every beam with web reinforcement was compared v/ith the calculated quantity $ir^r^$ and the results are shown in Table

5.3 and Figure 5,3, The relevant caluulations relating to figure 5,3 are presented in appendix E.

In this figure the results of the author¹s tests are cbmpared v/ith the results of Smith¹ s tests. It is observed that beams in group G-1 v/ith web reinforcement exceeded flexural capacity by up to 34/6. The high ultimate moments are discussed in Chapter 6.

5.3 PREDICTED WEB REII^OPrIP.T""hIN_T.

Equairion 5.10 was tentatively assumed to be applicable to beams with $x^ < 2x_2$. This equation

with the efficiency factor $V = 2/3$ as found by Smith was applied to estimate the quantity of web reinforcement that would have been sufficient for the beams tested by the author to fall in bending.

Since the age of the specimens at the time of testing was longer than 28 days on which the concrete mix design was based, the mean cube strength, $u = 45.8 \text{ N/mm}^2$ was used in the calculations.

Equation 5.-11 was used to calculate the shear-compression moment. For the beams tested,

$$p = 2.29 \frac{V}{b} \\ = 127 \text{ mm} \\ d-j = 200 \text{ mm}$$

and the equation reduces to

$M_s = 5.70 \text{ ft}^2 \text{ kNm}$ with ft' in N/mm^2 . Using Hognestad's (2) stress block factors with $u = 45.8$, $fc' = 35.8$, $ft' = 4.73 \text{ N/mm}^2$,

$$k_j k_j = 0.680 \\ *2 = 0.435 = 0.00320 = 0.496 \\ e_u = \text{ultimate neutral axis factor.}$$

From figure 4.1,

$$T = 581 \times 526 \times 10 \quad 306 \text{ kN}$$

$$\text{and } C = 0.680 \times 35.8 \times 0.496 \times 127 \times 200 = 306 \text{ M}$$

$$\text{Hence, } M_p = 306 \times \frac{200(1-0.49)}{c} \times 0.436$$

$$= 8.0 \text{ kNm}$$

$$M_s = 8.0 \times 4.73$$

$$= 27.0 \text{ KN m}$$

Thus for all groups,

$$c_p = \frac{M_s}{2M} = 0.281$$

' M.

G-roup Gr1: $L = 1.2 \text{ m}$, $\hat{c} = 0.150$ (from figure 5.2)

$$w = \frac{48.0 \times 8}{1.2^2} \quad \text{of span '}$$

$$x_1 = 9 - \frac{1}{2} V$$

$$= 0.128 \times 1200 = 220 \text{ mm}$$

$$2x_2 = 2 \times 0.15 \times 1200 = 560 \text{ mm}$$

$$r_{wy} = \frac{w}{4b} V^2$$

and with $\frac{1}{3}$

$$r_{wy} = \frac{3w}{4b} V^2$$

$$= 5 \times 266 \times 0.139$$

$$4 \times 127 \times 2.25 \times 10^{-2} = 9.70 \text{ N/mm}^2$$

Group G2: $l = 1.6 \text{ m}$, $\alpha = 0.126$

$$w = 48.0 \times 8_{150}$$

$$= \frac{1.6^2}{5^5} \times 1600 = 531 \text{ mm}$$

$$2x_2 = 2 \times 0.126 \times 1600 = 404 \text{ mm}$$

$$r_{wy} = \frac{180 \times 0.096}{4 \times 127 \times 1.58 \times 10^{-2}}$$

$$= 5.63 \text{ N/mm}^2$$

Group G5: $l = 2.0 \text{ m}$, $\alpha = 0.107$

$$w = 48.0 \times 8 = 96.0 \text{ N/mm}$$

$$x_j = \frac{Q > 170 \times 2000}{0.784} = 436 \text{ mm}$$

$$2x_2 = 2 \times 0.107 \times 2000 = 428 \text{ mm}$$

Note that $\alpha^2 = X^2$ and both equations 5.9 and 5.10 are applicable

$$r_{wy} = \frac{3 \times 96.0 \times 0.056}{4 \times 127 \times 1.14 \times 10^{-2}}$$

$$= 2.78 \text{ N/mm}^2$$

$$r_{wy} = \frac{3w}{4b}$$

Comparing with equation 5.9

$$\frac{1}{Q} = 2V(1 - V)$$

$$= \frac{3 \times 96.0}{4 \times 127} \left\{ \frac{0.438}{0.084} \right\}$$

$$= 2.96 \text{ N/mm}^2$$

The modes of failure, actual and predicted amounts of web reinforcements are given in Table 5.4. The predicted quantities for $\lambda = 1$ are based on actual concrete strengths while for $\lambda = 2/5$ the quantities are based on mean concrete strength, A comparison of modes of failure, the actual and predicted amounts of web reinforcements for $\lambda = 1$ indicates that a value of the efficiency factor between 2 and 4 would result in quantities of web reinforcement necessary for attainment of flexural capacity. If the modes of failure, the actual and predicted amounts of web reinforcement for $\lambda = 2/5$ are compared, it is noted that equation 5.10 yields overestimates of r for some of which are impracticable as in group G-1.

The overestimates are due to the fact that the derivation of equation 5.10 was based upon a tentative assumption that $x^*/x^* = 2$. As shown earlier for beams in groups G-1 and G2, x_q/x_2 varied from 1.25 to 1.66. In group G5 where x^*/x_2 varied from 2.02 to 2.15, the predicted quantity of web reinforcement v/a_s was not excessive.

It was therefore necessary to establish another equation which would predict reasonable estimates of r for beam of all L/d . In the following sections two empirical equations are developed based upon consideration of shear stresses and bending moments.

5.4 CONSIDERATION OF SHEAR STRESSES

After several attempts to establish an empirical equation for predicting the quantity of web reinforcement required to prevent failure below flexural capacity, it was found that the equation that gave the best results was of the form

$$\frac{q_u}{q_{cr}} = f \left(t + r_w f_y w \right) \dots \dots \dots (5.22)$$

cf

where q_u = ultimate shear stress

- q_{cr} = diagonal cracking shear stress determined by Som's equation (5.4)
- q_p = shear stress corresponding to the flexural capacity
- t = a constant which was assumed to have the same units as the web reinforcement $r_w f_y w$

The constant t was varied from 0 to 5.0 by increments of 0.1. For each value of t a regression equation was established in order to find constants A and B in equation 5.22. The results of the beams without web reinforcement were disregarded because a different mode of failure applies to such beams as a marked discontinuity was observed between the results for beams with and without web reinforcement. The amounts of web reinforcement predicted by the resulting equations were evaluated. It was found that for $0 < t < 0.5$ the derived equations predicted absurd results for all the beams studied. As t was

increased from 0.5 to 5.0 the predicted quantity r_{wf} increased for the beams tested by the author w_{yw} but decreased for cases 2 and 3 beams ($L/d^{\wedge} = 15$ and 18 respectively) tested by Smith; for case 1 beams, ($L/d^{\wedge} = 12$), r_{wf} decreased for $0.5 < t < 2.0$ and then increased for $2.0 < t < 3.0$. Table 5.5 shows the predicted quantity $r_{wf}^{\wedge v}$ for some values of t between 1.0 and 3.0 for all the beam groups. An examination of the results in table 5.5 indicates a discontinuity in the variation of r_{wfyw} between the two series of the test results. This is presumably due to the different properties of the beam.

When $t = 2.0$ equation 5.22 gave results with a good correlation with the results of equation 5.9 for the beams tested by Smith. Moreover at this value of t , r_{wfyw} for Smith's Case 1 beams was stationary. On these grounds $t = 2.0$ was substituted in equation 5.22 to give the required equation for predicting the quantity of web reinforcement necessary for attainment of flexural capacity. Figure 5.6 shows a plot of q_u/q_{cr} against $(2.0 + r_{wfyw})/cL$ from which the following equation was obtained.

$$\frac{q_u}{q_{cr}} = 7.09 - 5.6 (2.0 + r_{wfyw}) / cL$$

I_F

Coefficient of correlation = - 0.685.

For flexural capacity $q_u = q_r$

$$r_{wfyw} = (7.09 - \frac{q_r}{Q_{cr}}) \frac{I_F}{cL} - 2.0 \quad (5.23)$$

The amounts of v/eb reinforcement used in the beams tested by the author were less than those predicted by equation 5.23 because the design of web reinforcement was not based on the v. same theory as the derivation of this equation; the design was based on stirrup spacing which was maintained equal to or less than the effective depth except in beams G3/2 and G-3/3.

5.5 CONSIDERATION EOF BENDING- MOMENTS

As in the consideration of shear stresses, several attempts to establish an empirical expression for predicting the quantity of web reinforcement required for achievement of flexural capacity revealed that the best results were obtained by assuming an equation of the form

$$M_{cr}$$

i. e.,
$$M_{cr} = C + D \cdot r_v / f_{yw}$$

where M_{cr} = bending moment at ultimate load

at the section at which $M/Qd = 1.2 M_{cr}$ = bending moment corresponding to diagonal cracking load as predicted by Som's equation (5.4)

Figure 5.7 shows a plot of M^*/M_{cp} against

Again the results of the beams without web reinforcement were disregarded. The regression

equation obtained was

$$M_p / M_{cp} = 1.27 + 1.37 \cdot r_w / f_{yw}$$

Coefficient of correlation = 0.850 For

bending moment at
flexural capacity at the
section at which $M/Qd_1=1.2$

$$r_w f_{yw} = \left(\frac{M_F'}{M_{cr}} - 1.27 \right)^{1.37} \dots \dots \dots (5.24)$$

flexural capacity, $M_{cr} = M_j, '$

The quantities of web reinforcement predicted by equation 5.24 are contained in Table 5.6.

5.6 DISCUSSION OF EQUATIONS 5.25 AND 5.24.

It is noted that the amounts of web reinforcement predicted by equation 5.24 are far less than those predicted by equation 5.23. This is because equation 5.24 was based on a linear plot through the test results whereas in the derivation of equation 5.23 a value of t was selected to give amounts of web reinforcement to provide a margin of safety for attainment of flexural capacity. Consequently equation 5.23 is selected for predicting the quantity of web reinforcement required for attainment of flexural capacity.

5.7 MOMENT - ROTATION RELATIONSHIP

When some beams approached failure the limits of the deflection gauges at the quarter points were either exceeded .or the gauges were dismantled to avoid destruction by the beam after collapse. Thereafter only the central deflections were recorded and consequently the ultimate rotations could not be determined from the deflection readings for all the beams. The highest ultimate rotations occurred at the section of failure which were in

different regions depending upon the amount of web reinforcement provided. In beams failing in shear, the failure regions were between the supports and the mid span; in beams failing in flexure the failure regions were at mid span, and in combined shear and flexure failures, the beams sustained extensive diagonal cracking and finally collapsed by main steel yielding accompanied by concrete spalling at the top near mid span.

The calculations for the rotations given in Tables F1-F12 in appendix F were based upon the relative deflections of mid span and quarter points. Referring to figure 5.8, the rotations were calculated as

$$\begin{aligned} \text{Rotation at right support, } \theta^R &= 4A \theta^M \\ \text{Rotation at left support, } \theta^L &= 4A \theta^M \\ \text{Rotation at mid span, } \theta^M &= \frac{L}{\epsilon} \left(\frac{2A - A_1}{L} \theta^R - \frac{A_1}{L} \theta^L \right) \end{aligned}$$

The variations of bending moments and rotations at mid span for different amounts of web reinforcement are illustrated in figures 5.9(a), (b), and (c) for the three groups of beams tested with $L/d = 6, 8$ and 10 respectively. It is noted from these figures that the rotation capacity of the beams without web reinforcement is less than that of beams with web reinforcement.

Figure 5.9 (a) shows that for beams with $L/d = 6$, rotation capacity increased with the amount of web reinforcement. For the amounts of web reinforcement in group 02, the shear rotation impaired the flexural rotation and as seen in Figure 5.9 (b) beam G-2/4 was less ductile than beam G-2/2. In these two figures it is observed that beams G-1/2, G-1/3 and G-2/3 exhibited a peculiar characteristic towards the

failure load. The trend of the curves shown in Figure 5.9(c) suggests that had all the deflection readings been recorded up to the failure load it would have been possible to show that rotation capacity increased with the quantity of web 1 reinforcement. Moreover the trend of the curves in all the three figures suggests ductility increased with the span of the beam.

5.8 CONTRIBUTION OF WEB REINFORCEMENT

To estimate the total contribution of the web reinforcement towards the shearing resistance, it can be assumed that the contribution depends upon the strength of the beam without web reinforcement.

This can be expressed as

$$\frac{M_{uw}}{M_{u1}} = \frac{f_y A_{w1}}{f_y A_{w1} + f_y A_{w2}} \left(\frac{V}{V_{u1}} \right)$$

where M_{uw} = ultimate moment for beams with web reinforcement.
 M_{u1} = ultimate moment for beams without web reinforcement

as determined from the test evidence. A similar approach was used by Laupa (4), but Laupa assumed that the ratio M_{uw}/M_{u1} was independent of L/d ratio. An examination of the test results has indicated that L/d has an influence on M_{uw}/M_{u1} . The influence of the web reinforcement on M_{uw}/M_{u1} is shown in figure 5.10 and the applicability of Laupa's equation to the test results is also checked in the same figure. The following equation was derived from all the test results except those of group G1 which were disregarded because the ultimate moments exceeded the flexural capacity highly as discussed earlier.

$$\frac{M_{uw}}{M_{u1}} = 0.976 + 0.656 r_w f \dots \dots \dots (5.25)$$

M_{u1}

J

The influence of L/d_1 on M_{uw}/M_{u1} is shown in figure 5.11 and the following equation was derived

$$M_{uw} = 2.16 - 0,067 \frac{L}{d_1} \dots\dots\dots (5.26)$$

In order to establish the total effect of r^{\wedge} and L/d^{\wedge} on a coefficient, α , was introduced in equation 5.26 and the result added to equation 5.25 " such that the resulting expression was of the form

$$\frac{M_{uw}}{M_{u1}} = 0.576 + 0.656 r_w f_y w + \alpha (2.16 + \frac{0.067 L}{d_1})$$

The coefficient α was varied from 0 to 21. For each value of α , the correlation coefficient between

$\frac{M_{uw}}{M_{u1}}$ computed by the resulting equation and M^{\wedge}/M^{\wedge} from the test results was determined. The highest correlation coefficient was found to be 0.800 when $\alpha = 4.5$. Substituting for α in the above expression,

$$\frac{M_{uw}}{M_{u1}} = 1.94 + 0.119 r_w^{\wedge} f_y w - 0.055 \frac{L}{d_1} \dots\dots\dots (5.27)$$

The results calculated by 5.27 are compared with the test results in figure 5.12. The ultimate moment without web reinforcement corresponds to shear-

compression moment and may be obtained by Laupa's equation given in Chapter 5. Investigation into the applicability of 5.27 to predict the quantity of web reinforcement required for flexural capacity by assuming $M_{\#} = M_g$ indicated that r^{\wedge}

increases with span because M_p and M_s for the beams studied were not variables. This shows that equation 5.27 cannot be used to predict the quantity of web reinforcement.

TABLE 5.J.: SUMMARY OF GRAPHICAL SOLUTIONS FOR μ ; $\mu T(\mu C)$ and K

BEAM No.	ULTIMATE CONCRETE STRAIN ϵ_u	COEFFICIENT μ^2	COEFFICIENT μ	TENSILE OR COMPRESSIVE FORCE T or C (KN)
<*1/1	0.00315	0.431	0.478 %	310
81/2	0.00315	0.431	0.479	309
81/3	0.00315	0.431	0.478	310
81/4	0.00322	0.436	0.500	306
82/1	0.00322	0.437	0*501	305
82/2	0.00312	0.428	0.472	312
82/3	0.00325	0*439	0.509	303
82/4	0.00323	0.437	0.501	305
83/1	0*00323	0.439	0.504	304
83/2	0.00325	0.439	0.509	303
83/3	0.00312	0.428	0.472	312
83/4	0.00315	0.431	0.478	310

TABLE 5.2: TEST AND CALCULATED VALUES OF X_2

BEAM No	*2 test mm	mean *2 (test)	*2 (Calc.) mm	L	i, *i
G1/1 G1/2 G1/3 G1/4	210 250 140 160	185	180 %	0.150	6
G2/1 02/2 G2/3 32/4	205 270 140 180	199	205	0.124	8
33/1 33/2 33/3 33/4	230 185 230 235	220	220	0.110	10

TABLE 5.3. ACTUAL AND THEORETICAL WEB REINFORCEMENTS.

BEAM No.	STIRRUP SPACING	ACTUAL REINFORCEMENT (N/ mm ²)	THEORETICAL WEB REINFORCEMENT (N/∧)	$\frac{f_y A_{sv}}{s V}$
	S		$\frac{f_y A_{sv}}{s V}$	
	-	-	-	-
G1/2	100	1.25	6.51 %	0.192
01/3	75	1.67	6.50	0.257
G1/4	50	2.51	6.56	0.382
02/1	-	-	-	-
02/2	175	0.716	3.58	0.200
G2/3	150	0.858	3.72	0.225
G2/4	125	1.005	3.69	0.271
G3/1	-	-	-	-
G3/2	250	0.502	1.96	0.225
G3/3	225	0.560	1.79	0.313
03/4	200	0.627	1.81	0.347

TABLE 5*4: Comparison of modes of failure.
Actual and predicted neb reinforcements.

BEAM NO	MODE			
	OP	ACTUAL	Predicted	
	FAILURE		n = 1	U - 2/3
GI/I 81/2	DP SC-F	1.25	6.52 6.51	9.70
81/3	F	1.67	6.50	
81/4	F	2.51	6.56	
G2/1	DP	.	3.74	5.63
G2/2	SC	0.716	3.58	
Gf/3	SC-F	0.838 ..	3.72	
G2/4	F	1.005	3.69	
83A 83/2	SC SC7	0.502	1.83 1.96	2.78
83/3	SC	0.560 '	1.79	
•5/4	SC-F	0.627	1.80	

TABLE 5.5s Predicted values of web reinforcement,
r f by equation 5.22 for different values w yw,
of t.

t	BEAM O' R OUP					
	G 1	0 2	G 3	CASE 1 %	CASE 2	CASE 3
1.0	1.85	1.88	1.69	1.06	1.90	0.70
1.5	2.28	2.13	1.76	0.93	0.71	0.46
2.0	2.66	2.43	1.94	0.91	0.65	0.34
2.5	3.07	2.77	2.17	0.96	0.64	0.25
3.0	3.46	3.10	2.40	1.00	0.43	0.20

TABLE 5.6s VALUES OF WEB REINFORCEMENT PREDICTED BY
EQUATION 5.24.

BEAM	$M_p' / \gg cr$	V_{yw} (N/mm ²)
GROUP G1	3.18	1.39
GROUP G2	2.66	1.09
GROUP G3	2.12	; 0.62
CASE 1	1.65	0.28
CASE 2	1.45	0.13
CASE 3	1.24	- 0.02

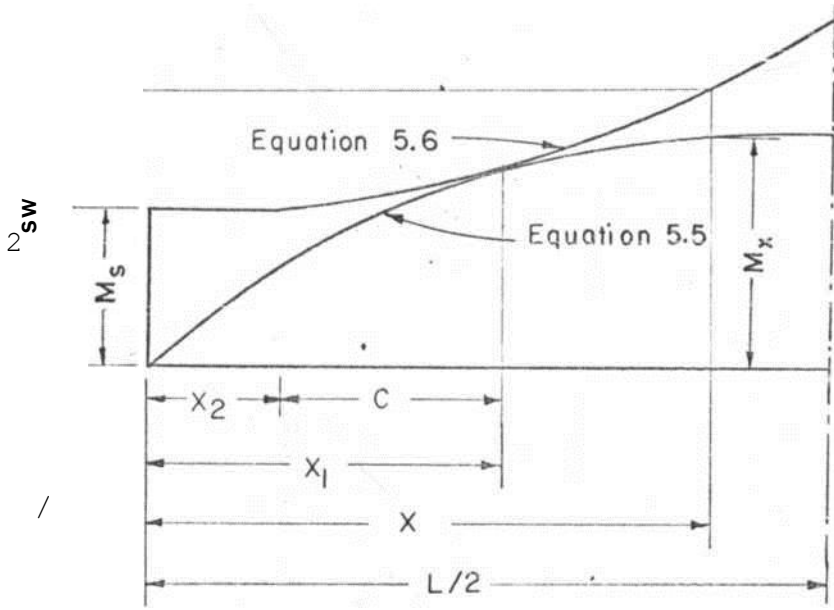


FIGURE 5. K Critical section.

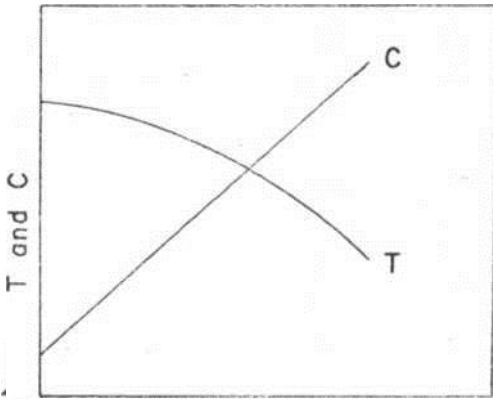


FIGURE 5-4: Concrete

and steel strain

of equations 5.12(b)

and
vari
ation.

5.17 for T (=C) and

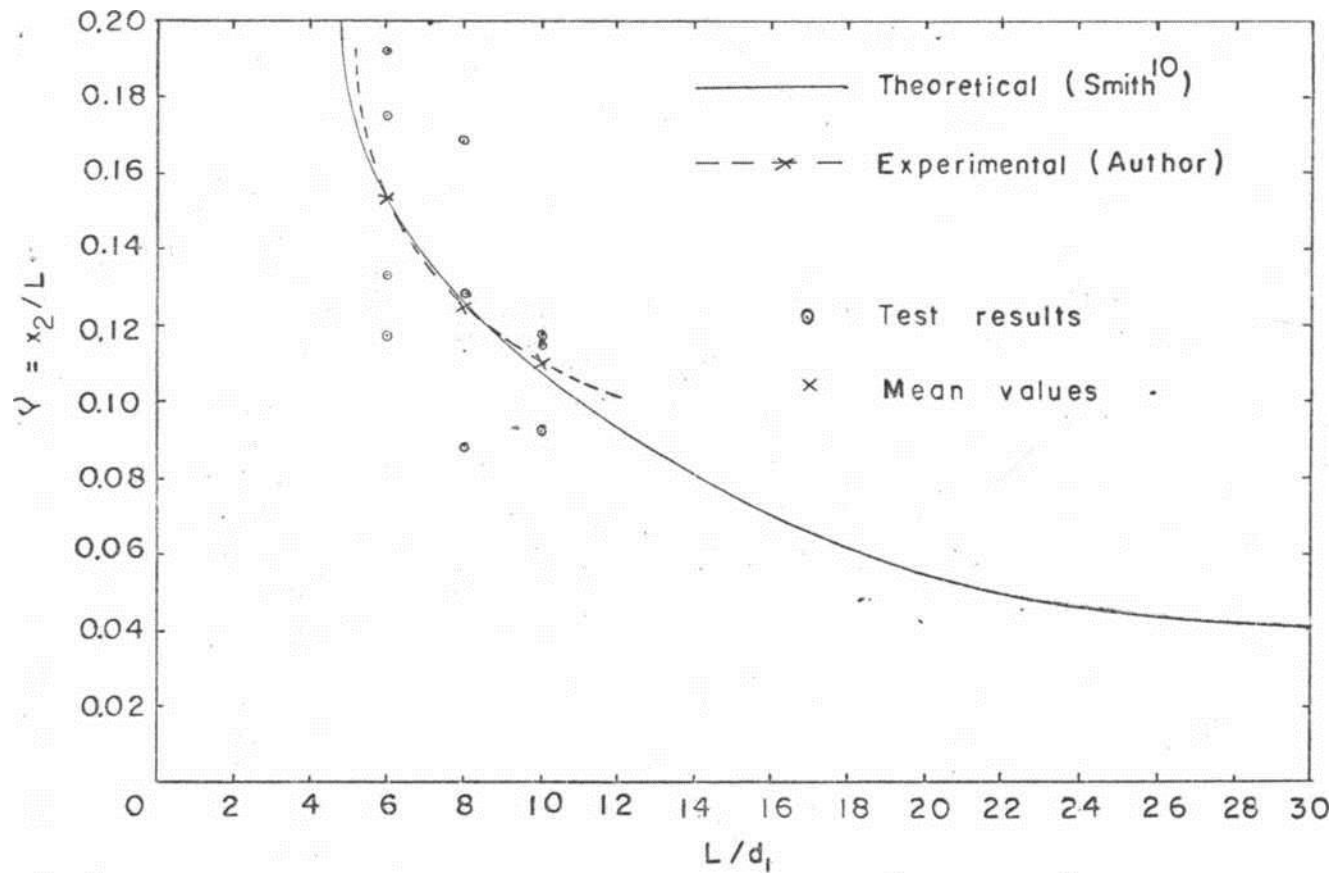


FIGURE 5.2: Relationship between x^2/L and L/d ,

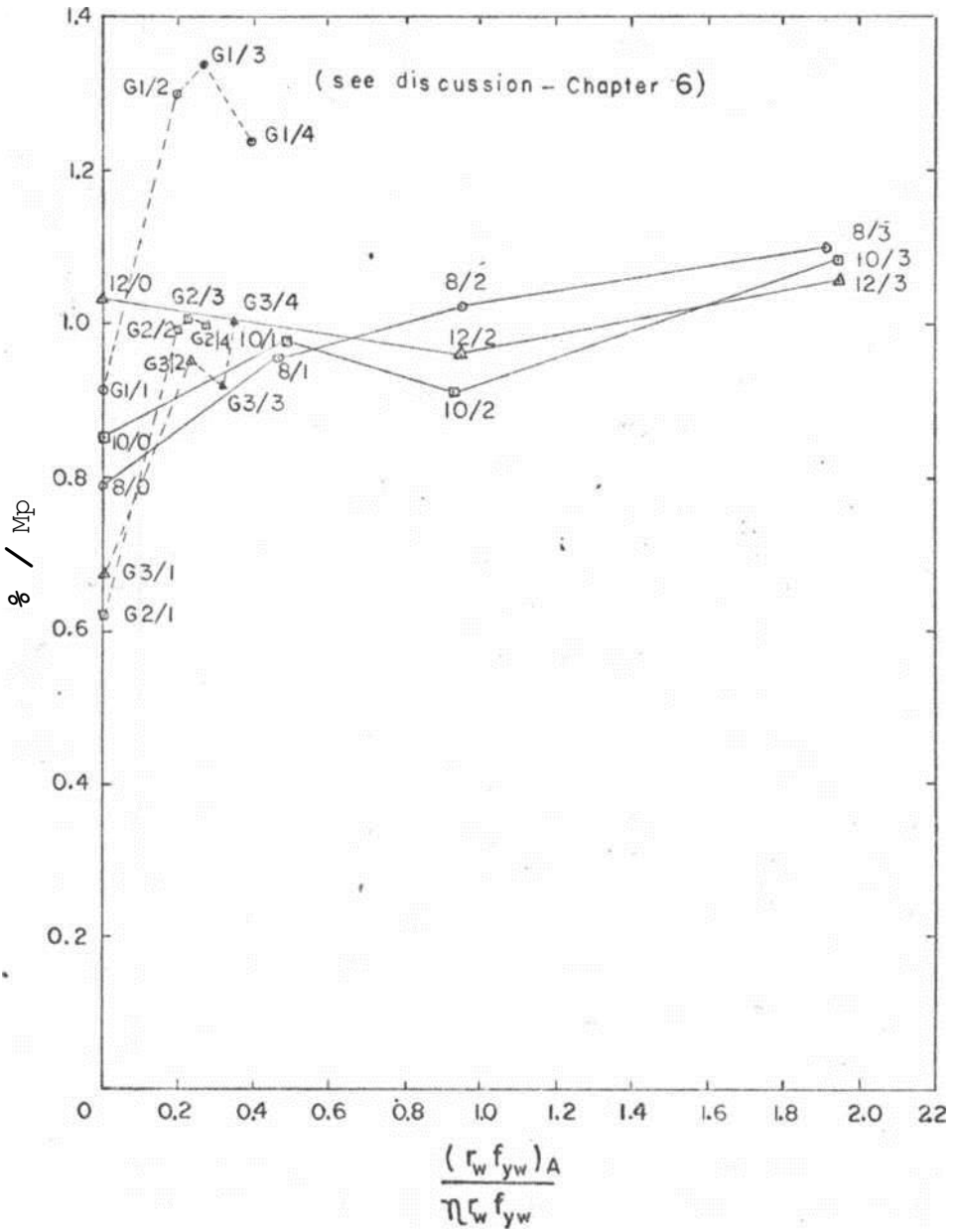


FIGURE 5.3: Relationship between ratio of actual web reinforcement to the calculated quantity and ratio of ultimate moment to flexural capacity.

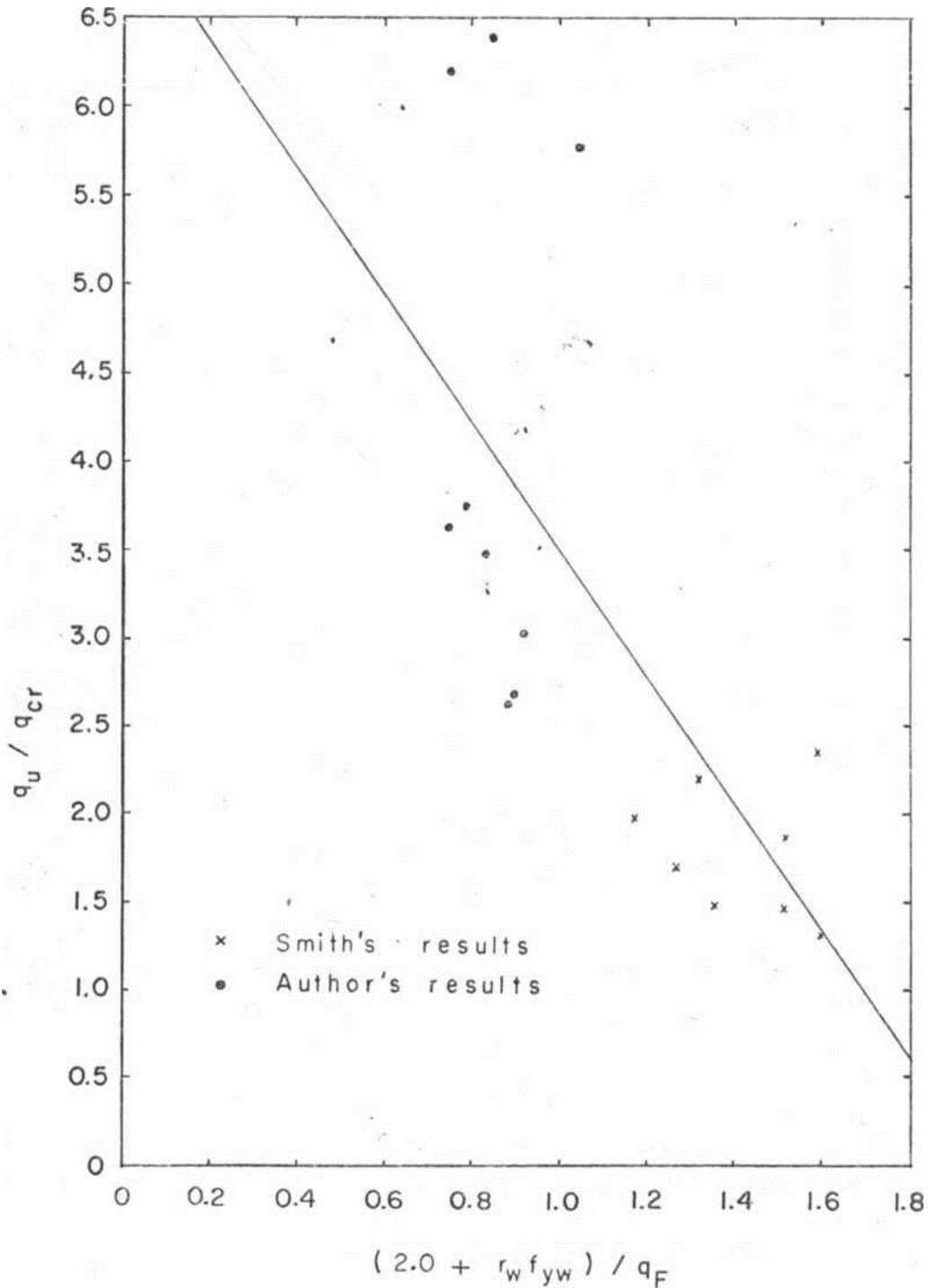


FIGURE 5.6; Development of regression equation

for predicting quantity of web reinforcement
considering shear stresses.

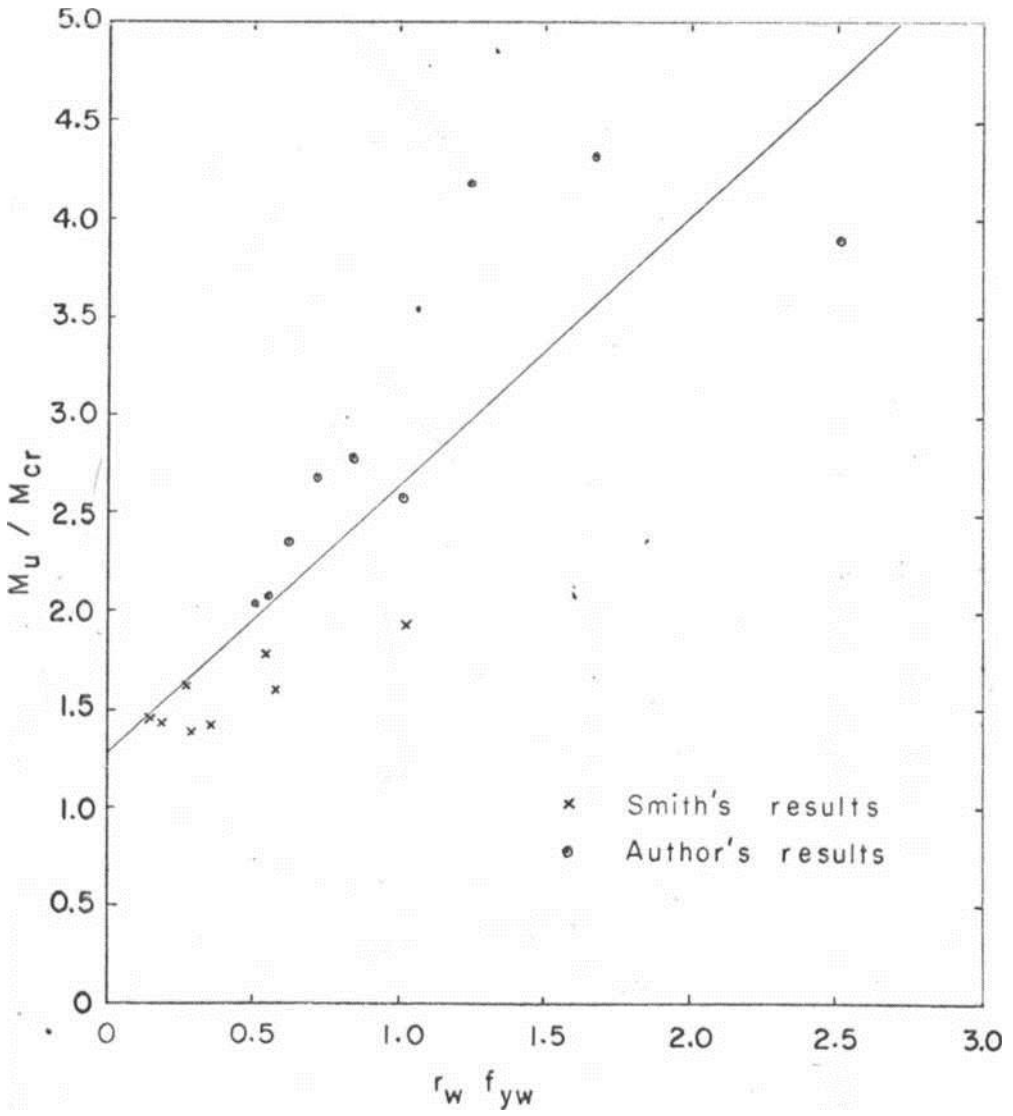
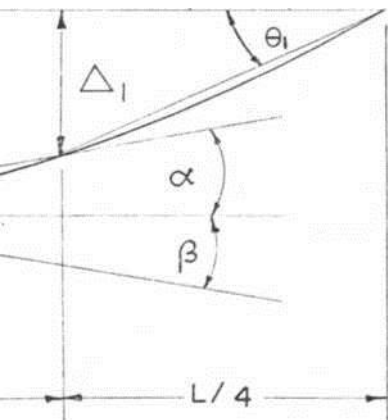


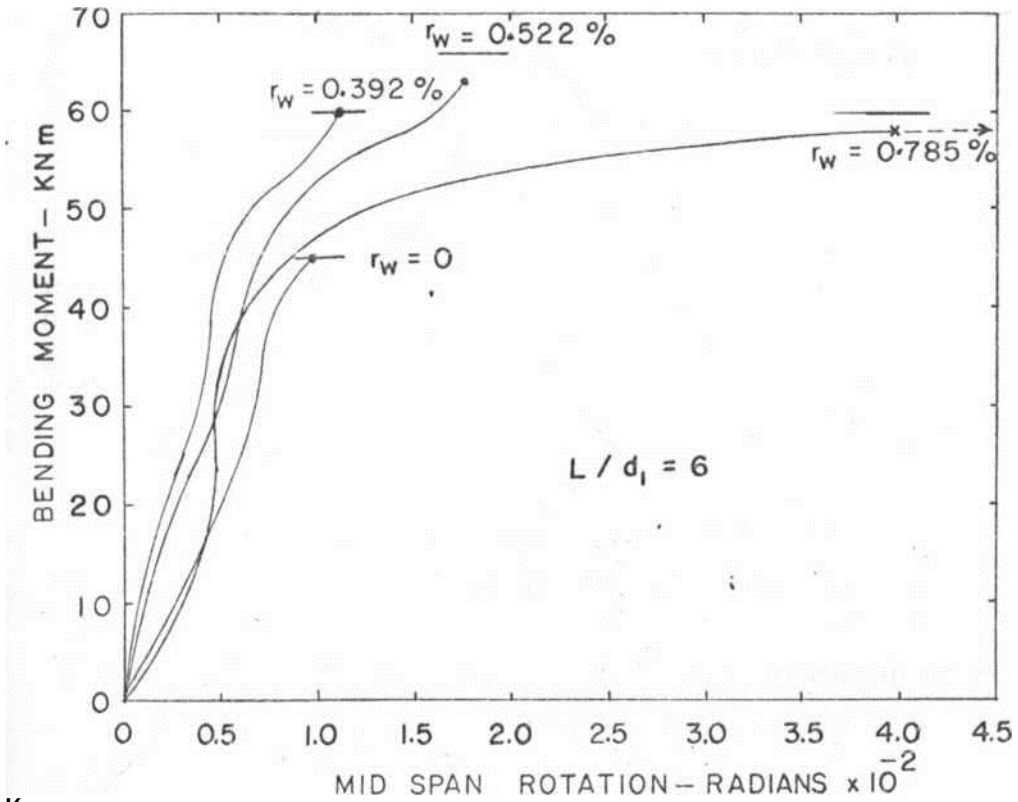
FIGURE 5.7'. Development of regression equation for predicting quantity of web reinforcement considering bending

mom e
nts.

FIGURE 5.8* Deflection **profile**
before failure.



of a beam



Key:

ultimate moment

indicates maximum rotation values
and ultimate moment at failure.

ultimate moment indicates the largest rotation values
measured due to removal of gauges and ultimate
moment at failure.



Influence of web reinforcement on mid
span rotations for $L/d_1 = 6$.

FIGURE 5.9(a):

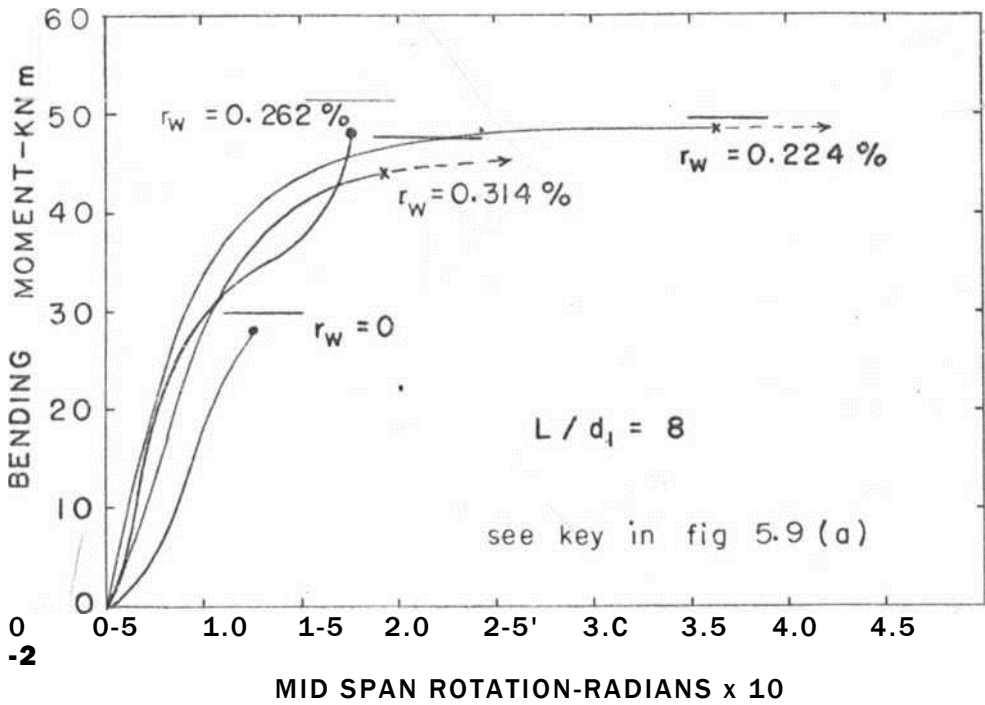


FIGURE 5.9(b): Influence of web reinforcement on mid span rotations for $L/d_1 = 8$.

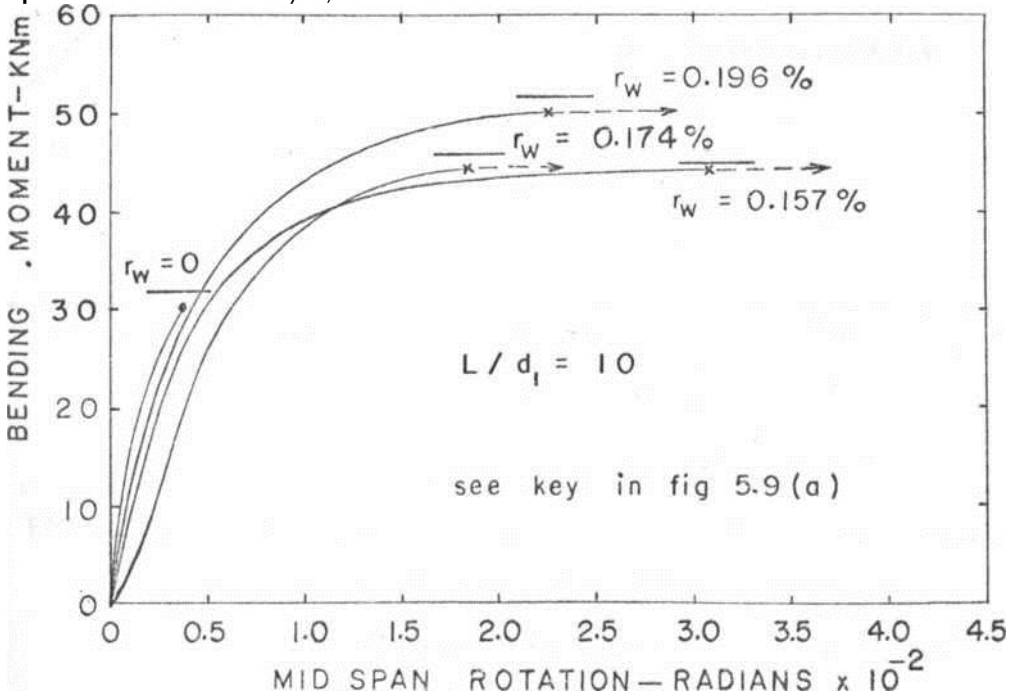


FIGURE 5.9(c): Influence of web reinforcement on mid span rotations for $L/d_1 = 10$.

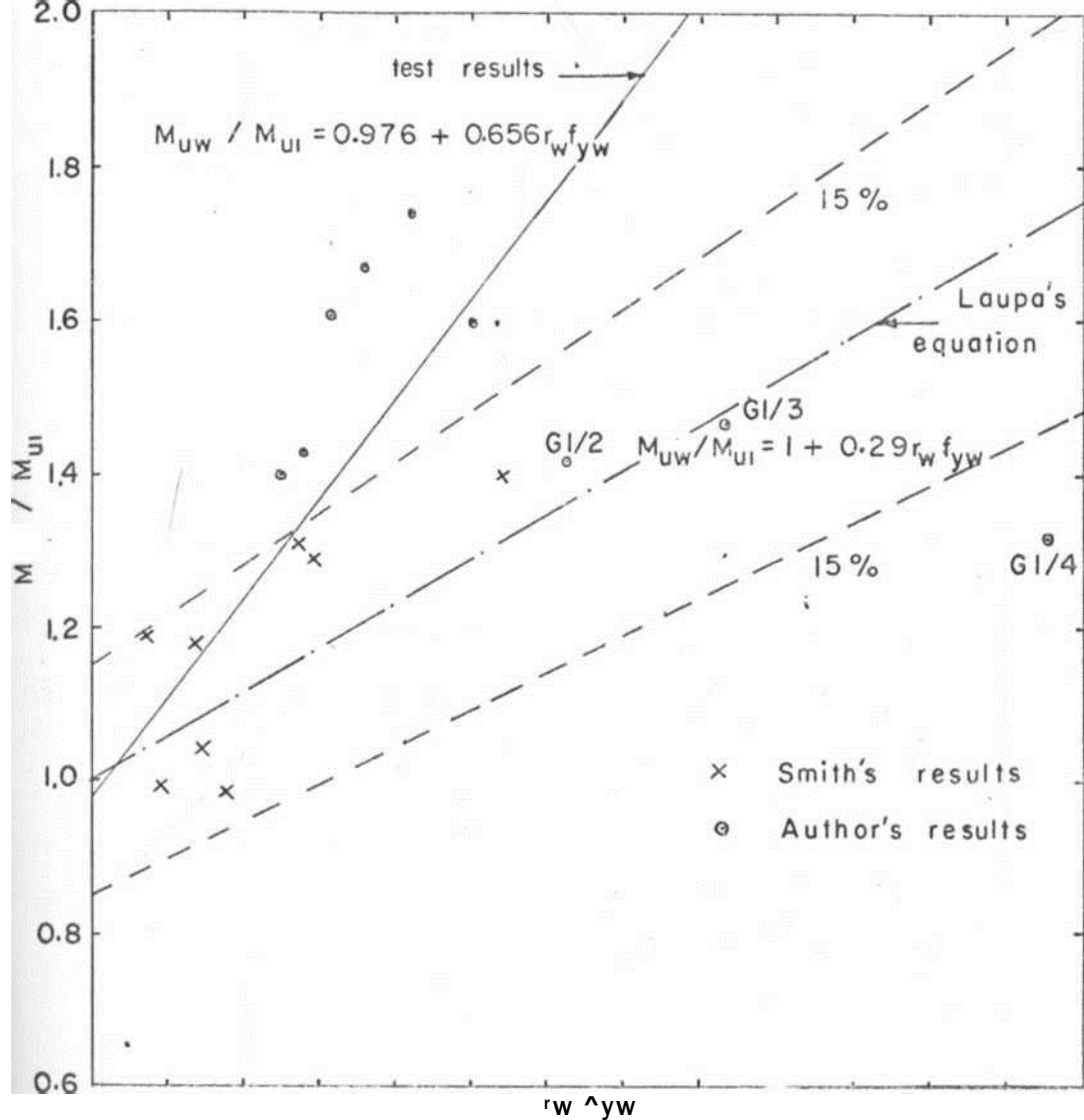


FIGURE 5.10.' Influence of web reinforcement on ratio of ultimate moment for beams with web reinforcement to ultimate moment for beams without web reinforcement.

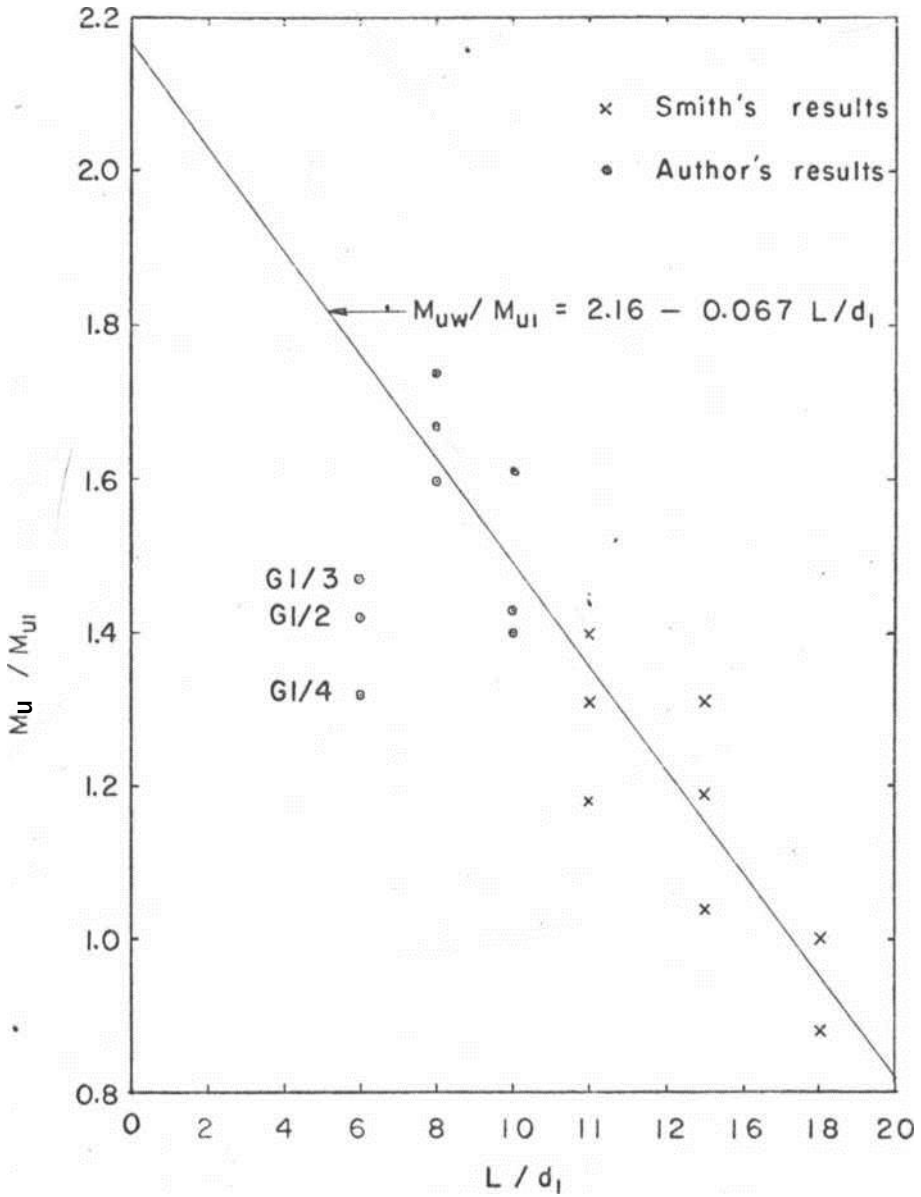
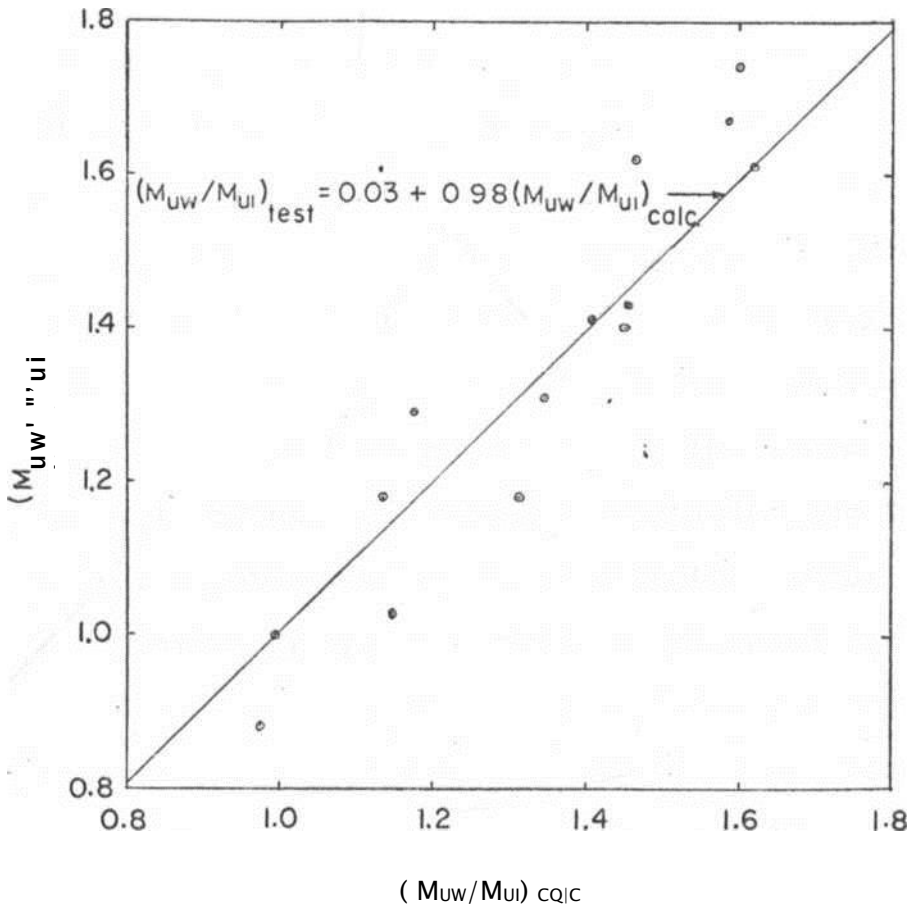


FIGURE 5.11! Influence of ratio of effective length to effective depth on ratio of ultimate moment for beams with web reinforcement to ultimate moment for beams without web r enforcement.



CHAPTER 6
CONCLUSIONS AND DISCUSSION

The modulus of rupture used for the calculations based on Smith's equations was calculated as defined in his paper, i.e. $f^* \approx 79/f_c^{0.2} U_{fnm}$.

It is noted from the strain readings that the maximum concrete strains recorded for the three beams of group G-1 with web reinforcement were very high relative to those of the other beams. It can be concluded from this evidence that the three beams did, in fact, exceed the flexural capacities and there was no experimental or testing machine error. An examination of the test results indicated that the

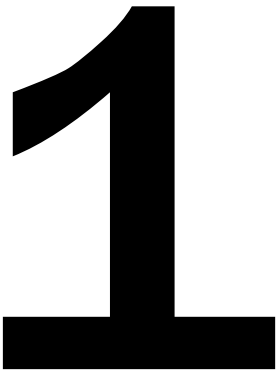


FIGURE 5.12. Comparison of test and calculated ratios of ultimate moment for beams with web reinforcement to ultimate moment for beams without web reinforcement.

closeness of the contact steel plates placed on the top of the beam for transmission of the point loads could be an influencing factor on the strength of the beams . in group G-1. The lever arms obtained from the ultimate moments and the tensile forces resisted by the main steel at failure and contained in Table 4.2. show that the lever arm was greatest in beams G1/2, G-1/3 and G1/4. Indeed in the first two, the calculated lever arm exceeded the effective depth and in G1/4 it was just less than the effective depth. In the remaining beams which failed in either flexure or combined shear and flexure, the lever arm was far less than the effective depth.

Since the testing programme and equipments were maintained the same for all the beams tested, it was not possible to account for the high values of lever arm for the three beams of group G-1. Probably in beam G1/2 which failed in combined shear and flexure, the increase beyond calculated flexural capacity was due to horizontal friction at the supports and to the closeness of the contact steel plates. These plates as shown in Figure 4.5 were 12.5 mm thick and the distance between them was only 50mm. In groups G-2 and G-3 the spacings were 100 and 150 mm respectively. It can therefore be stated that 12.5mm thick steel plates were bedded on to almost the entire top surface of the beams in group G-1. This method of loading where contact steel plates were too close is similar to the one employed by Krefeld and Thurston,

and was alleged by Smith (10) on the ground that it suggests a considerable gain of shear strength might have resulted. Since gain of shear strength does not strengthen beams failing in flexure, the increase beyond calculated flexural capacity in beams G1/3 and G1/4 which failed in flexure was probably due to horizontal friction at the supports. However this does not appear to have affected the beams of the other two series tested.

, The study of the strain distribution confirmed the result of the work of Watson and Mathey (8) "that following the formation of a diagonal crack, the upper

portion of the beam within the shear span become subjected to bending which causes it to develop a curved surface concave toward the mid plane.

The study of the crack formation revealed that diagonal tension cracks do not always originate as flexural cracks as generally accepted. It has been shown that the origin of the diagonal cracks depend the relationship of the bending moment and the shear force. While the diagonal cracks originate as flexural cracks in the regions of high $M/Qd-j$, they may also originate as pure web shear cracks in the regions already uncracked in bending. Such regions are always close to the supports where $M/Qd-j$ is low.

Within the variables studied, equation 5.23 was suggested for predicting the quantity of web reinforcement required to attain flexural capacity. This equation, however, has a shortcoming because its development was based on a limited number of test results and all the factors that influence shear resistance of reinforced concrete beams and their full range of variability had not been taken into account. The validity of the development of the reported equation needs to be established by a more comprehensive test programme.

Regarding rotations, it has been shown that the rotation capacity of beams without web reinforcement is less than that of beams with web reinforcement.

However the limited test results indicated no relationship

between rotations and either the amount of web reinforcement or the effective length/effective depth ratio.

The equation derived for the contribution of web reinforcement was based on a limited number of test results and the validity of its development needs to be established by more test results.

This investigation illustrates that an attempt to find a single equation applicable to all beams normally encountered in practice is only possible when all the factors that influence shear resistance have been fully studied. Unfortunately there is a considerable lack of test data of beams failing in shear under uniformly distributed loading.

Although the problem of predicting the amount of web reinforcement required for beams subjected to uniformly distributed loading to fail in flexure cannot be claimed to have been solved, this investigation has added some test data to the few already available.

CHAPTER 7

RBCOMIvIBNDATIONS FOR FUTURE

WORK 7. 1 TEST PROGRAMME

In view of the fact that the results of the equations established on the basis of shear stresses vary in opposite directions for the beams tested by Smith and by the author as the value of τ increases and that the results of the suggested equation have a discontinuity for the two sets of test data, it is apparent that further work in this field of reinforced concrete beams failing in shear under uniformly distributed loading is necessary. To this end, it is recommended that similar beams, of L/d varying from say, 4 to 20 be made and tested under the same conditions. The test data obtained would, it is hoped, enable the development of an empirical expression applicable to all beams used in practice. Future research would also be aimed at varying the flexural Capacity and shear-compression capacity in an attempt to find the influence of the web reinforcement on the ratio of the two capacities.

7.2 TESTING- ARRANGEMENT

Whereas the method of applying uniform loading by a system of point loads appears satisfactory, future work is needed to verify whether this is the best method or some other method should be used.

i

When a system of point loads is used to simulate uniform loading, it has been found that the clearance between the contact steel plates may be an influencing factor on the strength of beams failing in shear or combined shear and flexure. This aspect calls for future research to find whether applying the point loads through steel rollers only is sufficient.

7.3. OBSERVATION OF CRACKS.

For the purpose of determining the diagonal cracking load correctly, it is recommended that a more accurate method of observing crack propagation be employed. Such a method would enable accurate determination of the critical section for the major diagonal crack-initiation and for shear-compression failure. A suggested method would be to coat the surfaces of the beam with fluorescent penetrating dyes which pass into cracks and can be traced by illuminating them with a fluorescent light. Such dyes were not available for use in the testing of the beams considered in this study.

7.1. THEORETICAL APPROACH.

As more and more experimental work is done on beams failing in shear under uniform loading, there will be a better understanding of the factors that influence the behaviour and strength of such beams. It would be worthwhile to attempt a theoretical approach and perhaps use modern techniques to solve the problem.

Now computer methods are available which can be developed to treat the shear problem. An outstanding example of such a development is the 'finite element' technique which has gained popularity in recent years.

The application of the finite element technique would be based on the study of elastic and plastic behaviour of reinforced concrete beams. The analysis would involve the

idealisation of a reinforced concrete beam as an assemblage of finite elements interconnected at nodal points, the elements in concrete and steel being characterised *by* the different structural properties of the different materials, i.e. Young's modulus, Poisson's ratio and shear modulus and the thickness of the elements.

A computer program written such that the breakdown of the dowel force and the consequent redistribution of the internal stresses that occur after diagonal cracking are taken into account, may be used to determine stress and strain distributions, The author attempted to use finite element technique to treat the problem of shear failure in reinforced concrete beams under the guidance of Mr. D. Johnson, now of the University of Wales, Swansea, but the number of elements and nodal points suitable for the beams* considered exceeded the limitations of the computer at the University of Nairobi.

7.5 T-BEAMS.

Since T - beams provide a better representation of the reinforced concrete beams normally used in many civil engineering structures such as under building slabs and bridge decks, it is recommended that the experimentation discussed in this study be extended to T - beams where the uniformly distributed loading may be applied on the flanges•

BIBLIOGRAPHY

1. HOGNE3TAD, E. (1931) What do we know about diagonal tension and web reinforcement in concrete. University of Illinois Bulletin. No.5.
2. HOGNESTAD, E., HANSON, N.1. AND Me HENRY, D. (1933) Concrete stress distribution in ultimate strength design. Journal of the American Concrete Institute. **J1**, December, 433-479.
3. B.S.CP 114(1963) Code of Practice for Reinforced Concrete. British Standards Institution, London.
4. LAUPA, A., SIESS, C.P.and NEWMARK, N.M. (1933) Strength in shear of reinforced concrete beams. University of Illinois Bulletin. No. 428.
3. ZWOYER, E. M. and SIESS, C.P. (1934) Ultimate strength in shear of simply supported prestressed c concrete beams without web reinforcement. Journal of tie American Concrete Institute.
26. October. 181 - 200.
6. MOODY, K.G. and VIEST, I.M. (1933) Shear strength of reinforced concrete beams, Part 4 - Analytical • Studies. Journal of the American Concrete Institute. 26. March, 697 -730.
7. JONES, R. (1936) Ultimate strength of reinforced concrete beams in shear. Magazine of Concrete Resegrch, 8. August, 69-84.

8. WATSTEIN, D. and MATHEY, R.G. (1938) Strains in beams having diagonal cracks. Journal of the American Concrete Institute, 30. December, 717 - 728.
9. SMITH, R.B.L. (1966) The interaction of moment and shear on the failure of reinforced concrete beams without web reinforcement. Civil engineering and Public Works Review, 61, June, 723-723, July 869-872, August 967-970.
10. SMITH, R.B.L. (1970) Shear reinforcement of reinforced concrete beams subject to distributed loading. Magazine of Concrete Research. 22. March, 17-24.
11. RAMAIRISHNAN, V, (1969) Behaviour and ultimate strength of reinforced concrete in shear. PSG College of Technology, Coimbatore.
12. REGAN, P.E. (1971) Behaviour of reinforced and prestressed concrete subjected to shear force. Proc. of Institution of Civil Engineers. Supplement (XVII).
13. WHITNEY, C.S. (1937) Ultimate shear strength of reinforced concrete flat slabs, footings, beams and frame, Journal of the American Concrete Institute. 29. October, 263-298
- 1L. OJHA, S.K. (1971) The shear strength of uniformly loaded beams without web reinforcement. Magazine of Concrete Research. 23. September, **111-118**.
13. RENSAA, E.M. (1958) Shear, diagonal tension and anchorage in beams, Journal of the American Concrete

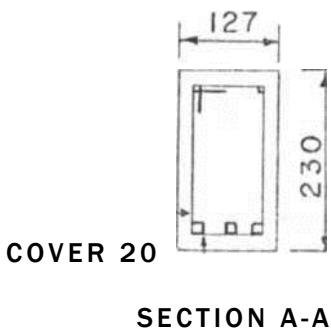
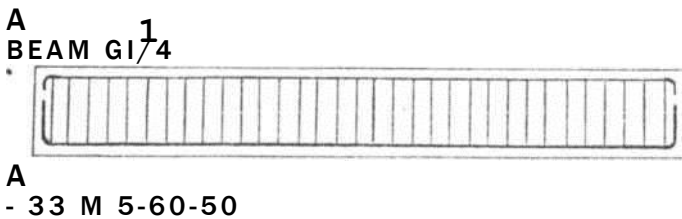
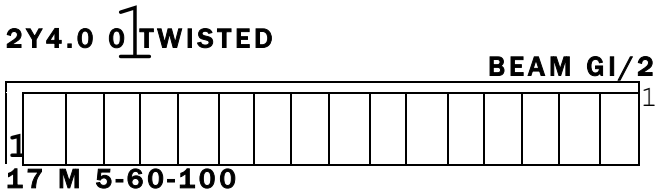
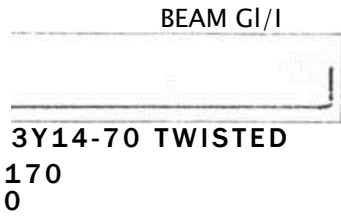
Institute, 30. December, 695-715.

16. EVANS, R.H. and KONG, F.K. (1967) Shear design and B.8. CP 114.. The structural Engineer. 45. April, 153-158.
17. SHEAR STUDY GROUP OF THE INSTITUTION OF STRUCTURAL ENGINEERS (1969) The shear strength of Reinforced Concrete Beams. Series No. 4-9. January.
18. B3 1881 (1970) Methods of Testing Concrete. British Standards Institution, London.
19. JONES, L.L. A Theoretical Solution for the Ultimate Strength of Rectangular Reinforced Concrete Beams Without Stirrups. Cement and Concrete Association.
20. BERNAERT, S. and SIESS, C.P. (1956) Strength in shear of reinforced concrete beams under uniform load. University of Illinois Bulletin No. 120.
21. SUBBIAH, K. and SMITH, R.B.L. (1958) The influence of shear on the moment of resistance of reinforced concrete beams. The Structural Engineer. 36. November, 377-384..
22. HOGNESTAD, E., HANSON, N.W., MAGURA, D.D. and MASS, M.A. (1963) Shear strength of slender continuous reinforced concrete T-beams. Journal of the Portland Cement Association. 3. September, 22-33.
23. PEREDY, J. and VISY, Z. (1961) The economic design of members subjected to shearing (ultimate- load method). Concrete and Constructional Engineering, February and March. Butler and Tanner Ltd., London.

22. BROCK, O. (1960) Effect of shear on ultimate strength of rectangular beams with tensile reinforcement. Journal of the American Concrete Institute. 31. January, 619-637.
23. ELSTNER, R.C. and HOGNESTAD, E. (1936) Shearing strength of reinforced concrete slabs. Journal of the American Concrete Institute, 28[^] July, 29-38.
26. MORROW, J. and VIEST, I.M. (1937) Shear strength of reinforced concrete frame members without web reinforcement. Journal of the American Concrete Institute. 28. March, 833-869.
27. HOGNESTAD, E. (1933) Shearing strength of reinforced concrete column footings. Journal of the American Concrete Institute. 23. November, **189-208**.
28. HAMMOND, F.A. and SMITH, R.B.L. (1960) A preliminary study of ultimate load moment-shear interaction in reinforced concrete beams. Civil Engineering and Public Works Review, **pb**. June, **792-791**.

APPENDICES

- A Physical properties of beams
- B Plates
- C Tables of concrete strains
- D Table of details of beams and test
results of Smith
- E Calculations for figure 5*3
- P Tables of rotations*

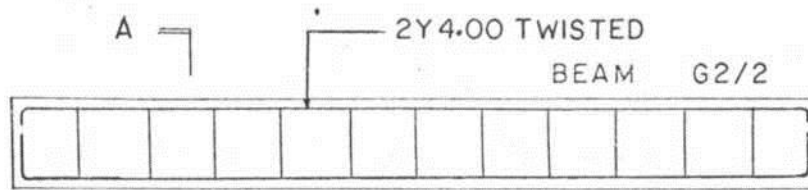
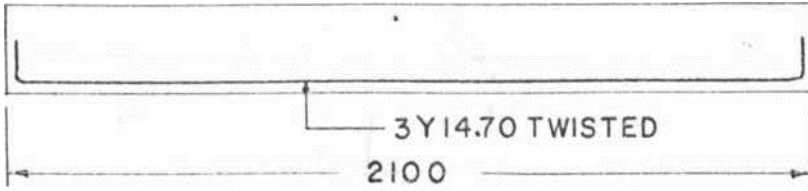


NOTES:

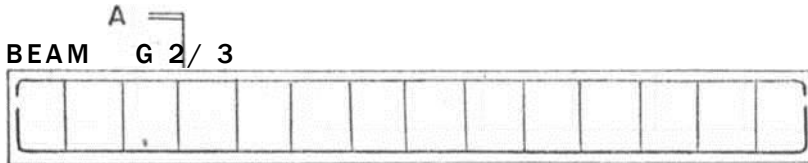
- (1) SECTION A-A HAS ALL BEAMS EXCEPT G1/1, G2/1 AND G3/1 WHICH HAVE NO TOP BARS AND STIRRUPS.
- (2) DIMENSIONS IN mm

FIGURE Ai: Physical properties of group G1 beams.

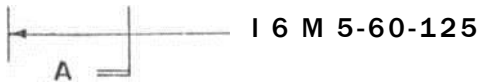
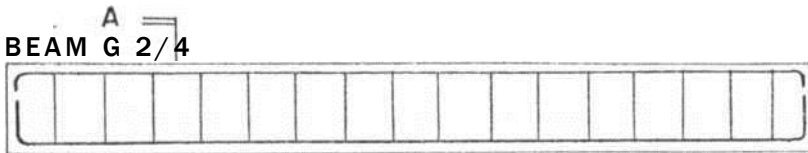
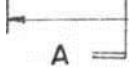
BEAM G2/1



I I M 5*60- 17 5- ----- v-



13 M 5.60-150



(SEE NOTES IN FIG. A1)

8

FIGURE A21 Physical properties of group G2 beams.

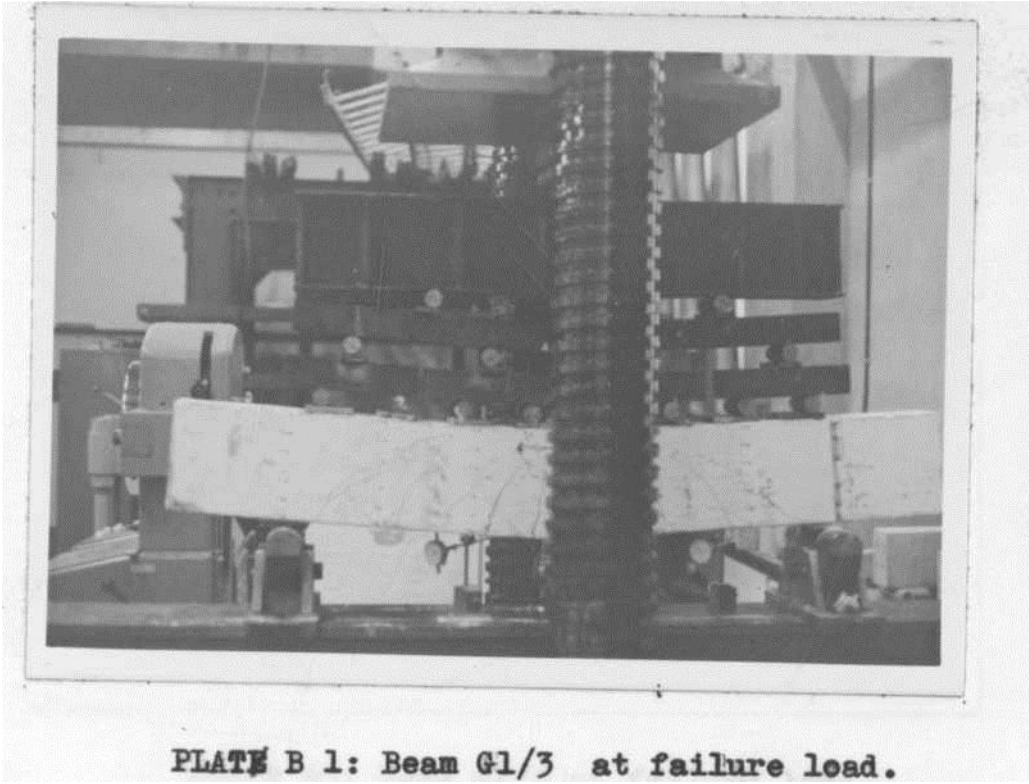
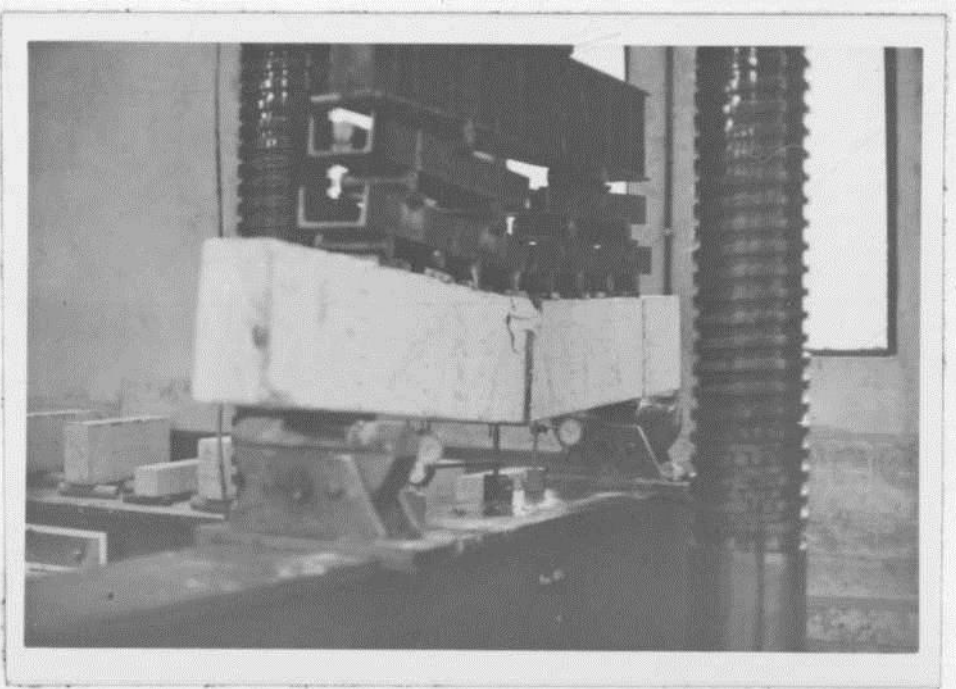


PLATE B 1: Beam G1/3 at failure load.



ms.

PLATE B 2s Beam G1/3 showing concrete spalling*

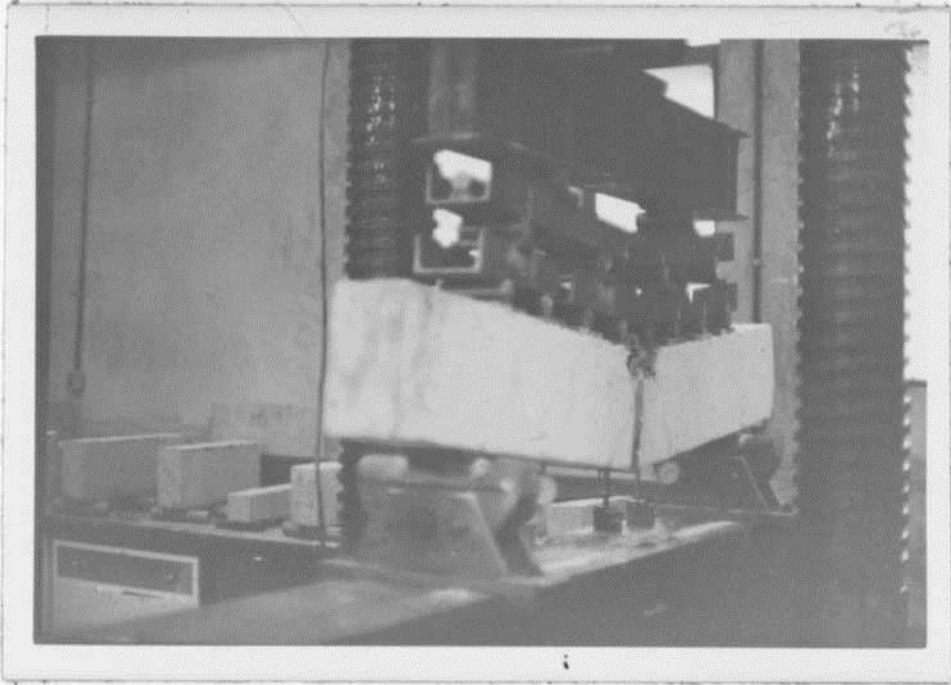


PLATE B3: Beam G1/4 at failure load.

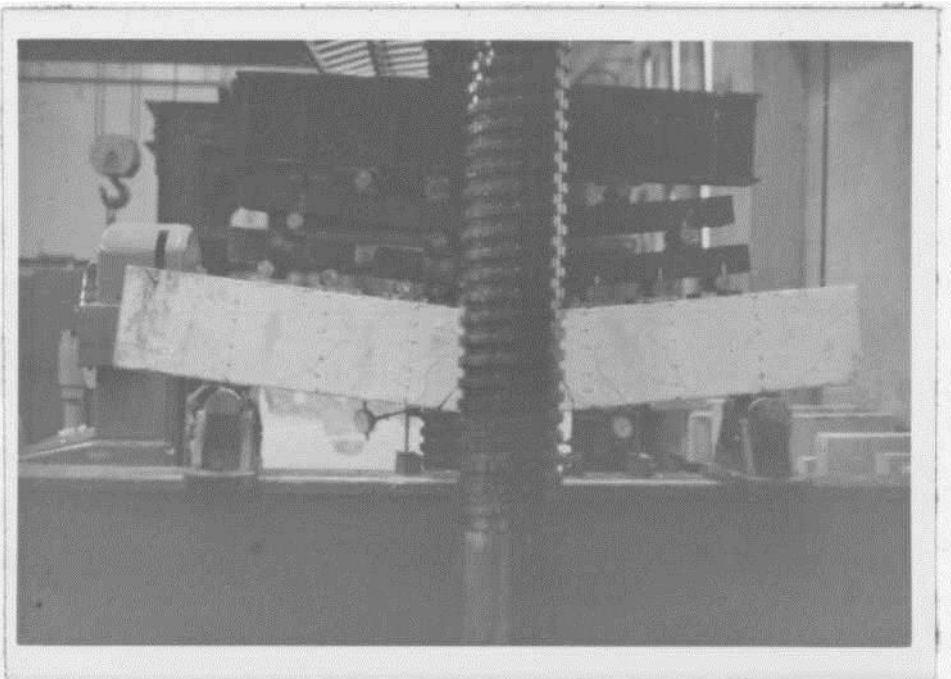
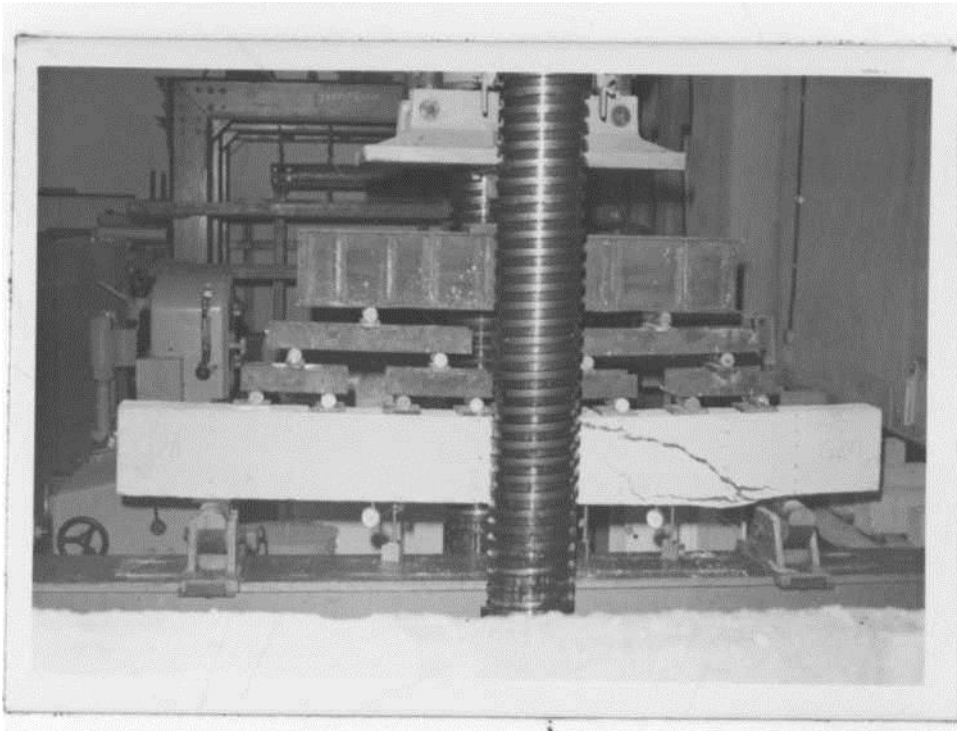


PLATE B4: Beam G1/4 showing concrete spalling.

PLATE B8: Shear-compression failure of
beam G2/2.



**PLATE B5: Diagonal tension failure of
beam**

G2/1.



**PLATE B6: Close-up of the failure diagonal
crack of beam G2/1***

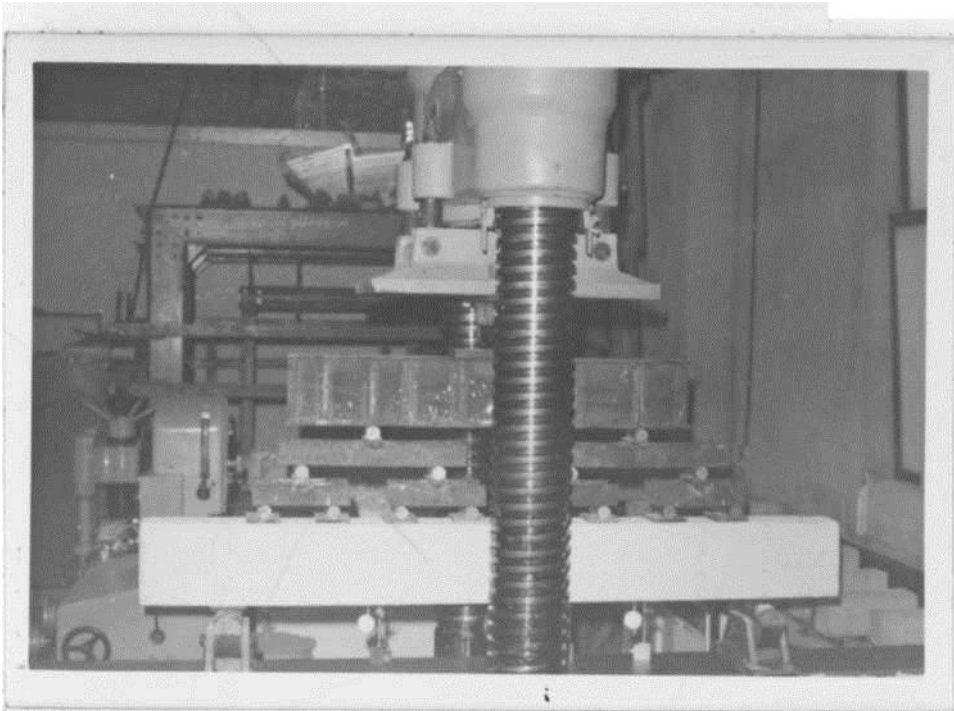


PLATE B7: Beam G2/2 before load application.

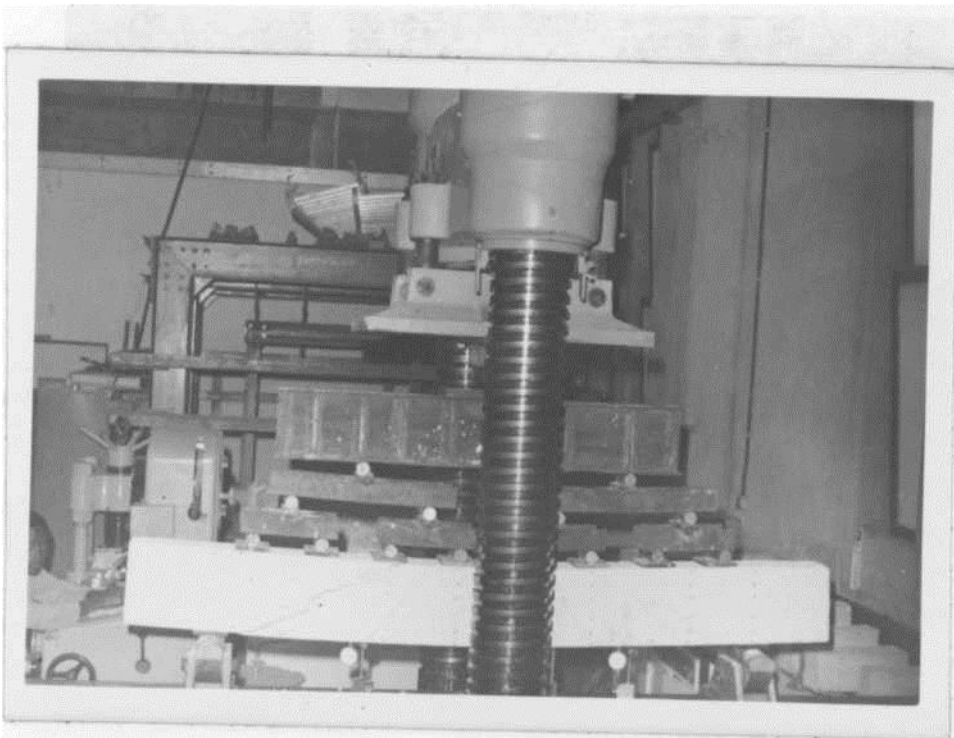


PLATE B8: Shear-compression failure of beam G2/2.

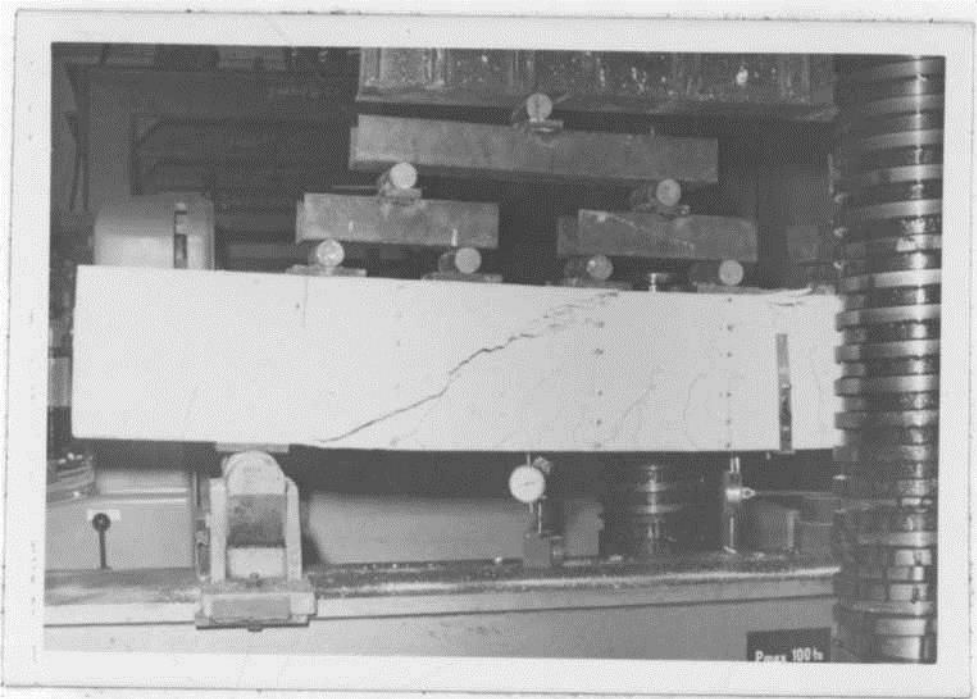


PLATE B 9: Close-up of failure section of beam G2/2.

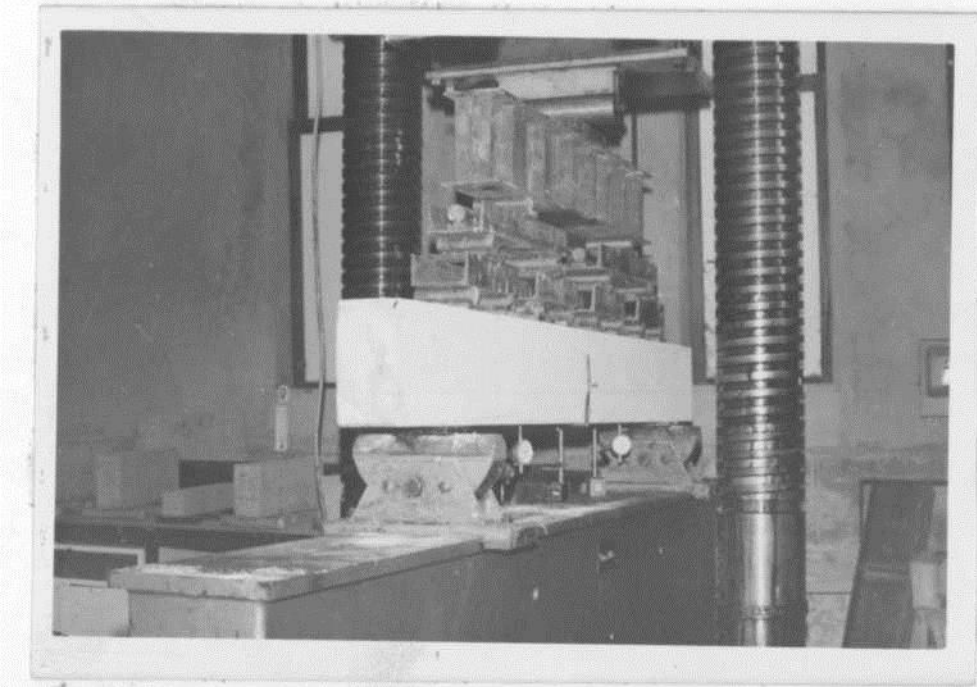
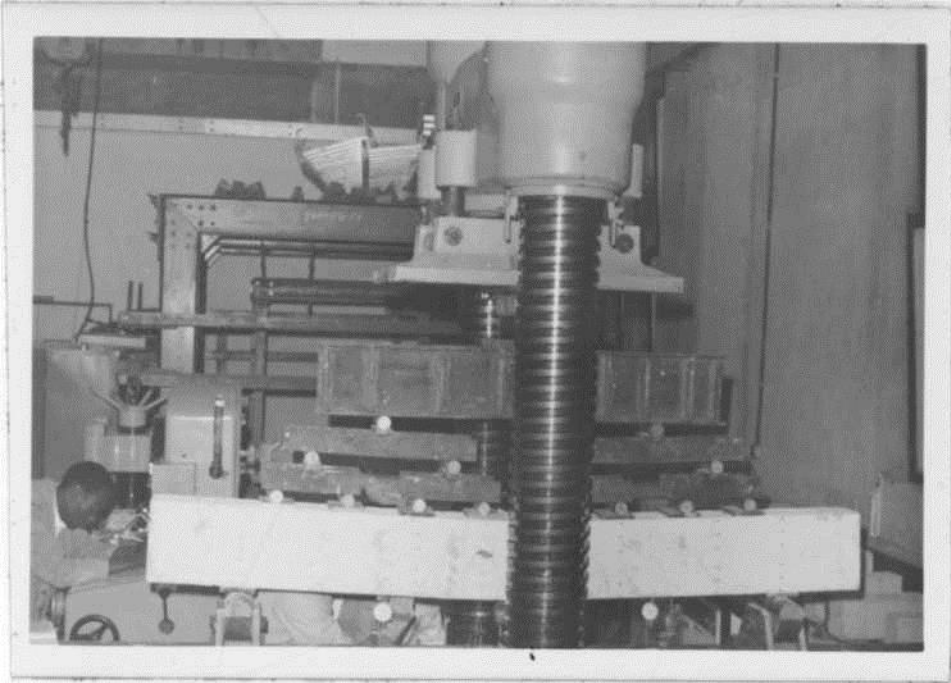


PLATE B 10: Beam G-2/3 before load application.



PLATS B 11: Diagonal cracking of beam
G2/3 during loading.

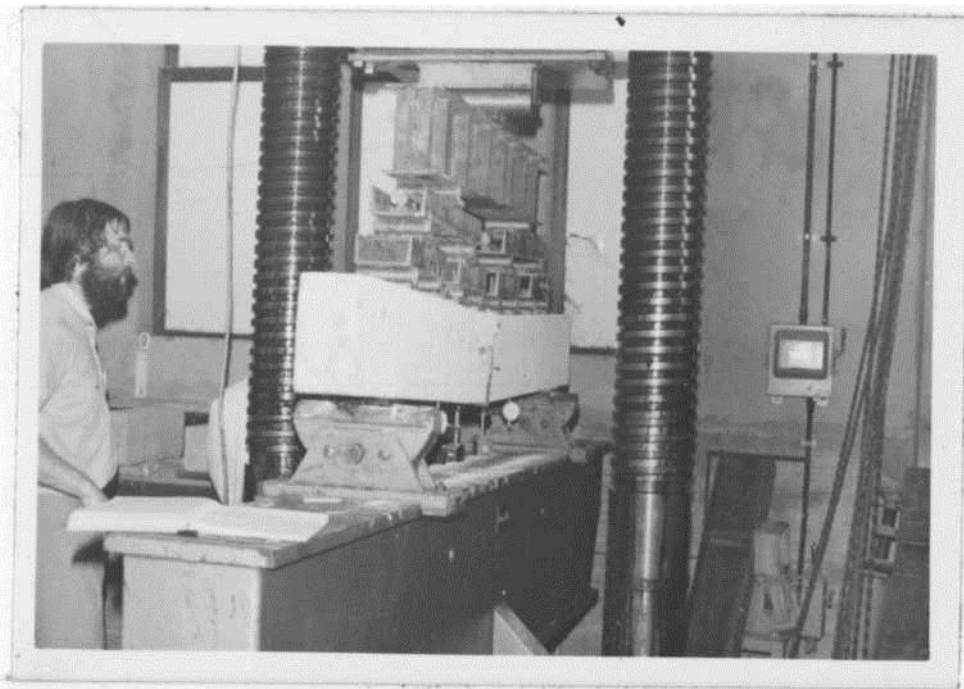


PLATE B 12: Combined shear and flexure failure
of beam G2/3. Note concrete spalling



PLATE B 13: Diagonal cracking of beam
G2/L during loading.

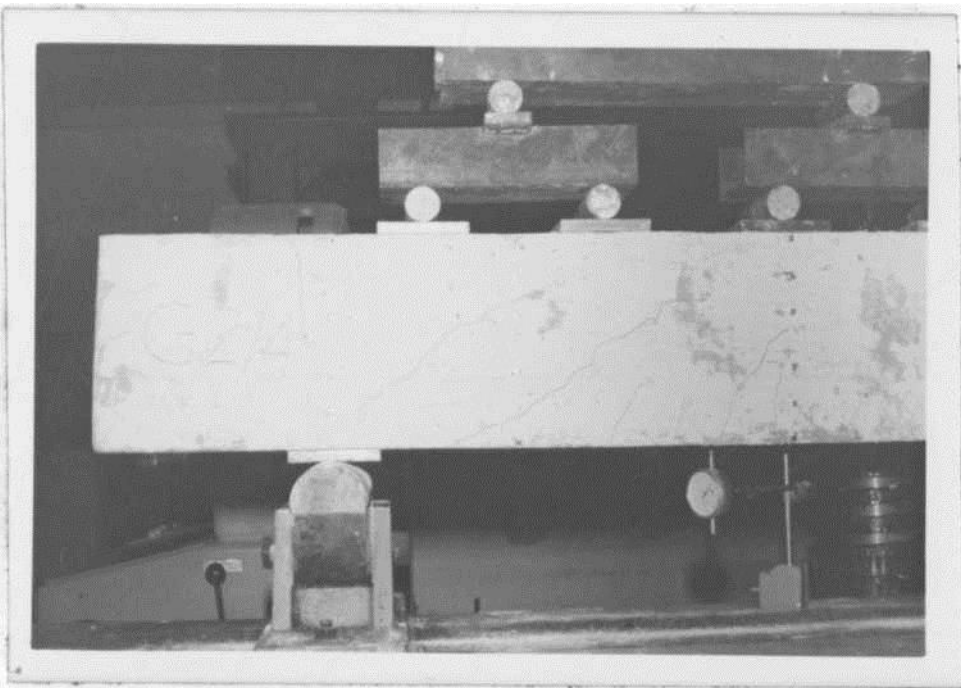


PLATE B 11: Close-up of diagonal cracks of
beam G2/L during loading.

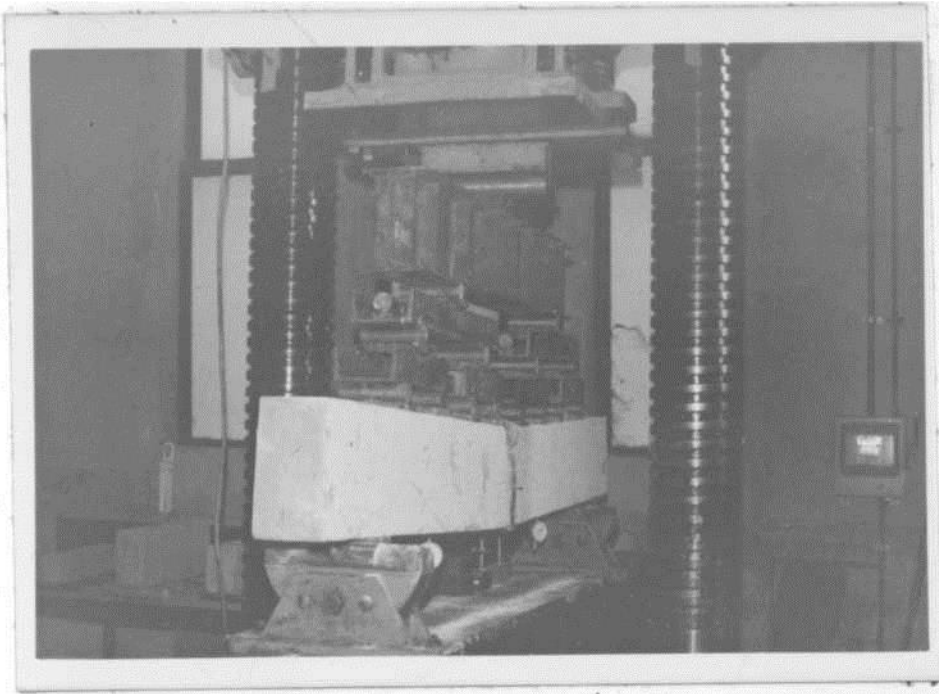


PLATE B 15: Flexural failure of beam G2/4.

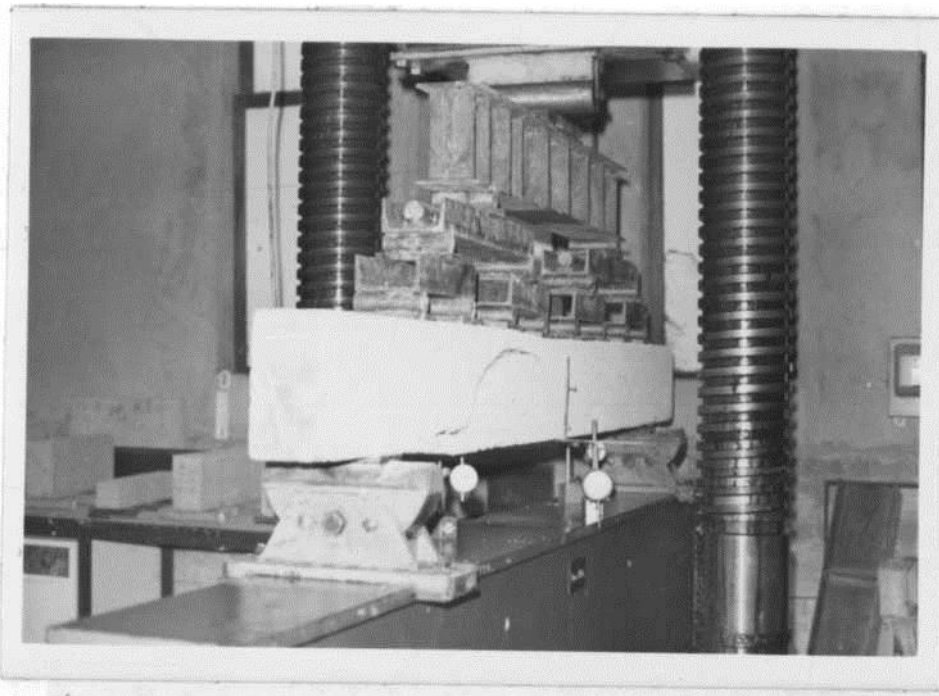


PLATE B 16: Diagonal tension failure of beam G3/1•

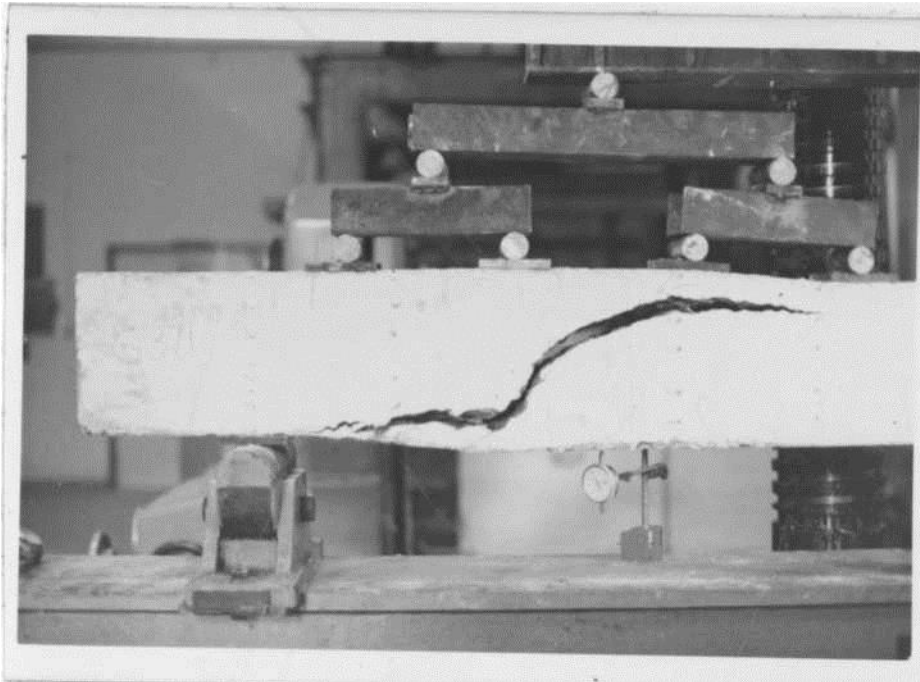


PLATE B 17: Close-up ϵ_t failure diagonal crack of beam G3/1*

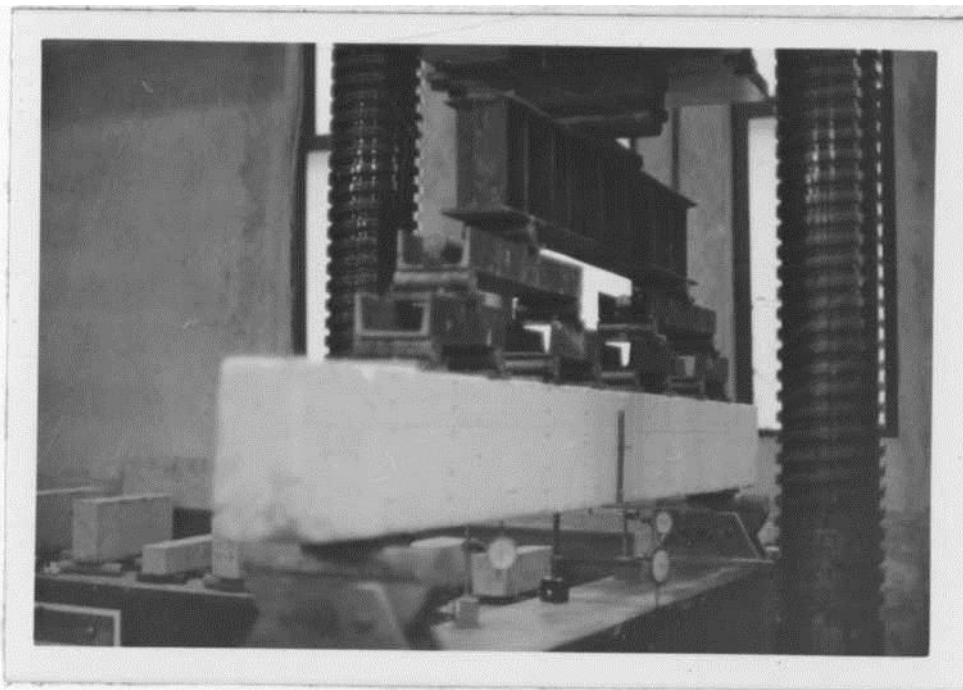


PLATE B 18: Beam G3/2 before load application.

PLATE B 16: Diagonal tension failure of
beam G3/1•

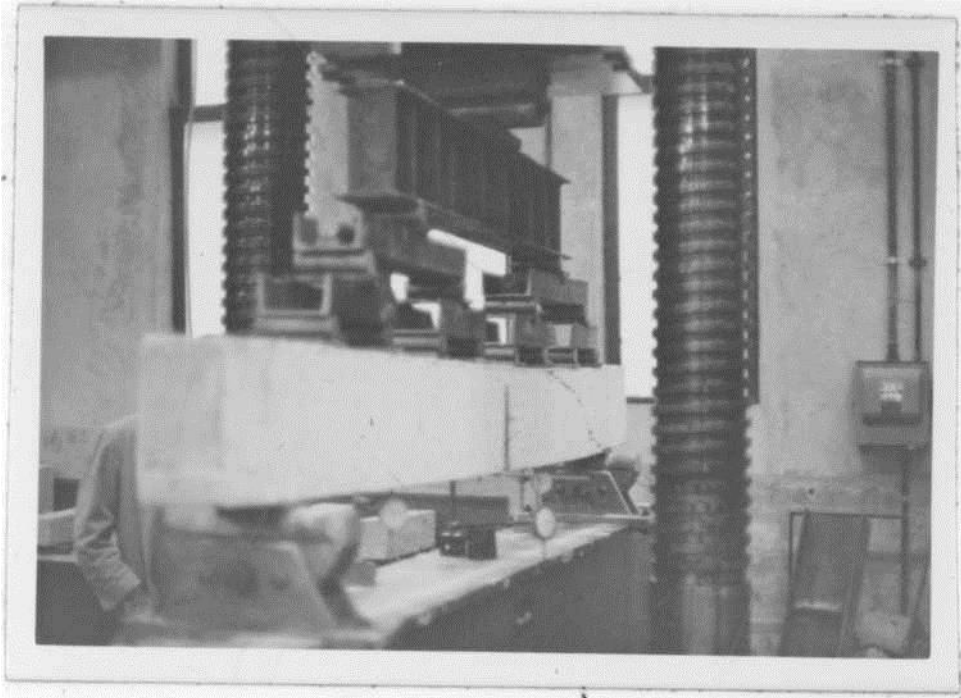


PLATE B 19: Shear-compression failure of beam G3/2.

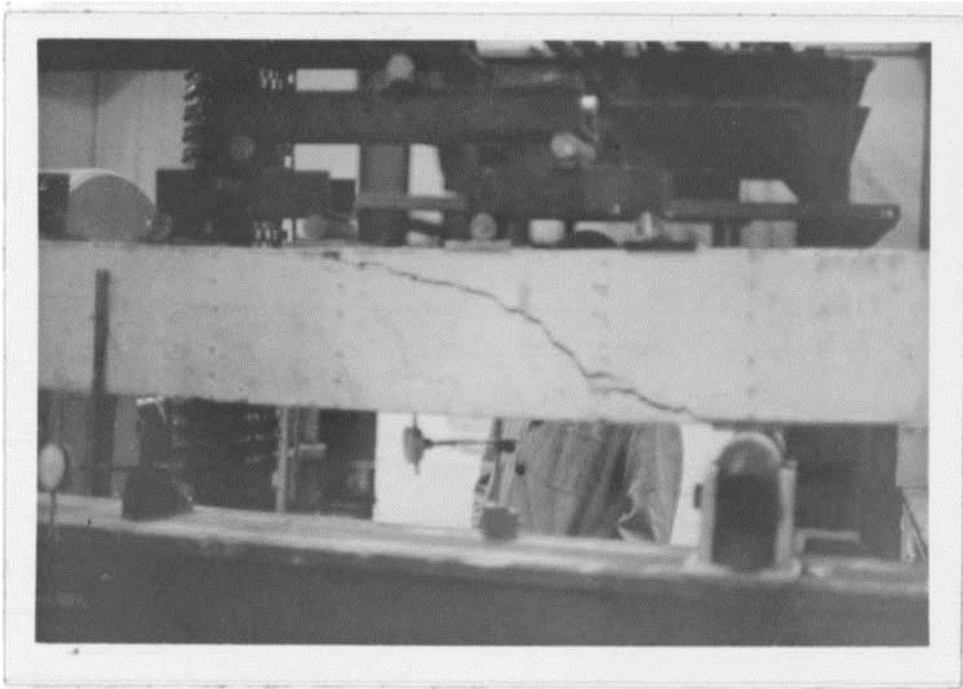


PLATE B 20: Shear-compression failure of beam G3/3.

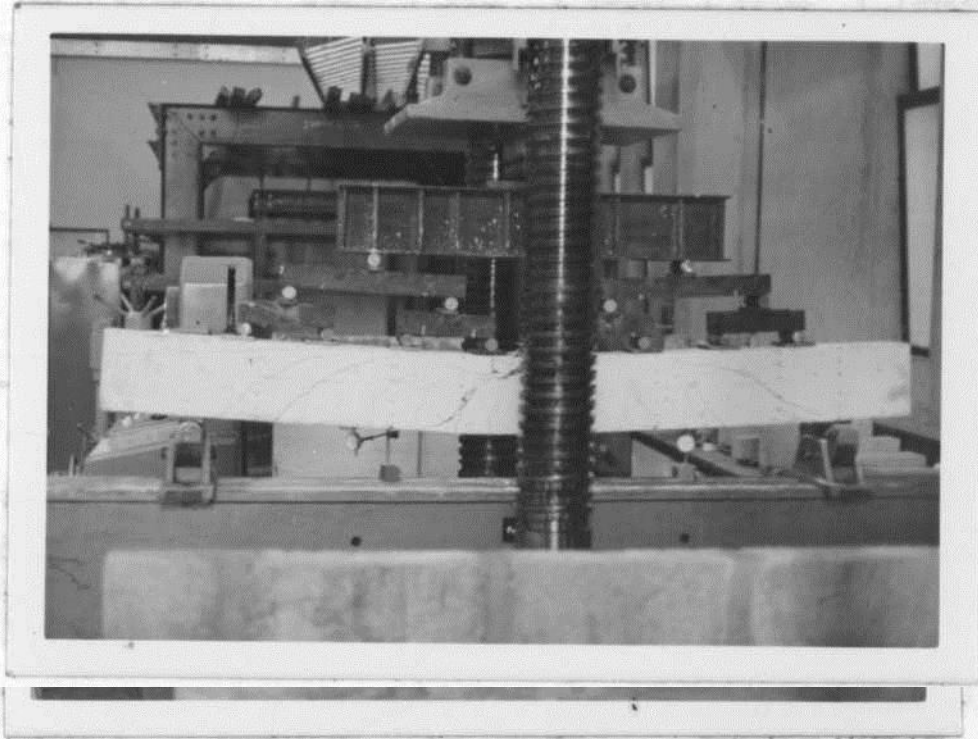


PLATE B 21: Beam G3/4 before load application.

PLATE B 22: Combined shear and flexure failure of beam G-3A* Note concrete spalling.

APPLIED LOAD (wO	CONCRETE STRAIN z 10 ⁻⁵					
	13 ^{***}	14	15	16	17	18
20	-4.1 [*]	-2.9	-1.6	0.0	+2.5 ^{**}	+1.6
40	-13.9	-6.9	-4.9	+2.3	+6.9	+9.0
60	-13.9	-8.4	-4.1	+3.3	+6.0	+10.2
80	-30.0	-17.5	-5.8	+10.0	+17.5	+30.3
100	-40.2	-21.7	-5.9	+13.8	+30.0	+42.5
120	-49.3	-26.4	-4.1	+23.2	+43.8	+59.2
140	-52.2	■*30.3	-4.9	+24.6	+49.2	+67.7
160	-70.4	-36.8	-2.7	+35.2	+62.3	+92.0
180	-85.7	-39.8	-4.1	+40.2	+67.2	+102.4
200	-102.0	-43.1	-4.9	+49.3	+82.7	+117.6
220	-115.6	-15.8	+4.1	+56.2	+95.6	+125.5
240	-141.4	-9.8	+6.9	+66.0	+109.0	+141.7
260	-162.1	-14.7	+8.2	+72.0	+117.4	+150.6
280	-201.6	-24.6	+10.8	+80.8	+130.5	+165.0

*** negative signs indicate compressive strains.**

••• positive signs indicate tensile strains.

*** Numbers denoting mid points of gauge lengths as shown in figure i»A.

**TABLE C1 (b) t STRAIN VALUES FOR BEAM G1/1
SECTION B**

CONCRETE STRAINS X10⁻⁵

	7	8	9	10.	11	12
	- 2.9	-1.2	-3.3	+ 1.6	+ 3.3	+ 2.9
(KN)	-9.0	-4.9	-2.7	+ 2.5	+ 6.9	+ 9.8
	-9.5	-6.1	-2.7	-h 4.2	+ 9.7	+12.9
20	-22.1	-13.1	-4.5	+ 7.8	+20.0	+26.0
40	-26.3	-15.0	-4.9	+12.0	+27.3	+37.2
60	-34.0	-17.2	-3.7	+24.0	+44.0	+59.9
80	-38.8	-19.9	-3.3	+27.8	+61.0	+73.2
100	-46.9	-21.0	+4.9	+50.7	+87.6	+104.6
120	-57.2	-18.9	+22.0	+92.0	+109.8	+144.0
140	-58*0	-20.0	+37.8	+115.3	+133.1	+173.7
160	-47.3	-20.7	+63.7	+156.2	+161.7	+218.2
180	-47.2	-30.3	+77.2	+185.5	+170.2	+244.1
200	-46.8	-37.4	+87.5	+218.4	+182.4	+271.0
220	-51.2	-47.4	+104.0	+256.2	+211.0	+303.8
240						
260						
280						

TABLE C2 (a) : STRAIN VALUES FOR BEAM G1/2-SECTION A.

APPLIED LOAD (KM)	CONCRETE STRAINS $\times 10^{-5}$					
	1*	2	3	4	5	6
20	-1.6	-2.5	-1.2	+0.8	+0.8	+12.0
40	-3.7	-2.9	-2.5	+0.8	+1.6	+14.3
60	-4.1	-3.3	-1.2	+1.2	+2.2	+15.1
80	-7.8	-6.3	-2.9	+0.5	+4.4	+19.3
100	-8.5	-6.5	-3.3	-1.2 %	+5.0	+20.5
120	-12.1	-8.5	-3.7	-1.2	+4.9	+20.5
140	-13.0	-9.4	-4.1	-1.2	+5.0	+23.2
160	-14.8	-9.8	-5.3	-2.9	+4.1	+35.8
180	-10.5	-10.0	-8.2	-6.4	+26.0	+59.2
200	-5.8	-11.2	-9.2	-9.0	+38.4	+65.7
220	-1.6	-12.3	-13.9	-15.8	+53.0	+87.1
240	+20.7	-13.0	-13.9	-19.2	+100.5	+122.0
260	+58.5	-13.8	-17.0	-20.2	+132.4	+151.3
280	+125.3	-15.9	-18.1	-10.9	+226.9	+197.0

* Numbers denoting mid points of gauge length as shown in figure.

TABLE C (c) 1 STRAIN VALUES FOR BEAM G1/1

APPLIED LOAD (WJ)	CONCRETE STRAINS x 10*5					
	13	14	15	16	17	18
20	-4.1	-4.5	-2.5	+1.6	+1.6	+3.6
* 40	-11.9	-6.9	-7.0	+3.7	+6.0	+10.7
60	-18.0	-11.2	-4.8	+6.0	+7.9	+14.9
80	-22.2	-12.5	-4.1	+10.3	+12.5	+18.5
100	-32.3	-18.8	-4.8	+20.4	+24.2	+36.0
120	-49.7	-23.1	-3.6	+21.2	+35.3	+48.5
140	-54.8	-33.2	-3.7	+35.8	+40.4	+59.3
160	-65.6	-53.6	-4.5	+41.7	+48.5	+69.2
180	-76.2	-40.7	-1.6	+49.6	+60.0	+87.3
200	-77.3	-37.5	-0.8	+58.0	+68.3	+96.6
220	-97.5	-44.0	-1.2	+75.5	+85.2	+120.0
240	-109.0	-53.3	0.0	+85.0	+100.0	+140.2
260	-121.1	-58.0	+5.8	+92.4	+107.3	+148.3
280	-122.3	-64.6	+5.8	+103.3	+122.2	+165.6
300	-154.6	-73.2	+10.0	+118.3	+140.7	+193.5
320	-169.8	-79.0	+21.2	+135.5	+158.8	+220.4
340	-211.3	-89.3	+27.8	+182.4	+217.3	+293.1
360	-238.0	-100.6	+35.0	+228.7	+273.1	+362.4
380	-296.4	-114.2	+64.3	+314.8	+323.2	+498.2
400	-446.7	-152.9	+127.5	+535.2	+682.0	+846.3

**TABLE 02 (b) { STRAIN VALUES FOR BEAM G1/2
SECTION B**

APPLIED LOAD (wO)	CONCRETE STRAINS <small>x10⁻⁵</small>					
	7	8	9	10	11	12
20	-4.1	-1.6	-1.6	+0.8	+1.6	+4.1
40	-9.0	-6.8	-2.2	+2.5	+5.6	+10.2
60	-13.9	-8.0	-3.9	+1.6	+9.2	+12.7
80	-16.2	-8.0	-4.0	+2.2	+12.3	+19.8
100	-17.4	-10.6	-3.5	+4.9	+18.0	+35.6
120	-16.3	-17.8	-4.9	+8.0	+35.3	+49.8
140	-30.5	-21.0	-4.9	+16.2	+48.2	+65.7
160	-39.0	-19.6	-6.3	+19.3	+58.1	+80.0
180	-40.8	-26.3	-8.9	+21.7	+68.0	+93.4
200	-55.3	-25.8	-6.0	+34.1	+80.2	+108.6
220	-60.3	-50.5	-0.5	+53.5	+91.3	+137.2
240	-72.4	-28.5	+3.3	+71.7	+113.2	+156.1
260	-77.8	-33.6	+4.0	+77.8	+122.5	+168.4
280	-84.2	-54.2	+6.9	+90.0	+137.3	+187.8
500	-94.5	-37.6	+9.1	+104.2	+149.8	+204.0
520	-106.6	-40.7	+11.0	+108.6	+165.1	+226.2
540	-109.8	-46.6	+16.2	+131.4	+170.0	+259.3
560	-120.0	-47.1	+19.3	+142.0	+174.6	+287.0
580	-127.8	-51.2	+20.5	+160.0	+248.3	+334.1
400	148.5	-56.4	+27.8	+173.6	+286.7	+375.2

APPLIED LOAD (wt)	CONCRETE STRAINS $\times 10^5$					
	1	2	3	4	5	6
20	-2.5	-1.6	-1.6	+1.2	+0.8	+2.5
40	-2.5	-2.5	-1.6	+1.6	+2.5	+4.1
60	-5.0	-4.4	-1.6	+1.6	+3.3	+1.6
80	-5.9	-4.4	-1.2	+2.9	+4.1	+1.8
100	-6.9	-5.3	-2.0	+2.5	+4.1	+3.3
120	-9.8	-7.0	-2.9	+3.3	+7.4	+4.9
140	-12.0	-7.9	+0.8	+3.5	+8.2	+6.0
160	-13.1	-11.3	+4.9	+6.5	+24.0	+14.6
180	-15.3	-9.8	+6.0	+16.0	+38.3	+24.6
200	-13.2	-10.4	+6.0	+18.8	+46.2	+36.2
220	-10.5	-9.2	+6.0	+16.2	+51.7	+49.8
2*0	-11.2	-7.9	+7.1	+19.2	+59.8	+70.0
260	-8.9	-7.8	+7.2	+18.8	+62.2	+74.2
280	-9.2	-8.3	+6.9	+16.8	+64.3	+82.6
500	-8.0	-9.4	+6.9	+14.7	+58.0	+88.7
320	-7.2	-10.2	+7.2	+12.9	+56.2	+94.8
340	-4.9	-9.8	+4.9	+9.0	+48.3	+106.0
360	-2.6	-9.2	+4.0	+8.8	+42.9	+114.3
380	-0.8	-10.0	+2.9	+9.0	+38.3	+145.4
400	-0.8	-8.2	+1.8	+10.2	+39.4	+141.0

**TABLE C2 (c) : STRAIN VALUES FOR BEAM G1/2
SECTION C**

TABLE C3 (a) STRAIN VALUES FOR BEAM G1/3 SECTION A

APPLIED LOAD V^m , t	-5 CONCRETE STRAINS x10					
	13	14	15	16	17	18
20	-0.8	-0.8	0.0	+2.6	+0.8	+0.8
40	-10.8	-4.1	0.0	+4.9	+11.0	+7.4
60	-17.2	-9.2	0.0	+6.0	+11.8	+18.2
80	-23.3	-10.6	-3.3	+10.7	+18.1	+22.0
100	-31.5	-17.4	-2.5	+15.1	+27.3	+39.1
120	-37.4	-19.6	-2.6	+18.3	+33.0	+47.9
140	-50.8	-27.0	-5.3	+24.6	+43.4	+66.2
160	-58.7	-28.1	-1.2	+32.0	+51.2	+79.8
180	-67.0	-33.0	+0.8	+39.2	+59.8	+89.3
200	-80.5	-40.2	+0.8	+44.8	+71.9	+112.7
220	-96.4	-46.3	+2.0	+57.6	+81.1	+130.4
240	-107.7	-52.5	+3.3	+67.7	+95.3	+147.6
260	-123.6	-58.7	+4.9	+75.0	+101.7	+162.5
280	-128.2	-59.8	+4.1	+85.0	+114.6	+178.0
300	-151.1	-69.6	+10.8	+96.7	+132.4	+195.1
320	-168.3	-74.2	+14.6	+120.5	+143.0	+247.3
340	-177.6	-80.0	+30.9	+128.6	+168.5	+260.6
360	-216.9	-88.1	+61.7	+179.1	+220.6	+332.9
380	-263.5	-99.0	+62.4	+260.3	+327.6	+320.4
400	♦ -337.0	-122.4	+114.2	+481.0	+622.4	+879.7
420	-400.0	-299.2	+270.5	-	-	-

**TABLE C5 (b) : STRAIN VALUES FOR BEAM G1/3
SECTION B**

APPLIED LOAD (kN)	CONCRETE STRAINS $\times 10^{-5}$					
	7	8	9	10	11	12T* ----
20	-1.2	-1.2	+6.0	+1.2	+1.2	+2.0
40	-8.9	-4.9	+6.0	+2.8	+6.0	+7.0
60	-12.7	-8.3	+4.2	+4.9	+9.8	+11.8
80	-16.1	-14.1	+2.9	+6.0	+13.2	+14.6
100	-19.8	-13.6	+1.6	+8.0	+14.4	+23.1
120	-27.0	-16.7	0.0	+10.2	+23.6	+27.2
140	-31.2	-21.2	-1.6 ;	+17.5	+56.1	+39.6
160 *	-39.8	-23.6	-2.9	+22.5	+44.7	+52.3
180	-45.3	-25.0	-4.5	+33.5	+63.0	+69.0
200	-55.4	-20.9	-7.1	+53.4	+84.2	+91.9
220	-65.3	-22.1	-24.2	+62.3	+97.5	+107.7
240	-68.9	-21.8	-25.8	+67.8	+105.7	+119.2
260	-69.0	-22.2	-33.3	+75.2	+117.4	+130.4
280	-77.2	-22.7	-35.6	+82.1	+130.2	+145.5
300	-87.5	-25.5	-44.5	+88.7	+141.0	+160.0
320	-94.6	-26.6	-46.4	+96.0	+152.6	+179.8
540	-96.7	-26.4	-47.7	+104.2	+169.8	+188.7
360	-104.1	-30.5	-50.3	+116.0	+196.1	+225.3
380	-113.3	-31.0	-53.2	+130.5	+236.6	+270.2
400	-128.7	-37.9	-55.0	+148.3	+295.2	+541.4
420	-158.4	-40.1		+193.6	+528.3	+396.5
420			-50.2			

APPLIED LOAD (wO)	CONCRETE STRAIN $\times 10^{-5}$					
	1	2	3	4	5	6
20	-0.8	-2.0	-3.3	-0.8	+2.5	+0.8
40	-2.5	-3.7	-2.5	0	+2.7	+4.9
60	-3.3	-5.3	-4.8	+1.6	+4.9	+5.7
80	-5.0	-7.4	-4.8	+1.6	+6.5	+6.6.
100	-6.3	-8.3	-6.9	+2.5	+10.5	+6.6
120	-9.8	-9.0	-8.4	+1.6	+12.1	+8.9
140	-7.7	-11.5	-8.4	+1.6	+13.3	+14.0
160	-23.8	-11.5	-8.9	+1.6	+12.1	+16.2
180	-22.1	-11.5	-8.9	+4.9	+14.5	+27.9
200	-21.7	-12.7	-10.3	+30.8	+24.7	+51.3
220	-23.0	-13.5	-13.5	+48.0	+34.8	+79.8
240	-7.7	-14.0	-17.5	+65.2	+47.3	+89,4
260	-5.3	-14.0	-20.6	+64.3	+50.0	+96.7
280	-4.9	-15.2	-21.2	+73.6	+60.2	+112.2
300	-5.7	-16.6	-23.2	+84.5	+74.4	+125.5
320	-4.5	-16.4	-23.7	+93.1	+79.3	+136.6
340	-1.5	-15.8	-24.8	+103.3	+86.6	+146.3
360	+0.5	-15.5	-24.8	+111.0	+93.1	+149.4
380	+3.3	-15.3	-27.1	+119.7	+101.7	+166.8
400	+7.0	-15.0	-28.4	+129.6	+106.2	+183.0
420	+9.0	-12.6	-30.3	+130.5	+102.5	+187.4

TABLE C 4(a) : STRAIN VALUES FOR BEAM G1/4 SECTION A

**TABLE C3 (c) : STRAIN VALUES FOR BEAN G1^
SECTION C**

APPLIED LOAD (MJ)	CONCRETE STRAINS $\times 10^{-5}$					
	13	14	15	16	17	18
20	-5.0	-1.8	-2.5	+2.9	+2.4	+5.0
40	-7.8	-7.8	-9.8	+4.9	+23.0	+16.2
60	-17.2	-13.0	-8.2	+8.0	+26.6	+40.9
80	-21.3	-16.1	-15.3	+11.7	+30.7	+56.7
100	-40.6	-27.2	-16.4	+22.2	+43.2	+71.1
120	-44.3	-25.9	-9.3 ¹	+32.0	+55.4	+92.3
140	-59.0	-33.7	-11.8	+32.8	+61.2	+114.0
160	-64.7	-43.6	-7.3	+48.7	+92.7	+125.5
180	-83.8	-37.8	-6.5	+49.0	+103.3	+137.8
200	; -85.5	-44.0	-2.6	+57.7	+114.5	◆158.9
220	-100.0	-56.1	-1.6	+ 65.6	+124.8	+172.7
240	i -106.2	-54.8	+3.7	+79.2	+141.4	+231.4
280	-150.1	i -70.3	+14.6	+104.4	+185.6	+232.0
320	-167.4	-92.4	+35.0	+194.3	+281.9	+358.1
360	-373.7	-148.6	+26.4	+470.6	+718.0	+859.3

TABLE C 4 (b) ; STRAIN VALUES FOR BEAM G1/4
SECTION B

APPLIED LOAD (wr)	CONCRETE STRAINS $\times 10^5$					
	7	8	9	10	11	12
20	-11.0	-1.6	-1.8	-1.2	+6.0	+0.8
40	-11.9	-3.8	-3.3	+1.6	+7.8	+5.7
60	-14.1	-3.7	-5.2	+2.5	+13.1	+14.6
80	-14.4	-7.0	-7.8	+4.1	+15.9	+21.7
100	-20.2	-11.9	-4.2	+5.0	+30.2	+35.4
120	-22.5	-11.3	-10.0	+16.2	+35.4	+42.0
140	-23.2	-13.2	0	+27.7	+51.6	+67.3
160	-34.8	-20.4	+4.5	+51.2	+76.7	+94.4
180	-40.1	-17.0	+9.9	+68.3	+85.2	+111.0
200	-48.7	-22.8	+13.3	+80.4	+94.3	+123.5
220	-63.6	-24.0	+12.4	+94.2	+100.0	+137.6
240	-60.2	-24.0	+22.5	+106.5	+111.2	+159.2
280	-76.4	-30.7	+26.7	+149.2	+167.8	+192.4
320	-92.0	-37.6	+28.2	+183.1	+189.2	+236.6
360	-102.5	-40.3	+25.3	+155.4	+198.0	+329.7

TABLE C 5(a); STRAIN VALUES FOR BEAM C2/1
SECTION A

APPLIED LOAD (wo)	CONCRETE STRAINS $\times 10^{-5}$					
	1	2	3	4	5	6
20	-3.7	-1.2	+1.6	-8.0	-0.5	+8.0
40	-3.7	-4.5	+5.1	+4.2	-2.1	+12.2
60	-4.1	-0.8	+6.3	0.0	+6.0	+16.9
80	-9.0	-4.9	-11.4	+11.0	+4.8	+14.7
100	-4.9	-11.0	-1.6	+9.8	+10.2	+13.3
120	-2.8	-7.2	+0.8	+13.7	+13.8	+11.5
140	-8*0	-15.3	-1.2	+15.2	+20.3	+18.8
160	-6.7	-7.8	-0.5	+16.3	+18.8	+22.4
180	-3.6	-7.4	+4.0	+7.1	+34.0	+26.6
200	-12.2	-20.5	-7.8	+4.9	+43.2	+34.1
220	-0.8	-14.7	+1.8	+1.8	+54.5	+51.0
240	-4.1	-8.0	+0.8	+5.2	+44.3	+62.2
280	-3.9	-6.7	-2.2	+6.0	+94.4	+75.0
320	-2.9	-6.7	-2.2	+1.2	+105.0	+112.3
360	-4.0	-10.3	-3.3	0.0	+114.6	+127.7

**TABLE C1e), Sm. IM VALUES FOR BEAM OI/4
SECTION C**

APPLIED LOAD (EH)	CONCRETE STRAINS × 10 ⁻⁵					
	13	14	15	16	17	18
10	-11.0	-7.7	-14.2	+4.2	+4.0	+8.3
20	-16.2	-8.9	-13.0	+6.0	+8.3	+9.4
50	-24.9	-14.0	-13.0	+8.3	+13.4	+17.7
40	-50.7	-15.8	-12.4	+19.7	+18.5	+30.8
50	-41.1	-18.0	-12.4	+30.4	+28.8	+47.0
60	-43.5	-21.1	-16.3	+35.1	+31.7	+58.0
80	-58.8	-25.5	-16.3	+51.5	+61.2	+89.1
100	-76.8	-27.2	-16.3	+62.8	+94.6	+117.4
120	-81.2	-41.2	-12.5	+71.0	+102.0	+130.4
140	-103.4	-47.0	-5.8	+87.3	+130.5	+164.5

TABLE C 5(b) : STRAIN VALUES FOR BEAM G2/1 SECTION

B

APPLIED LOAD (kw)	CONCRETE STRAINS ×10 ⁻⁵					
	7	8	9	10	11	12
10	-6.8 *	-3.3	-2.5	-3.3	+4.2	+6.0
20	-7.9	-5.0	-4.3	-2.0	+6.6	+9.0
30	-14.0	-9.1	-6.0	-1.6	+8.0	+11.5
40	-20.3	-12.8	-7.2	-1.0	+10.6	+14.4
50	-28.2	-18.2	-6.4	-1.2	+15.3	+19.8
60	-31.8	-20.3	-5.8	-2.0	+17.4	+26.2
80	-42.1	-27.4	-6.0	-3.3	+29.0	+40.8
100 •	-54.7	-33.8	-6.0	-4.1	+42.7	+59.3
120	-61.2	-40.0	-1.6	-6.3	+57.1 .	+75.5
140	-70.4	-29.1	-0.8	-7.2	+70.0	+93.4

TABLE C 5(c) : STRAIN VALUES FOR BEAM G2/1 SECTION C

APPLIED LOAD (KN)	CONCRETE STRAINS $\times 10^{-5}$					
	1	2	3	4	5	6
10	-5.7	-4.1	-2.5	-1.6	+1.6	+18.2
20	-4.9	-4.1	+3.7	-0.8	+5.7	+17.3
30	-4.9	-4.9	+6.0	+1.6	+5.7	+7.9
40	-4.1	-8.2	+5.7	+4.1	+10.7	+8.5
50	-5.7	-8.2	+7.4	+4.1	+10.7	+7.5
60	-4.1	-9.8	+6.2	+4.9	+11.5	+12.0
80	-7.4	-12.3	+10.3	+6.6	+12.3	+15.7
100	-9.8	-14.0	+7.4	+7.4	+14.0	+12.0
120	-9.8	-14.8	+5.8	+4.9	+15.0	+5.3
140	-7.4	-14.8	+4.1	+6.6	+15.0	+4.1

TABLE C 6(a) : STRAIN VALUES FOR BEAM G2/2 SECTION A

APPLIED LOAD (K.N)	CONCRETE STRAINS $\times 10^{-5}$					
	13	14	15	16	17	18
20	-	-17.6	-8.0	+16.1	-	+25.0
40	-	-24.7	-21.6	+40.7	-	+32.7
60	-	-58.0	-25.2	+41.4	-	+40.8
80	-	-55.2	-16.0	+32.8	-	+53.3
100	-	-57.6	-14.3	+38.0	-	+74.5
120	-	-81.5	-16.5	+43.4	**	+98.4
140	-	-74.0	-15.8	+74.5	-	+122.7
160	-	-61.9	-16.3	+88.7	-	+130.9
180	-	-70.4	-12.0	+82.2	-	+168.0
200	-	-81.7	0.0	+127.0	-	+197.3
220	-	-86.3	+11.3	+160.4	-	+270.5
240	-	-106.2	+103.4	+360.0	-	+417.4

TABLE C 7(a) : STRAIN VALUES FOR BEAM 02/5

APPLIED LOAD (MO)	CONCRETE STRAINS $\times 10^{-5}$					
	7	8	9	10	11	12
20	-4.0	-8.2	-3.3	+3.3	+3.3	+3.3
40	-21.1	-14.3	-4.2	+6.2	+45.4	+21.2
60	-32.8	-20.0	-9.1	+21.3	+52.7	+30.4
80	-40.6	-42.4	-6.0	+29.1	+85.8	+52.4
100	-40.6	-43.3	-6.0	+34.0	+85.8	+89.0
120	-82.2	-50.7	-2.2	+52.3	+116.5	+120.6
140	-98.4	-66.8	-2.2	+61.1	+106.3	+150.0
160	-102.5	-52.1	0.0	+72.5	+107.0	+171.4
180.	-123.0	-66.3	+4.0	+92.6	+160.5	+210.6
200	-148.7	-70.5	+16.1	+104.7	+192.4	+261.0
220	-194.3	-72.0	+28.3	+107.8	+267.0	+334.4
240	-260.0	-72.0	+55.4	+274.0	+340.6	+555.0

TABLE C 6 (c) : STRAIN VALUES FOR BEAM G2/2 SECTION C

APPLIED	CONCRETE STRAINS $\times 10^{-5}$					
	1	2	3	4	5	6
20	-3.3	-7.0	-0.4	-7.4	+4.5	+20.7
40	-8.2	-4.3	-0.8	-7.0	+5.7	+33.2
60	-8.2	-4.3	-1.2	-8.2	+4.9	+39.3
80	-10.1	-14.5	-2.8	-8.2	+6.5	+41.0
100	-12.3	-14.5	-1.6	-6.0	+5.3	+55.4
120	-14.8	-12.3	-0.4	-7.3	+8.3	+55.4
140	-20.0	-12.5	-2.0	-12.3	+14.0	+58.0
160	-12.3	-14.0	-2.8	-16.5	+21.2	+58.0
180	-14.4	-8.2	-6.6	-19.6	+31.7	+91.4
200	-8.2	-10.0	-12.3	-23.0	+44.8	+120.0
220	-8.2	-6.6	-3.3	-29.8	+57.5	+152.3
240	-8.0	-8.4	-8.7	-32.7	+82.5	+187.4

TABLE 6 (b) - STRAIN VALUES FOR BEAM 02/3

APPLIED LOAD (kN)	CONCRETE STRAINS $\times 10^{-5}$					
	13	14	15	16	17	18
20	-7.4	-4.1	-0.8	+4.3	+4.0	+8.2
40	-21.3	-13.4	-6.3	+8.2	+15.7	+27.0
60	-35.2	-20.8	-7.4	+16.4	+29.8	+48.7
80	-49.2	-21.2	-7.4	+24.6	+43.4	+96.8
100	-66.3	-37.3	-10.4	+33.7	+59.2	+98.0
120	-84.5	-48.0	-12.3	+38.9	+71.4	+121.2
140	-110.0	-61.6	-15.6	+48.8	+91.0	+153.6
160	-122.3	-66.9	-15.6	+54.7	+93.4	+173.4
180	-163.5	-89.1	-20.7	+59.0	+126.7	+217.7
200	-185.7	-102.0	-22.9	+68.1	+136.8	+248.6
220	-240.2	-128.4	-24.6	+101.0	+186.0	+308.5
240	-306.0	-161.5	-23.4	+140.5	+250.2	+392.4

TABLE F - STBATW VALUES FOR BEAM 02/3

SECTION B

APPLIED LOAD (kN)	CONCRETE STRAINS $\times 10^{+5}$					
	7	8	9	10	11	12
20	-7.4	-5.6	-1.2	+1.6	+4.9	+7.8
40	-19.6	-13.7	-2.8	+4.1	+12.7	+14.0
60	-32.2	-21.1	-4.5	+9.4	+19.6	+22.7
80	-47.5	-28.0	-6.0	+15.6	+32.7	+35.2
100	-60.0	-36.2	-7.0	+22.0	+43.4	+51.5
120	-74.6	-44.4	-7.4	+28.5	+54.0	+65.4
140	-93.7	-53.1	-7.4	+37.4	+70.7	+81.2
160	-109.4	-56.3	-8.7	+46.3	+82.7	+93.9
180	-136.6	-76.6	-10.5	+55.0	+106.0	+120.1
200	-164.2	-89.6	-12.0	+66.2	+121.2	+137.8
220	-197.4	-104.2	-13.1	+88.7	+159.6	+180.0
240	-240.0	-122.4	-13.5	+110.8	+197.4	+231.6

TABLE C 7 (c) i STRAP) VALUES FOR BEAM 02/3
SECTION C

APPLIED LOAD (KN)	CONCRETE STRAIN $\times 10^{-5}$					
	1	2	3	4	5	6
20	-2.0	-2.2	-1.6	-0.5	0.0	+5.3
40	-5.0	-3.3	-2.5	-0.7	+2.1	+7.0
60	-8.2	-4.1	-2.5	+1.2	+2.5	+7.0
80	-9.1	-6.6	-2.8	+0.8	+1.6	+5.5
100	-11.8	-8.2	-5.0	+0.8	+1.6	+12.0
120	-14.2	-11.4	-6.5	-0.4	+4.1	+12.0
140	-10.7	-12.3	-7.0	-6.2	+3.7	+22.3
160	-12.5	-11.7	-8.2	-9.4	+3.7	+26.7
180	-11.8	-11.0	-10.3	-12.7	+8.2	+33.8
200	-8.4	-11.5	-13.6	-17.0	+20.5	+42.5
220	-7.5	-11.7	-14.8	-22.5	+28.0	+40.0
240	-7.0	-25.0	-17.6	-25.3	+32.7	+41.4

TABLE 0 8 (ah STRAIN VALDES FOR BEAK G2/4

APPLIED LOAD (KN)	CONCRETE STRAIN $\times 10^{-5}$					
	13	14	15	16	17	18
20	-12.3	-5.0	-3.3	+0.8	+11.0	+18.6
40	-23.5	-11.8	-8.2	+2.0	+24.3	+30.7
60	-40.9	-20.6	-10.6	+3.3	+37.2	+51.1
80	-52.7	-25.1	-12.2	+7.4	+52.1	◆75.4
100	-75.2	-38.4	-14.0	+8.8	+70.0	+87.2
120	-99.0	-51.7	-17.8	+14.7	+90.0	+124.6
140	-129.1	-62.2	-24.6	+20.8	+105.4	+140.0
180	-160.4	-80.9	-27.1	+29.2	+126.3	+164.7
200	-192.8	-102.0	-30.4	+35.0	+138.7	+188.3
220	-254.2	-131.5	-30.5	+70.0	+182.4	+250.0
240	-405.6	-202.4	-17.3	+205.5	+331.3	+442.0

TABLE C 9(a) : STRAIN VALUES FOR BEAM G5/1

SECTION A

APPLIED LOAD (wt)	CONCRETE STRAINS $\times icr5$					
	7	8	9	10	11	12
20	-7.0	-4.1	-7.0	+7.8	+7.0	+19.2
40	-17.6	-6.6	-10.7	+18.4	+18.2	+30.3
60	-34.4	-11.9	-9.2	+16.5	+32.7	+49.7
80	-48.4	-18.0	-15.4	+24.2	+43.8	+67.6
100	-62.8	-17.5	-12.6	+28.1	+61.2	+95.4
120	-87.7	-48.0	-16.8	+44.7	+85.5	+117.6
140	-110.0	-56.4	-15.6	+51.6	+103.0	+145.3
160	-138.0	-72.1	-13.5	+56.0	+126.4	+173.0
180	-164.5	-84.2	-17.6	+81.5	+154.6	+205.2
200	-208.5	-103.5	-16.0	+103.0	+225.5	+261.4
220	-279.0	-140.3	-26.5	+120.4	+240.0	+380.5

TABLE C 8 (c) : STRAIN VALUES FOR BEAK 02/4 SECTION

C

APPLIED LOAD (RK)	CONCRETE STRAINS $\times 10^{15}$					
	1	2	3	4	5	6
20	-4.9	-13.9	0.0	+0.8	+5.7	+2.5
40	-9.4	-14.8	-0.8	+7.4	+5.7	+4.1
60	-14.0	-4.9	-1.6	+11.5	+7.4	+7.8
80	-15.6	-9.8	-2.0	+7.0	+7.5	+10.3
100	-16.4	-9.4	-4.5	+5.4	+19.3	+19.8
120	-14.1	-11.5	-6*1	+13.9	+53.6	+56.5
140	-11.9	-11.1	-4.9	+18.0	+49.7	+52.8
160	-9.0	-13.1	-7.2	+6.5	+65.5	◆71.7
180	-3.3	-12.7	-9.4	+8.2	+67.0	+86.5
200	+0.5	-12.8	-11.9	-1.6	+61.7	+98.5
220	+9.0	-10.6	-11.9	-11.6	+56.7	+111.0

TABLE C 8C1d)» STRAIN VALUES FOR BEAM G2/4

APPLIED	CONCRETE STRAINS $\times 10^5$					
	7	8	9	10	11	12
20	-12.7	-4.9	-4.5	+3.3	+13.9	+14.8
40	-25.9	-13.1	-7.3	+9.4	+17.2	+33.6
60	-39.7	-18.4	-5.7	+28.7	+44.2	+62.1
80	-50.6	-29.0	-3.3	+40.9	+65.8	+90.0
100	-73.3	-33.6	-2.9	+59.4	+81.2	+118.0
120	-91.0	-41.3	-2.5	+72.8	+96.4	+138.0

TABLE C q(b)i STRAIN VALUES FOR BEAM G5/1 SECTION B

APPLIED LOAD (kN)	CONCRETE STRAINS $\times 10^5$					
	1	2	3	4	5	6
20	-3.3	-2.0	-1.6	0.0	+1.6	+3.3
> 40	-4.1	-3.3	-1.6	+1.6	+3.7	+3.7
60	-4.9	-5.7	-2.5	+3.6	+4.5	+4.9
80	-9.0	-7.4	-4.6	+4.5	+5.3	+11.5
100	-9.8	-7.4	-5.3	+5.3	+7.4	+10.2
120	-11.0	-9.0	-5.3	+5.3	+7.4	+22.6

TABLE C 10 (a) : STRAIN VALUES FOR BEAM G3/2

SECTION A

APPLIED LOAD (kN)	CONCRETE STRAINS $\times 10^{-5}$					
	7	8	9	10	11	12
20	-15.5	-9.4	-2.8	+8.6	+4.9	+4.1
40	-26.6	-16.4	-0.5	+23.1	+19.7	+20.5
60	-45.5	-26.2	+1.2	+40.0	+37.8	+43.6
80	-44.6	-25.4	+10.2	+66.8	+67.6	+186.8
100	-71.7	-30.4	+7.8	+70.5	+80.0	+106.6
120	-80.4	-63.3	+11.5	+75.6	+99.4	+137.5
140	-119.2	-84.5	+6.1	+88.1	+120.0	+170.0
160	-133.6	-108.2	+9.4	+102.5	+140.5	+215.3
180	-220.0	-147.5	+14.0	+115.0	+241.6	+426.1

TABLE C 10 (b) : STRAIN VALUES FOR BEAM G3/2 SECTION

B

APPLIED LOAD (kN)	CONCRETE STRAINS $\times 10^{-5}$					
	1	2	3	4	5	6
20	-4.1	-3.3	-2.0	+0.8	-1.6	0.0
40	-9.0	-5.3	-1.1	+1.6	+1.6	-4.9
60	-15.0	-6.1	-4.1	+1.6	-1.6	+0.8
80	-13.0	-4.1	-5.0	-2.1	+4.9	+9.8
100	-14.3	-8.2	-2.5	-4.2	+17.2	+14.8
120	-10.2	-16.0	-11.8	-6.0	+41.0	+20.5
140	-8.2	-16.0	-12.7	-12.3	+72.4	+44.2
160	-8.2	-18.8	-9.8	-10.5	+100.5	+72.0
180	-2.5	-16.8	-15.9	-12.0	+125.3	+97.6

TABLE C 12 (a) : STRAINS VALUES FOR BEAM G5/4
SECTION A

APPLIED LOAD (kw)	CONCRETE STRAINS $\times 10^{-5}$					
	7	8	9	10	11	12
20	-9.0	-6.6	-1.2	+9.0	+8.2	+11.1
40	-19.6	-12.3	+2.5	+16.0	+18.5	+22.9
60	-32.0	-18.0	+1.6	+27.5	+28.6	+47.5
80	-44.6	-22.5	+5.7	+48.0	+59.4	+80.2
100	-57.3	-27.1	+8.6	+60.0	+86.5	+100.0
120	-71.5	-32.8	+12.3	+71.6	+106.4	+131.5
140	-88.6	-36.8	+18.8	+89.5	+132.6	+162.5
160	-112.5	-41.0	+27.9	+115.0	+171.3	+210.0

TABLE C 11 * STRAIN VAH SECTION B

APPLIED LOAD (ML)	CONCRETE STRAINS $\times 10^{-5}$					
	1	2	3	4	5	6
20	-1.2	-1.6	+0.4	+0.4	+4.5	+8.2
40	-2.9	-2.1	+1.2	+0.8	+3.3	+7.0
60	-7.0	-4.1	+0.4	+1.6	+4.1	+7.4
80	-7.6	-7.4	+1.2	+3.4	+5.0	+10.6
100	-10.2	-5.3	+0.4	+2.1	+6.1	+10.2
120	-11.1	-4.6	-0.4	+1.6	+12.9	+17.0
140	-5.7	-5.3	-0.4	-3.7	+20.9	+20.2
160	-2.8	-4.1	-2.5	-2.8	+32.4	+39.0

TABLE C 11(a) i STRAIN VALUES FOR BEAM G5/5

APPLIED <i>m</i>	CONCRETE STRAIN $\times 10^{-5}$					
	7	8	9	10	11	12
20	-9.8	-4.9	-2.5	+2.0	+5.3	+9.0
40	-20.5	-11.5	-6.6	+7.4	+10.7	+23.3
60	-35.2	-18.0	-4.1	+18.9	+27.1	+47.1
80	-47.5	-22.5	-3.3	+31.2	+43.2	+73.3
100	-57.3	-26.6	+0.8	+46.8	+64.8	+96.2
120	-70.5	-27.2	+4.9	+59.5	+84.0	+122.8
140	-83.6	-28.6	+9.0	+75.2	+109.6	+155.0
160	-104.0	-42.2	+14.0	+91.0	+127.5	+186.2
180	-205.5	-37.7	+29.5	+122.2	+165.4	+243.4
200	-195.6	-28.6	+96.8	+231.3	+315.0	+350.3

TABLE C 12(b) : STRAIN VALUES FOR BEAM G5/4 SECTION B

APPLIED LOAD O'®)	CONCRETE STRAINS $\times 10^{-5}$					
	1	2	3	4	5	6
20	-3.7	-4.1	-4.5	+0.4	+7.0	+0.8
40	-7.4	-5.7	-2.9	+0.8	+10.6	+2.0
60	-10.2	-6.6	-2.8	+1.6	+10.6	+4.5
80	-11.9	-7.4	-5.3	+1.6	+10.0	+6.5
100	-13.9	-7.4	-2.8	+4.1	+7.8	+11.9
120	-15.1	-7.4	-3.7	+4.4	+15.3	+24.2
140	-13.5	+0.8	-7.3	+26.0	◆38.1	+78.8
160	-2.5	+1.6	-9.0	+35.4	+39.4	+102.8
180	-2.0	+2.5	-10.6	+42.2	+59.2	+125.0
200	+1.6	+5.7	-12.7	+56.0	+117.4	+142.5

BEAM No,	F _{CONCRETE} STRENGTH (N/mm ²)			CRACKING LOAD (KN)		SI	A	K M p	MP	OP FAILURE	S	V _{yjA}	f _{yv} (N/mm ²)	(w ^f _{yv}) A V _{yv}
	u	fc*	ft ¹	(Sic)	"cr test									
8/0	35.0	28.0	4.16	90.8	90	118.2	35.9	45.3	0.790	SC	-	-	-	-
8/1	32.2	25.7	4.00	87.2	90	139.2	42.4	44.1	0.960	SC	100	0.271	0.583	0.465
8/2	35.7	28.6	4.22	92.5	100	154.1	47.0	45.6	1.025	p	50	0.543	0.566	0.956
8/3	35.1	28.1	4.18	90.8	105	165.1	50.4	45.4	1.105	F	25	1.080	0.568	1.910
10/0	34.5	27.5 j	4.15	87.2	95	101.0	38.7	45.1	0.855	sc	-	-	-	-
10/1 j	37.2	29.7	4.30	90.0	90	119.5	45.5	46.4	0.980	sc	190	0.145	0.297	0.487
10/2	30.8	24.6	3.91	82.8	90	104.0 1	39.6	43.5 !	0.910	sc	95	0.290	0.310	0.933
10/3	36.7	29.3	4.27	90.0	85	131.5	50.0	46.2	1.085	p	47	0.578	0.297	1.95
12/0	36.2	29.0	4.24	81.9	80	104.0	47.5	46.0	1.035	DT	-	-	-	-
12/2	31.0	24.8	3.93	80.0	85	91.5	41.8	43.6	0.960	sc	150	0.181	0.190	0.95
12/3	33.0	26.4	4.06	83.2	90	103.5	47.3	44.4	1.060	F	76	0.361	0.185	1.95

* approximate values

APPENDIX E

CALCULATIONS FOR FIGURE 5.3 E.1

GROUP G 1

Beam G1/1; $u = 48.0$, $f_c' = 38.4$, $f_t' = 4.90 \text{ K/mm}^2$

$$\frac{1.3 \times 26.9 + 0.35 \times 38.4 \times 0.667}{22.1 + 38.4}$$

$$\frac{0.5 \times 38.4}{552} \times 0.431$$

$$u = \frac{0.004 \times 38.4}{44900} \times 0.00315$$

$$k = 0.478$$

$$C = T = 310 \text{ kN}$$

$$M_p = 310 \times 200 (1 - 0.478 \times 0.431) = 49.2 \text{ kNm}$$

$$M_u = 300 \times \frac{1.2}{17} = 45.0 \text{ kN} \quad \mathbf{9}$$

$$M_u = 45.0 = 0.915$$

$$M_n = \frac{49.2}{49.2}$$

$$F \ll \frac{49.2 \times 8}{1.2} = 328 \text{ kN}$$

$$W \ll \frac{328}{1.2} = 273 \text{ N/mm of span}$$

$$V = 0.15 \times 2 = 192 \text{ mm}$$

$$c_r = 7.27 \times 4.9 = 35.5 \text{ kN}$$

$$c_r = 2 \times 35.5 \times \frac{600}{408} = 104.5 \text{ kN} \quad \mathbf{BN}$$

Beam Q1/2: u = 47.5, fc¹ = 38.0, ft' = 4.86 N/mm²

CM i n E

$$k_1 \ll \frac{26.9 + 0.35 \times 38.0}{22.1 + 38.0} \quad * 0.668$$

$$= 0.5 - \frac{38.0}{552}$$

$$* 0.004 - 38.0$$

$$u = \frac{44900 \text{ " } O^{*00\wedge}}{\quad}$$

$$k = 0.479$$

$$C^* = \Gamma = 309 \text{ kN}$$

$$M_j \gg = 309 \times 200 (1 - 0.479 \times 0.431) = 49.0 \text{ Kin}$$

$$M_u = 425 \times 1^2 = 65\#7 \text{ KNm } 8$$

$$M_u * 63.7$$

$$M_p = 49.0 \text{ ' } ^$$

$$W_p = 49.0 \times \underline{8} \text{ . } 32g \text{ kN } 1.2$$

$$W = 272 \text{ N/mm } 1.2$$

$$Q_{\text{oz}} = 7.27 \times 4.86 = 35.3$$

$$W_{cr} = 2 \times 35.3 \times 600 = 104.0 \text{ kN } 408$$

$$M_s = 5.70 \times 4.86 = 27.7 \text{ kHm}$$

$$= 27.7 / 98.0 = 0.283$$

$$\blacksquare \frac{272 \times 0.137}{(0.15r)^2} * 6.51 \text{ N/inm}^2 254 \times$$

$$(V_{yw}) A$$

$$* 49.75 \times 320 \ll 1.25 \text{ N/mm}^2 127 \times 100$$

$$\frac{\wedge^t W_{yw}^e A}{W|,}$$

$$* 1.25 = 0.192$$

$$6.51$$

0.192

W|,

Beam 61/3:

$$u = 48.0, f_c' = 38.4, f_t' = 4.90 \text{ N/m}^2$$

Beam Q1/2: $u = 47.5, f_c^1 = 38.0, f_t' = 4.86 \text{ N/mm}^2$

$$k, k_3 = \frac{26.9 + 0.35 i 38.4 \ll 0.667}{22.1 * 38.4}$$

$$k_2 = \frac{0.5 - 38.4}{552} = 0.431$$

$$\ll u = \frac{0.004 - 38.4}{44555} = 0.00315$$

$$k = 0.478$$

OT- 310 kN

$$M_p = 310 i 200 (1.0478 \times 0.431) = 49.2 \text{ kNm}$$

$$M_u = 440 \times 1.2 * 66.0 \text{ kNm}$$

ft:

$$M_u = 6.0 = 1.34$$

$$J: 49.0$$

$$W_p = \frac{49.2 \times 8}{172} = 328 \text{ kN}$$

$$W = \frac{328}{1.2} = 273 \text{ N/mm}$$

$$Q_{cr} = 7.27 \times 4.90 = 35.6 \text{ KN}$$

$$V_{cr} = 2 \times 35.6 \times \frac{600}{408} = 105.0 \text{ kN}$$

$$M_g = 5.70 \times 4.90 = 28.0 \text{ kNm}$$

$$V = 28.0 / 98.4 = 0.284$$

$$W_y \gg \frac{273 \times 0.136}{254 \times (0.19)} = 6.50 \text{ N/mm}^2$$

$$= \frac{49.75 \times 320}{127 \times 75} = 1.67 \text{ N/mm}^2$$

$$\frac{(P_n * y_w) A_w}{1.67} = 0.257$$

$$|T_w^{\wedge} y_v| = 6.50$$

$$\frac{B_{ftm} a_i // L_i}{u} \ll 44 \cdot 0, f_{c^*} = 35 \cdot 2, f_{t'} = 470 \text{ N/mm}^2$$

$$k_{1k3} = \frac{26.9 \cdot 0.35 \cdot 35.2}{22.1 \cdot 35.2} = 0.684$$

$$*_{2} = \frac{0.5 - 35.2}{552} = 0.436$$

$$\bullet_u = \frac{0.004 - 35.2}{44900} = 0.00322$$

$$1 \quad * 0.500$$

$$C^* = T = 306 \text{ kN}$$

$$M_p = 306 \cdot 200(1 - 0.500) \cdot 0.436$$

$$\ll 47.8 \text{ KNm}$$

$$M_u = 396 \cdot 1.2 \cdot 5 \cdot T = 59.5 \text{ KNm}$$

$$M_u = \frac{59.5}{47.8} = 1.24$$

$$W_p = 47.8 \cdot 8 = 319 \text{ kN}$$

$$W = \frac{319}{1.2} = 266 \text{ N/mm}$$

$$Q_{cr} = 7.27 \cdot 4.70 = 34.1 \text{ kN}$$

$$v_{cr} = 2 \cdot 34.1 \cdot \frac{600}{455} = 100.0 \text{ kN}$$

$$M_g = 5.70 \cdot 4.70 = 26.7 \text{ KNm}$$

$$\ll -26.7/95.6 = 0.279$$

$$\frac{266 \cdot 0.141}{254 (0.15)^2} = 6.56 \text{ N/mm}^2$$

$$\sigma_{rW^f yw}^A = \frac{49.75 \cdot 320}{127 \cdot 50} = 2.51 \text{ N/mm}^2$$

$$\sigma_{rW^* yv}^A = \frac{2.51}{6.56} = 0.382$$

$$\sigma_{rW^{\wedge} yv}$$

E. 2 GROUP G2

$$u = 43.8, f_c \ll 35.0, f_t \bullet = 4.67 \text{ N/mm}^2$$

$$k_1 = \frac{26.9 + 0.35 \times 35.0}{22.1 + 35.0} \bullet 0.685$$

$$k_2 = 0.5 - \frac{35.0}{552} = 0.437$$

$$e_u = \frac{0.004 - \frac{35.0}{44900}}{\bullet} \bullet 0.00322$$

$$k \ll 0.501$$

$$C = T = 305$$

$$= 305 \times 200 (1 - 0.501 \times 0.437)$$

$$= 47.7 \text{ KN}$$

$$M_u = \frac{148 \times 1.6}{8} = 29.6 \text{ kNm}$$

$$\frac{M_u}{M_n} = \frac{29.6}{47.7} = 0.620$$

$$w_p = \frac{47.7 \times 8}{1.6} = 238.5 \text{ KN}$$

$$V = \frac{w_p}{\bullet} = 149 \text{ N/ipm}$$

$$\bullet 0.126, \bullet 2 = 202 \text{ mm}$$

$$V_{cr} = 2 \times \frac{7.27 \times 4.67}{33.8 \times 800} = 90.2 \text{ KN}$$

$$\frac{V}{V_{cr}} = \frac{149}{90.2} = 1.65$$

Bam G2/2:

$$u = 49.3, f_c \bullet = 39.5, f_t \bullet \ll 4.96 \text{ N/mm}^2$$

$$k_1 = \frac{26.9 + 0.35 \times 39.5}{22.1 + 39.5} \bullet = 0.660$$

$$k_2 = 0.50 - \frac{39.5}{552} = 0.428$$

$$e_u = \frac{0.004 - \frac{39.5}{44900}}{\bullet} = 0.00312$$

$$k = 0.472$$

$$C = T = 312$$

$$= 312 \times 200 (1 - 0.472 \times 0.428) = 49.8 \text{ kNm}$$

$$M_u = 248 \times 1.68 = 418.56 \text{ kNm} = 49.6 \text{ kNm}$$

$$M_{-JA} = 49.6 / 49.8 = 0.995$$

$$w = 49.8 \times \frac{1}{T6} = 2.9 \text{ kN}$$

$$w = 249 / 1.6 = 155.5 \text{ N/m}$$

$$Q_{cr} = 7.27 \times 4.96 = 36.0 \text{ kN}$$

$$W_{cr} = \frac{2 \times 36.0 \times 800}{598} = 96.5 \text{ kN}$$

$$M_s = 5.70 \times 4.96 = 28.2 \text{ kNm}$$

$$M_{cp} = 28.2 / 99.6 = 0.284 \text{ in}$$

$$T_{r_w f_y w} = \frac{155.5 \times 0.095 \times 25 \text{ in} \times (0.1 \text{ 2b})}{(r_{y w}^2 \times w) A} = 3.58 \text{ N/mm}^2$$

$$\frac{(r_{y w}^2 \times w) A}{(r_{y w}^2 \times w) A} = \frac{49.75 \times 320 \times 127 \times 175}{0.176} = 0.716$$

$$\frac{3.58}{\text{Beam G2/3: ...}} = 0.200$$

$$u = 4.2, r_c = 33.8 \text{ mm}$$

$$k_1 k_2 = \frac{26.9 + 0.35 \times 33.8}{22.1 + 33.8} = 0.692$$

$$k_2 = 0.5 \times 2.8 = 0.439$$

$$f_t = \frac{h \cdot p}{552} = 0.00325$$

$$e_Q = 0.04 - 33.8 \times 44900$$

$$k = 0.509 \text{ C=T} = 303$$

$$M_F = 303 \times 200 (1 - 0.509 \times 0.439) = 47.2 \text{ kN}$$

$M = 257 \times 1.6 \cdot 8$	= 51.4 KNm
	= 1.09
$M_U = aiti$	
$M_p = 47.2$	
$\frac{, = 47 \cdot 2 \times 8}{** 1.6}$	236 kli
$w = 236/1.0$	= 147.5 N/mm
$Q = 2 \times 36.0 \times 800 \text{ cr } 598$	= 96.9 kN
$M_g = 5.70 \times 4.59$	= 26.0 KN
$\phi = 26.0/94.4$	= 0.275 m
$Y \setminus r f = 147.5 \times 0.102^{\wedge}$	= 3.72 N/num
$^{\wedge} w y * 25iU1'0.126')^2$	
2	
$(r f) A = \frac{U9.75 \times 720}{127 \times 150}$	= 0.338 t%
$(r f) A = 0.838 \frac{w_{yw}}{v 70''}$	0.225
rv r-? -----	
' V. r_w I yw	
Seam G-2/4:	
= 43.4, f = 34.6, f_t	4.64 N/2
kk = 26.9 + 0.35 \times 34.6	= 0.689
13	
$22.1 + 34.6$	
*2 = 0.5 - 3,4.6	= 0.437
552	
e = 0.004 - 34.6	= 0.00323
..	
44900	
k = 0.501	
C=T = 305	
m_p = 305 \times 200 (1 - 0.501 \times 0.437)	
= 47.6 KK_m	
M_u = 238 \times 1.6/8	= 47.7 KN
M_u = 47.7	
47.6	= 1.00

$$\begin{aligned} I_{VJ} &= & &= 238 \text{ XK} \\ 1+7.6 \times 8 / 1.6 & & &= 11+9 \text{ N/ m} \\ w &= 238 / 1.6 & &= 33.7 \text{ kN} \\ Q_{cr} &= 7.27 \times 1+.65 & &= 90.1+ \text{ KIT} \\ W_{//} &= & &= 26.5 \text{ xisr} \\ 2 \times 33.7 \times 800 & & 598 &= 0.277 \text{ m} \\ K_g &= 5.70 \times 1+. \\ 65 & & & \end{aligned}$$

$$f_{wy} = \frac{11+9 \times 0.100}{727 \times 125} = 3.69 \text{ V mm}$$

$$W_{yw} = 1.00 = 0.271$$

$$Y_{iw} = 3.69$$

B. 3 GROUP

Beam G3/1: $u = 1+3.3$, $f_c' = 31+5$, $f_t' = 1+62$

$$k_1 = \frac{26.9+0.35 \times 51+5}{22.1+31+5} = 0.688$$

$$k_2 = \frac{0.5-31+5}{552} = 0.1+39$$

$$e_u = \frac{0.001+31+5}{1+1+900} = 0.00323$$

$$k = 0.501+$$

$$C=T = 301+$$

$$M_p = 304 \times 200 (1 - 0.501 + 0.1+39)$$

$$0? = 26.5/95.2$$

$$M = \frac{1+7.1+KK_{j \neq 1}}{128 \times 2/8}$$

$$M_u = \frac{32.0}{kl.k} = 32.0 \text{ kK m} = 0.675$$

$$w_F = 1+7.1+X8/2 = 189.6 \text{ kK}$$

$$w = 189.6/2 = 94.8 \text{ N/mm}$$

$$= 0.107, x^{\wedge} = 7.27 \times 1+ = 211+ \text{ mm} =$$

$$33.7 \text{ kN}$$

$$= 86.0 \text{ kN}$$

* >> 2

Beam G3/2: $u = 42.4$, $f_Q = 33.8$, $f_t = 4.59$ M/mm

k_k

$$1.3 = \underline{26.9 + 0.35 \times 33.8} = 0.692$$

$$k_k = 0.5 - 22 \times 8$$

552

		0.439
e u	0.004-33.8 44900	0.00325
k C=T	0.509 =303	
M _j ,	303x200 (1-0.509x6.439) =47.2 kN _m	
u _u	=1 80x2/8	= 45.0 kN _m
"u M _p	=45.0 <hr style="width: 50%; margin-left: 0;"/> 47.2	0.954
w _p	=47.2x8/2	= 183.8 kN
w	=188.8/2	= 94.4 N/mm
Q _{cr}	=7.27x4.59	= 33.2 kN
w _{cr}	= 2x33.2x100 0	= 84.0 kN
M _s	=5.70x4.59 =26.1/94.4	= 26.1 kN _m 0.276
ifir f L w y ^w	=94.4x0.448 254x0.085	= 1.96 N/ mm
(r f)A w y ^w A	49.75x320	= 0.502 N/ 2
(y ^w) T ₁ r _w ^f y ^w	= 125x250 0.502 1.96	= 0.255

22.1+33.8

Beam 03/3: $u = 49.2$, $f_t = 39.5$, $f_t' = 4.96 \text{ N/mm}^2$

$$k_1 = \frac{26.9 + 0.35 \times 39.5}{22.1 + 39.5} = 0.660$$

$$k_2 = \frac{0.5 \times L^4}{552} = 0.1 + 28$$

$$e_u = \frac{0.004 \times 39.5}{44900} = 0.00312$$

$$k = 0.472$$

$$C = T = 312$$

$$M_u = \frac{312 \times 200}{m} (1 - 0.472 \times 0.428) = 49.8 \text{ kN}$$

$$M_u = 183 \times 2 / 8 = 45.8 \text{ kNm}$$

$$M_u = \frac{45.8}{49.8} = 0.920$$

$$V_F = 49.8 \times 8 / 2 = 199.5 \text{ kN}$$

$$w = 199.5 / 2 = 99.7 \text{ N/mm}$$

$$Q_{cr} = 7.27 \times 4.96 = 36.1 \text{ kN}$$

$$W_{cr} = \frac{2 \times 36.1 \times 1000}{786} = 92.0 \text{ kN}$$

$$M_S = 5.70 \times 4.96 = 28.4 \text{ kNm}$$

$$g = 28.4 / 99.6 = 0.285$$

$$U_{Vyw} = \frac{99.7 \times 0.11 \times 30}{254 \times 0.094} = 1.79 \text{ N/mm}^2$$

$$(r_f)_A = \frac{49.75 \times 320}{127 \times 225} = 0.500 \text{ N/mm}^2$$

$$\frac{(V_{yw})^A}{n_f L w yw} = \frac{0.560}{1.70} = 0.313$$

TABLE FI: ROTATIONS FOR BEAM G1/1

M kNm	SLOPES x 10 ⁻² (RADIANS)		ROTATIONS x 10 ⁻² RADIANS		
	a	3	9	0i	©2
3	.03	.07	.10	.12	.08
6	.05	.15	.20	.25	.16
9	.08	.18	.26	.32	.22
12	.10	.21	.31	.37	.26
15	V ¹⁴	.26	.40	.44	.33
18	.16	.28	.44	.52	.40
21	.19	.31	.50	.56	.43
24	.21	.36	.57	.67	.52
27	.21	.39	.60	.84	.67
30	.23	.42	.65	.95	.77
33	.25	.45	.70	1.20	.96
36	.28	.47	.75	1.49	1.13
39	.29	.47	.76	1.77	1.30
42	.32	.53	.85	2.07	1.58
45	.35	.61	.96	2.73	2.32

TABLE F2: ROTATIONS FOR BEAM G1/2

M	SLOPES x 10 ²		ROTATIONS x 10 ²		
	(RADIANS)		(RADIANS)		
KNm	a	3	0	©1	02
3	.02	.05	.07	.13	.10
6	.02	.06	.08	.31	.14
9	.03	.08	.11	.28	.23
12	.04	.10	.14	.35	.29
15	.05	.13	.18	.43	.35
18	.07	.16	.23	.51	.42
21	.07	.17	.24	.59	.48
24	.08	.21	.29	.64	.51
27	.11	.25	.36	.74	.63
30	.12	.25	.37	.83	.70
33	.14	.29	.43	.98	.80
36	.13	.32	.45	1.09	.89
39	.13	.32	.45	1.13	.94
42	.15	.34	.49	1.23	1.03
45	.17	.36	.53	1.33	1.13
48	.20	.36	.56	1.42	1.23
51	.26	.46	.72	1.64	1.44
54	.31	.52	.83	1.81	1.60
57	.42	.64	1.06	2.08	1.86
60	.43	.67	1.10	2.81	2.57

TABLE F4: ROTATIONS FOR BEAM G1/4

M KNm	SLOPES $\times 10^{-2}$ (RADIANS)		ROTATIONS $\times 10$ (RADIANS)		
	a	3	Q	9 ₁	02
3	.03	.01	.04	.05	.07
6	.07	.01	.08	.20	.28
9	.10	.02	.12	.27	.35
12	.12	.03	.15	.32	.41
15	.16	.03	.19	.41	.54
18	.18	.04	.22	.47	.62
21	.24	.09	.33	.51	.67
24	.26	.10	.36;	.57	.74
27	.30	.12	.42	. 6 3	.81
30	.36	.15	.51	.76	1.00
33	.39	.16	.55	.83	1.05
36	.42	.18	.60	.89	1.12
39	.43	.19	.62	.96	1.20
42	.46	.21	.67	1.05	1.30
45	.46	.21	.67	1.13	1.41
48	.55	.27	.82	1.28	1.56
51	.59	.29	.88	1.37	1.63
. 54	.69	.37	1.06	1.49	1.82
57	.88	.47	1.35	1.72	2.11
60	.63	.72	1.35	2.34	2.91
63	.67	1.08	1.75	0.67	1.08

TABLE F4: ROTATIONS FOR BEAM G1/4

M KNm	SLOPES x 10 ⁷ (RADIANS)		ROTATIONS x 10 ² (RADIANS)		
	a	3	0	0i	02
3	.09	.02	.11	.06	.13
6	.12	.02	.14	.11	.21
9	.19	.09	.28	.20	.29
12	.22	.11	.33	.24	.36
15	.28	.13	.41	.32	.46
18	.27	.12	.39	.36	.51
21	.28	.12	.40	.44	.59
24	.31	.15	.46	.57	.72
27	.31	.15	.46	.66	.81
30	.32	.16	.48	.70	.86
33	.32	.15	.47	.78	.95
36	.35	.18	.53	.87	1.05
42	.45	.28	.73	1.10	1.27
48	.67	.39	1.06	1.37	1.64
54	1.15	.99	2.14	2.31	2.54
57	1.84	1.78	3.62	4.40	4.50

TABLE F7: ROTATIONS FOR BEAM G2/3

M t	SLOPES × 10 ⁻² (RADIANS)		ROTATIONS × 10 ⁻² (RADIANS)		
	a	6	0	0i	02
4	.14	.13	.27	.09	.10
8	.15	.14	.29	.11	.19
12	.19	.17	.36	.25	.26
16	.21	.20	.41	.33	.34
20	.26	.25	.51	.43	.45
24	.32	.32	.64	.58	.53
28	.29	.44	.73	.92	.77

TABLE F6: ROTATIONS FOR BEAM G2/2

M	SLOPES × 10 ⁻² (RADIANS)		ROTATIONS × 10 ⁻² (RADIANS)		
	a	6	0		02
4	.01	.03	.04	.12	.09
8	.01	.03	.04	.18	.15
12	.03	.05	.08	.24	.22
16	.08	.11	.19	.41	.38
20	.10	.13	.23	.52	.43
24	.13	.16	.29	.56	.54
28	.21	.22	.43	.76	.76
32	.20	.24	.44	.90	.86
36	.27	.30	.57	1.06	1.30
40	.37	.38	.75	1.26	1.26
44	.52	.50	1.02	1.51	1.54
48	.83	1.00	1.83	2.24	2.42
. 48.5	1.40	1.75	3.15	3.35	3.30

TABLE F5: ROTATIONS FOR BEAM G2/1

M KNm	SLOPES x 10 ⁻² (RADIANS)		ROTATIONS x 10 ⁻² (RADIANS)		
	a	3	0	e _i	°2
4	.05	.04	.09	.09	.10
8	.08	.04	.12	.18	.21
12	.11	.05	.16	.25	.32
16	.14	.05	.19	.33	.42
20	.20	.08	.28	.45	.58
24	.25	.10	.35	.57	.72
28	.29	.13	.42	.71	.87
32	.29	.17	.46	.86	.98
36	.68	.50	1.18	.98	1.15
40	.68	.47	1.15	1.15	1.34
44	.69	.49	1.18	1.38	1.59
48	.71	.51	1.22	1.64	1.84

TABLE F8: ROTATIONS FOR BEAM G2/4

M kNm	SLOPES x 10 ⁻² (RADIANS)		ROTATIONS x 10 ⁻² (RADIANS)		
	a	3	e	e _i	°2
4	.04	.04	.08	.09	.09
8	.07	.06	.13	.15	.16
12	.11	.07	.18	.25	.29
16	.15	.10	.25	.38	.43
20	.18	.13	.31	.52	.57
24	.24	.19	.43	.68	.74
28	.25	.20	.45	.81	.88
32	.34	.26	.60	1.00	1.08
36	.40	.31	.71	1.18	1.25
40	.54	.41	.95	1.44	1.57
44	.84	.59	1.43	1.91	2.16

TABLE F9: ROTATIONS FOR BEAM G3/1

M KNm	SLOPE $\times 10^{-2}$ S (RADIANS)		ROTATIONS $\times 10^{-2}$ (RADIANS)		
	a	e	0	9i	0 ₂
5	.00	.00	.00	.11	.10
10	.01	.03	.04	.23	.22
15	.06	.07	.13	.37	.36
20	.09	.10	.19	.51	.50
25	.12	.11	.23	.70	.71
30	.19	.17	.36	.82	.84

TABLE F10: ROTATIONS FOR BEAM G3/2

M XNm	SLOPES $\times 10^{-2}$ (RADIANS)		ROTATIONS $\times 10^{-2}$ (RADIANS)		
	a	g	9	©1	02
5	.10	.01	.11	.10	.18
10	.11	.02	.13	.23	.34
15	.14	.03	.17	.36	.47
20	.19	.09	.28	.55	.65
25	.24	.10	.34	.66	.80
30	.31	.19	.50	.94	1.06
35	.38	.27	.65	1.19	1.30
40	.58	.46	1.04	1.60	1.72
44	L. 58	1.55	3.13	2.64	2.67

TABLE F11: ROTATIONS FOR BEAM G3/3

M KNm	SLOPES $\times 10^{-2}$ (RADIANS)*		ROTATIONS $\times 10^{-2}$ (RADIANS)		
	a	8	0	01	02
5	.05	.10	.15	.16	.06
10	.05	.18	.23	.29	.17
15	.08	.22	.30	.46	.31
20	.12	.28	.40	.64	.47
25	.14	.35	.49	.79	.61
30	.22	.39	.61	.94	.77
35	.29	.47	.76	1.16	.98
40	.42	.59	1.01	1.45	1.28
44	.65	1.21	1.86	2.71	2.07

TABLE F12: ROTATIONS FOR BEAM G3/4

M KNm	SLOPE S $\times 10^{-2}$ (RADIANS)		ROTATIONS $\times 10^{-2}$ (RADIANS)		
	a	8	0	0i	02
5	.01	.01	.02	.07	.07
10	.03	.02	.05	.17	.17
15	.08	.07	.15	.28	.29
20	.13	.10	.23	.40	.43
25	.18	.18	.36	.54	.56
30	.22	.21	.43	.68	.69
35	.33	.30	.63	.98	1.01
40	.39	.38	.77	1.17	1.18
45	.56	.62	1.18	1.50	1.56
50	1.18	1.07	2.25	2.46	2.57